STUDIES ON SCATTERING AND QUASI-NORMAL MODES IN BLACK HOLE SPACE-TIMES

Thesis submitted to
Cochin University of Science and Technology

in partial fulfillment of the requirements
for the award of the degree of

DOCTOR OF PHILOSOPHY

by

Sini R
Theory Division
Department of Physics
Cochin University of Science and Technology
Kochi - 682022

September 2008

Studies on scattering and quasi-normal modes in black hole space-times

PhD thesis in the field of black hole physics

Author

Sini R

Dept of Physics

Cochin University of Science and Technology

Kochi - 22

rsin2002@gmail.com

Research Supervisor

Prof V. C. Kuriakose

Dept of Physics

Cochin University of Science and Technology

Kochi - 22

vck@cusat.ac.in

Dedicated to Achan, Amma, Renjiettan &
Binojettan

CERTIFICATE

Certified that the work presented in this thesis is a bonafide research work done by Ms. Sini R under my guidance in the Department of Physics, Cochin University of Science and Technology, Kochi, India - 682022, and has not been included in any other thesis submitted previously for the award of any degree.

Kochi-22
September 05, 2008

Prof. V. C. Kuriakose
(Supervising Guide)

DECLARATION

I hereby declare that the work presented in this thesis is based on the original research work done by me under the guidance of Prof. V. C. Kuriakose, Department of Physics, Cochin University of Science and Technology, Kochi, India - 682022, and has not been included in any other thesis submitted previously for the award of any degree.

Kochi-22
September 05, 2008 Sini R

Contents

Preface

A black hole is an object so compact that, within a certain distance of it, even the speed of light is not fast enough to escape. Black holes can be created in the collapse of a star having mass about 10 to 20 times the mass of the sun. If a massive star undergoes supernova explosion leaving behind a fairly massive stellar remnant, there will be no outward forces to oppose gravitational forces and the remnant will collapse on itself. The star eventually collapses to the point of zero volume and infinite density, creating what is known as a "singularity ". As the density increases, the paths of light rays emitted from the star are bent and eventually wrapped irrevocably around the star. Photons emitted are trapped into an orbit by the intense gravitational field; they will never leave it. Since no light escapes from the star when it reaches this infinite density, hence the name black hole. The spherical surface which acts like one-way membrane: particles and radiation can cross it from outside, but they cannot escape from its interior, is known as the horizon of the black hole. It is the place where escape velocity equals the velocity of light, so if we cross the horizon, we are doomed eventually to hit the singularity.

Black holes have begun to be entities of theoretical interest when they have been found as exact solutions of the Einstein equations for theory of general relativity with peculiar features. Even though, the name black hole was only introduced by Wheeler in 1968, the first black hole solution has been found by Schwarzschild in 1916, just a few months after the publication of the theory of General Relativity by Einstein. It is well known that the black holes, unlike other astrophysical objects, cannot be observed directly. Therefore, the only way to discover its presence is through its gravitational interaction with the surrounding matter. Currently, about 20 stellar binaries are known in our galaxy which are believed to contain black holes of some solar masses, whereas super massive black holes may exist

in the centers of active galaxies. The gravitational wave detectors GEO , VIRGO and LIGO, are used to directly observe processes involving black holes. As our observational and theoretical capabilities continue to advance, the ability to probe these strong field regions steadily improves. The essential aim of this thesis is to study theoretical aspects of scattering off waves by black holes, which is considered as a most useful way of exploring black holes.

Even though the theoretical idea of black holes is more than 200 years old, interest in the absorption of quantum waves by black holes was reignited after Hawking's discovery that black holes can emit, as well as scatter and absorb radiation. And there is another interesting fact that the event horizon need not be fully absorptive type but can reflect waves falling on it. Thus, we are interested in finding absorption cross section in various black hole space-times perturbed by various matter fields, using the fact that the reflection from the horizon can take place.

A characteristic feature of the response of a black hole to external perturbations is the appearance of quasi-normal modes. Quasi-normal modes of black holes have been studied ever since the seminal work of Vishveshwara in the early 1970s. Within general relativity, it is well-known that there are three stages to the dynamical evolution of field perturbation on a black hole background: the initial outburst from the source of perturbation, the damping (quasi-normal) oscillations and asymptotic tails at very late time. These damped oscillations, which are intrinsic characteristics of the black hole exterior geometry and depend only on the black hole parameters, imply that they are the imprint of a black hole in its response to external perturbations. And thus, they provide a unique opportunity to identify a black hole, and that hopefully will become a reality when large-scale laser-interferometric detectors for gravitational waves come into operation in the near future. In order to extract as much information as possible from a gravitational-wave signal it is important to study

about quasi-normal modes in various black hole space-times.

Chapter 1 gives a basic introduction to the concept of black holes. Starting from the simplest scattering problems involving black holes, we discuss the fundamental equation in black hole scattering. Also historical developments, different terms and concepts associated with quasi-normal modes are also introduced.

In **Chapter 2**, Schwarzschild-de Sitter, RN extremal and SdS extremal space-times scattered off by scalar waves are studied. In the SdS black hole case, it possesses two horizons: black hole horizon r_b and cosmological horizon r_c. We considered the scattering effect near the black hole horizon r_b. Since here the scattering is by scalar waves the equation of motion will be Klein-Gordon equation and its radial part is solved in regions outside the black hole horizon. Here we split the region outside the horizon into 3 regions: vicinity of the horizon, sufficiently away from the horizon and very far away from the horizon. The wave function in the vicinity of horizon containing the incident wave and the wave reflected from the horizon, is obtained using WKB approximation. Here, reflection from the black hole horizon r_b is used as an alternative way to derive the Hawking temperature of SdS black hole. The behavior of scattered scalar waves in the regions $r > r_b$ and $r \gg r_b$ in low energy limit are also studied. The solutions in the 3 regions are compared and found the S-matrix and the absorption cross section for SdS black hole in the low energy limit. Deduction of absorption cross section of Schwarzschild black hole in the presence of reflection and in the absence of reflection has been made, from the expression for absorption cross section of SdS black hole. Similar studies are extended to RN extremal and SdS extremal cases also and expressions for absorption cross sections for these two black holes are obtained.

In **Chapter 3**, scattering studies are extended to charged scalar field. For that we consider the Reissner-Nordstrom space-time. The dynamical behavior of a massive charged scalar field under RN back-

ground is taken account. For that we have studied the behavior of scattered charged scalar waves in different regions outside the event horizon r_+. Absorption cross section for RN black hole in the low energy limit and its depends on the Hawking temperature are found. By plotting σ_{abs} versus ϵ, the behavior of absorption cross section with increasing of charge in the RN black hole has been found.

Chapter 4 contains the study of scattering of Dirac waves in a Schwarzschild space-time in the low energy limit. The Dirac radial equation in a general background space-time is taken and applied it for Schwarzschild space-time. For the Schwarzschild metric the singularity is at $r = 1$ which is considered as the Schwarzschild horizon. The wave functions $G_I(r)$ in the vicinity of event horizon of Schwarzschild black hole, $G_{II}(r)$ in the region $r > 1$ and $G_{III}(r)$ for the case $r >> 1$ are obtained. Using these solutions we obtain the absorption cross section of Schwarzschild black hole in Dirac field for $k = 1$ case and compared with absorption cross section of Schwarzschild black hole in scalar field. The absorption cross section for $k = 2$ in Dirac field is also derived and the absorption cross section versus energy graphs for $k = 1$ and $k = 2$ are plotted. Emission spectrum for Schwarzschild black hole in Dirac field with and without reflection is plotted.

In **Chapter 5**, we have studied the QNMs of various black hole background space-times pierced by cosmic strings which are perturbed by a massless Dirac field. The Dirac equation in a spherically symmetric space-time with a cosmic sting is deduced into a set of second order differential equations. Using WKB approximation we have evaluated the quasi-normal mode frequencies for Schwarzschild, RN extremal, SdS and near extremal SdS black hole space-times having cosmic string perturbed by massless Dirac field and studied the effect of cosmic string in the quasi-normal modes. The influence of cosmic string on the QNMs of RN black hole background space-time which are perturbed by positively and negatively charged Dirac fields is

studied in **Chapter 6**. Dirac equation in RN black hole space-time with a cosmic sting is reduced into a set of second order differential equations and evaluated the quasi-normal mode frequencies using Pöschl-Teller potential method. Here the effect of cosmic string in the RN black hole background, perturbed by positively charged Dirac field and negatively charged Dirac field are studied. And the special behavior of negatively charged Dirac field on the RN black hole having cosmic string for low and high values of Q are also studied. The main results and conclusion of this thesis are given in **Chapter 7**. The future prospects are also presented.

Part of the results contained in this thesis has been published in journals and presented in conferences.

Publications

In refereed journals

1. R. Sini, and V. C. Kuriakose, "Absorption cross-section of a Schwarzschild-de Sitter black hole," Int. J. Mod. Phys.D **16**, 105-116 (2007).

2. R. Sini, and V. C. Kuriakose, "Absorption cross section of Reissner Nordstrom black hole," (accepted for publication in International Journal of Modern Physics D), arXiv:0708.3146 (gr-qc).

3. R. Sini, and V. C. Kuriakose, "Absorption cross section and Emission spectra of Schwarzschild black hole in Dirac field," (accepted for publication in Modern Physics Letters A).

4. R. Sini, Nijo Varghese, and V. C. Kuriakose, "Absorption cross sections of Reissner Nordstrom extremal and Schwarzschild-de Sitter extremal black holes," (accepted for publication in International Journal of Modern Physics A) arXiv:0802.4374 (gr-qc).

5. Quasi-normal modes of spherically symmetric black hole space-times with cosmic string in a Dirac field, R. Sini, Nijo Varghese, and V. C. Kuriakose (under review: General Relativity and Gravitation), arXiv:0802.0788v2 (gr-qc).

6. Quasi-normal modes of RN black hole space-time with cosmic string in a Dirac field, R. Sini, and V. C. Kuriakose, (to be submitted)

In conferences/seminars

1. Absorption cross section and Hawking temperature of SdS black hole, R. Sini, and V. C. Kuriakose, Young Astronomers Meet, IUCAA, Pune, India, November 2005.

2. Absorption cross section SdS Extremal black hole, R. Sini, and V. C. Kuriakose, Young Astronomers Meet, IIA, Bangalore, India, January 2007.

3. Absorption cross section of RN extremal black hole, R. Sini, Nijo Varghese, and V. C. Kuriakose, New Horizons in Theoretical and Experimental Physics, CUSAT, Cochin, India, October 2007.

4. Dirac Quasi-normal modes of RN extremal black hole with cosmic string, R. Sini, Nijo Varghese, and V. C. Kuriakose, International conference on Gravitation and Cosmology, IUCAA, Pune, India, December 2007.

ACKNOWLEDGEMENTS

Interdependence is certainly more valuable than independence. This thesis is the result of four and half years of work whereby I have been accompanied and supported by many people. I have now an opportunity to express my gratitude to all of them.

First of all, I would like to thank my supervisor, Professor V. C. Kuriakose for his guidance, inspiration, support and encouragement throughout my research work. When difficulties appeared he was always present with his scientific help, suggestions in the right direction, and also with his motivating word. His perpetual energy and enthusiasm in research have motivated all his students, including me. I am fully aware that this acknowledgement cannot express my gratitude towards him for his entire support and affection.

I was delighted to interact with Prof. Dr. Ramesh babu T. and I express my heartfelt gratitude to him.

I extend my sincere thanks to Prof. Godfrey Louis, Head of the Department for providing me the necessary facilities for the smooth completion of this research. I am also thankful to all my teachers of the Department of Physics, for their support and encouragement right from my post graduation days. I am thankful to all the office and library staff, present and former, of the Department of Physics for all the help and cooperation extended to me.

I am very grateful to all members of the theory group for their cooperative spirit and bulding an excellent working atmosphere. I am very much indebted to Vivek, Vinayaraj, Nijo, Priyesh and Radhakrishnan for their brotherly considerations, Subha teacher for all her advices and Nima, Bhavya, Lini for their friendship. I am thankful to my senior colleague Dr. Minu Joy for her love and care. I thank Jisha C. P. for her sincere support and affection and also for clearing my simple doubts in LATEX and graciously providing the very useful document class used to typeset this thesis. I am very

much grateful to the careful and critical eye of Chitra R. for keeping me in right track and also for understanding what I said.

I would like to thank all the other fellow research scholars, M.Phil. and M.Sc. students of Physics Department for the nice moments I had with them.

I am very much grateful to my friends who made my hostel life in CUSAT lively and funny: It is a great pleasure to thank Mangala, Sheeba, Ragitha, Swapna & Rosemary, for being with me in both good and bad times. Special thanks goes to Chithra K, for being a kind, helpful and honest friend. I will keep in my heart: wonderful memories of hostel fests, late night conversations, movies, and "egg bajies" with my friends Gleeja, Reena, Nimmi, Nisha, Vineetha, Geetha, Subha, Subitha, Sreeja and joyni. Thank you dears.

This research has been supported by CUSAT for providing me research fellowship and U.G.C, New Delhi for providing fellowship through a Major Research Project. I thank them for their confidence in me.

I express my deep gratitude to my parents, for their affection, care and support provided during my student life. I am grateful to my brother Ranjith, who supports my interests and leads me in the right way. I thank my uncle Sumodh, sister in law Ragna, and Savithri for their mental support and encouragement. I am forever grateful to my in-laws and Anoop for their unconditional support. Finally, I wish to thank my husband Binoj, although words cannot capture his impact on me: Thank you for accompanying me through this amazing life. You mean the world to me!

Finally, I thank the Almighty for making me what I am.

Sini R

1 Introduction

1.1 Black holes: Basic concepts

The concept of black holes consistently grips the human imagination. There are many strange, frightening creatures and objects which have been invented in mythology, fiction and even modern scientists have revealed a number of equally bizarre and disquieting things in the world. But none of them will be a substitute to the idea of a black hole, an object whose gravitational pull is so great that not even light can escape from it, and a place where all the laws of nature break down. In the words of Kip Thorne:[1]

"Of all the conceptions of the human mind, from unicorns to gargoyles to the hydrogen bomb, the most fantastic, perhaps, is the black hole: a hole in space with a definite edge into which anything can fall and out of which nothing can escape, a hole with a gravitational force so strong that even light is caught and held in its grip, a hole that curves space and warps time."

1.1.1 Formation of black holes

Black holes are the evolutionary endpoints of certain stars that have mass 10 to 15 times the mass of our Sun. There is always a constant tug of war between gravity pulling in and pressure pushing out in

the case of ordinary stars. Inside the star, enough energy for the outward push is obtained from nuclear reactions taking place in the core. Pressure and gravity are balanced exactly each other for most of a star's life, and thus stars are stable. Young stars are hydrogen rich, and the nuclear reactions inside it convert hydrogen to helium with energy created. Part of the energy creates necessary outward pressure to balance the inward gravitational pull and part is emitted as radiation. When all the hydrogen inside a star is converted to helium, a new nuclear reaction begins which converts the helium to carbon and the process continues converting the carbon to oxygen, then to silicon and finally to iron where the nuclear fusion stops. Then the star will run out of nuclear fuel. So, the gravity gets the upper hand and the material in the core becomes more compressed. The more massive the core of the star, the greater will be the force of gravity which compress the material, and thus collapse under its own weight.

In the case of small stars, when the nuclear fuel is exhausted and there are no more nuclear reactions to fight against gravity, the repulsive forces among electrons within the star create enough pressure, which is called electron degeneracy pressure, which will halt further gravitational collapse. The star then cools and dies and this type of star is called "white dwarf". The maximum mass of a star that can be supported by electron degeneracy pressure is $1.4M_{\odot}$, a result due to Subramanyan Chandrasekhar and this limit known as the famous Chandrasekhar limit. If the mass of the collapsing star exceeds the Chandrasekhar limit, collapse will continue until neutron degeneracy pressure comes into play. If neutron degeneracy pressure can balance gravity then a "neutron star" is born. When a very massive star exhausts its nuclear fuel, it explodes as a supernova. The outer parts of the star are expelled violently into space, while the core completely collapses under its own weight.

If the mass of the core is greater than, approximately 2.5 times

mass of the Sun, then no known repulsive force inside a star can prevent gravity from complete collapse of the core into a black hole. The term 'black hole' was coined by Wheeler in 1968.[2] Once, a giant star dies and a black hole has formed, all its mass is squeezed into a single point where, both the space and time stop.[3] It's very difficult to think a place where mass has no volume and time does not pass, but it happens at the center of a black hole.

1.1.2 Singularity and horizon

The idea of high concentration of mass in a region where even light would be trapped goes all the way back to Laplace in the 18th century. Even scientists speculated that such objects could exist in Newtonian theory, they are more accurately described using Einstein's General Theory of Relativity. Almost immediately after Einstein developed general relativity, a mathematical solution to the equations of the theory describing such an object was derived by Karl Schwarzschild. It was only much later, in 1930's, with the work of Oppenheimer, Volkoff, and Snyder,[4,5] people thought seriously about the possibility that such objects might actually exist in the Universe. These researchers showed that when a sufficiently massive star runs out of fuel, it is unable to support itself against its own gravitational pull, and it should collapse into a black hole.

Gravity is a manifestation of the curvature of space-time in general relativity. Since massive objects distort space and time, we cannot use the usual rules of geometry here. Near a black hole, this distortion of space is extremely severe and causes black holes to have some very strange properties.

The point at the center of a black hole is the singularity, where matter is crushed to infinite density, the force of gravity is infinitely strong, and space-time has infinite curvature. Here, it's no longer meaningful to speak of space and time, much less space-time. Jum-

bled up at the singularity, space and time cease to exist as we know them. Every thing that falls into a black hole eventually reach the singularity of the black hole.

Within a certain distance of the singularity, the gravitational pull is so strong that nothing–not even light–can escape. The spherical surface that marks the boundary of the black hole is called the event horizon. The event horizon is not a physical boundary but the point-of-no-return for anything that crosses it. When people talk about the size of a black hole, they are referring to the size of the event horizon. More massive the singularity, larger will be the radius of the event horizon.

The horizon has some very strange geometrical properties. If we are sitting still somewhere far away from the black hole, the horizon seems to be a nice, static, unmoving spherical surface. But when reach close to the horizon, we feel its pressure and it is easy to cross the horizon in the inward direction. Once we are inside the horizon, space-time is distorted so much that the coordinates describing radial distance and time change their roles. "r" is the coordinate that describes how far we are from the center, becomes a time like coordinate, and "t" becomes space like.[6] A consequence of this is that we can't stop ourselves from moving to smaller and smaller values of r, just as under ordinary circumstances we can't avoid moving towards the future (that is, towards larger and larger values of t). Eventually, we are bound to hit the singularity at r = 0. After crossing the horizon, trying to avoid the center of a black hole is like trying to avoid next week.

1.1.3 As Einstein solutions

Mathematically black holes can be the solutions of Einstein's equations. In 1916 a few months after the publication of Einstein's theory of general relativity Karl Schwarzschild,[7] a German mathematician,

solved Einstein field equations for the gravitational field out side a static, non-rotating spherically symmetric body. He showed that space curvature varied as a function of distance from the center of the object. His results predicted a critical point at which the curvature is so strong that matter could not escape from its gravitational attraction. And his solution to Einstein's equation is named as Schwarzschild metric and is given by,

$$ds^2 = (1 - \frac{2M}{r})dt^2 - \frac{dr^2}{(1 - \frac{2M}{r})} - r^2 d\theta^2 - r^2 \sin^2\theta d\phi^2, \qquad (1.1)$$

where M is the mass of the black hole and $r = 2M$ is the Schwarzschild radius (here $c = 1$). Depending on the conditions imposed on solving Einstein equation we will get different black holes. In 1963, the Newzealandian mathematician named Roy Patrick Kerr solved the Einstein equation for an uncharged rotating black hole and is known as Kerr black hole. The Kerr black hole is characterized by two parameters M (mass) and J(angular momentum). Since J has dimension of m^2, we can define a quantity "a" as $a \equiv \frac{J}{M}$ which has the same dimension as that of M. The metric equation for Kerr black hole[8] is given by,

$$\begin{aligned} ds^2 = -\frac{\Delta - a^2 sin^2\theta}{\rho^2} dt^2 - 2a\frac{2Mrsin\theta}{\rho^2} dtd\phi + \\ \frac{r^2 + a^{2^2} - a^2\Delta sin^2\theta}{\rho^2} d\phi^2 + \frac{\rho^2}{\Delta} dr^2 + \rho^2 d\theta^2, \end{aligned} \qquad (1.2)$$

where,

$$\begin{aligned} \Delta = r^2 - 2Mr + a^2, \\ \rho^2 = r^2 + a^2 cos^2\theta. \end{aligned} \qquad (1.3)$$

The Kerr black hole is rotationally symmetric about ϕ axis. Solution to the Einstein field equations in a gravitational field of a charged, non-rotating, spherically symmetric body of mass M was discovered independently by Gunnar Nordstrm and Hans Reissner,

and the black hole is named as Reissner-Nordsrom black hole[9,10] and their metric can be written as,

$$ds^2 = (1 - \frac{2M}{r} + \frac{Q^2}{r^2})dt^2 - \frac{1}{(1 - \frac{2M}{r} + \frac{Q^2}{r^2})}dr^2 - r^2(d\theta^2 + \sin^2\theta d\phi^2). \tag{1.4}$$

where Q represents the charge of the RN black hole and the outer and inner horizons are at $r_\pm = M \pm \sqrt{M^2 - Q^2}$. The space-time geometry in the region surrounding a charged rotating black hole is given by Kerr-Newman metric and is given by,

$$\begin{aligned} ds^2 = -\frac{\Delta}{\rho^2}[dt - asin^2\theta d\phi]^2 + \frac{sin^2\theta}{\rho^2}[(r^2 + a^2)d\phi - adt]^2 \\ + \frac{\rho^2}{\Delta}dr^2 + \rho^2 d\theta^2, \end{aligned} \tag{1.5}$$

where,

$$\begin{aligned} \Delta = r^2 - 2Mr + a^2 + Q^2, \\ \rho^2 = r^2 + a^2 cos^2\theta. \end{aligned} \tag{1.6}$$

Inclusion of cosmological constant in the Einstein's general theory of relativity leads to other types of black hole solutions. Some of these solutions are discussed in Chapter 2.

1.2 Thermodynamics of black holes

During the past 40 years, research in the physics of black holes has brought to light strong hints of a very deep and fundamental relationship between gravitation, thermodynamics, and quantum theory. The first hint for this connection came with the discovery of area theorem by Hawking which states that: in any physical process involving a horizon, the area of the horizon cannot decrease in time. This property suggests that there is a resemblance between the area of the event horizon of a black hole and the concept of entropy in

thermodynamics. The cornerstone of this relationship is black hole thermodynamics, where it appears that certain laws of black hole mechanics are, in fact, simply the ordinary laws of thermodynamics applied to a system containing a black hole. The properties of black holes are explained through four laws known as four laws of black hole mechanics which bear close resemblance with the four laws of thermodynamics. Thus[11] :

The Zeroth law: The horizon has constant surface gravity for a stationary black hole. The zeroth law is analogous to the zeroth law of thermodynamics which states that the temperature is constant throughout a body in thermal equilibrium. It suggests that the surface gravity is analogous to temperature.

The First law: The first law of black hole mechanics expresses the conservation of energy by relating the change in the black hole mass M to the changes in its area A, angular momentum J and electric charge Q in the following way:

$$dM = \frac{\kappa}{8\pi} dA + \Omega dJ + \Phi dQ \tag{1.7}$$

where κ is the surface gravity, Ω is the angular velocity and Φ is the electrostatic potential. This is analogous to the first law of thermodynamics which is a statement of energy conservation, which contains on its right hand side the term TdS.

The Second law: In all physical process, the sum of the surface areas of all black holes involved can never decrease. The second law is the statement of Hawking's area theorem. Analogously, the second law of thermodynamics states that the entropy of a closed system is a non-decreasing function of time.

The Third law: By no finite series of operation the surface gravity of a black hole is brought to zero. i.e., $\kappa = 0$ is not possible to achieve. Statement that κ cannot go to zero is analogous to the third law of thermodynamics which states that it is impossible to reach absolute zero temperature in a physical process.

1.2.1 Hawking radiation

Normally, a black hole is considered to draw all matter and energy in the surrounding region into it, as a result of the intense gravitational pull due to the black holes. However, in 1972 the Israeli physicist Jacob Bekenstein[12,13] suggested that black holes should have a well-defined entropy, and initiated the development of black hole thermodynamics, including the emission of energy. If a black hole has a finite entropy that is proportional to the area of the horizon, it also has a finite temperature, which would be proportional to its surface gravity. This would imply that a black hole could be in equilibrium with thermal radiation at some temperature other than zero. Yet according to classical concepts, no such equilibrium is possible, since a black hole would absorb any thermal radiation falling on it but by definition a black hole would not be able to emit anything in return.

In 1974 Hawking published a shocking result:[14] if one takes quantum theory into account, it seems that black holes are not quite black! Instead, they should glow slightly with "Hawking radiation", consisting of photons, neutrinos, and to a lesser extent all sorts of massive particles. The radiation theory of Hawking states that, virtual particle pairs are constantly being created near the horizon of the black hole. Normally, they are created as a particle-antiparticle pair and they quickly annihilate each other. But near the horizon of a black hole, it's possible for one to fall in before the annihilation can happen, in which case the other one escapes as Hawking radiation. The particle which is escaped from the black hole, takes away energy from the black hole, and thus may be explained as black hole evaporation. Hawking showed that the photons which come out have the spectrum characteristic of a black body with a temperature,[15]

$$T = \frac{\hbar}{8\pi k M}, \tag{1.8}$$

where k is the Boltzmann's constant and the entropy of a black hole

is given by,

$$S = \frac{A}{4h}. \tag{1.9}$$

1.3 Evidence for the black holes

So far, there are only indirect evidences for the existence of black holes. To check whether there is a black hole in a region of space, first we have to measure how much mass is present in that region. If we have found a huge mass concentrated in a small volume then there will be a great chance for a black hole. In the search using Hubble Space telescope, it is found that centers of many galaxies including our milky way contain such massive dark objects.[16,17] In the outer parts of galaxies the stars are far apart compared to the central region of galaxies where they are very closely packed together. Thus everything in the central region of the galaxy is tightly packed, a black hole in the center of a galaxy becomes more and more massive, and the stars orbiting the event horizon can ultimately be captured by gravitational attraction and add their mass to the black hole. Matter swirling around a black hole heats up and emits radiation that can be detected.

The instrument inside the Hubble Space Telescope, called the Space Telescope Imaging Spectrograph (STIS) which was installed in February 1997 is the space telescope's main "black hole hunter." Inside STIS, provision is made to split the incoming light into its spectrum and spectrographs having prisms or diffraction gratings are used to analyze the spectrum. The position and strength of the line in a spectrum gives scientists valuable information. The instrumental range of STIS is from ultraviolet to near-infrared wavelengths. So, this instrument can take the spectrum of many places at once across the center of a galaxy and each spectrum tells scientists how fast the stars and gas are swirling at that location. Faster the orbital speeds, the stronger will be the gravitational force required to hold the stars

and gas in their orbits.

These massive dark objects in galactic centers are thought to be black holes for at least two reasons. First, it is hard to think of anything else they could be, because they are too dense and dark, so can't be stars or clusters of stars. Second, the only promising theory to explain the enigmatic objects known as quasars and active galaxies, states that such galaxies have super massive black holes at their cores. If this theory is correct, then a large fraction of galaxies must have super massive black holes at the center. The signature of a super massive black hole in the center of the galaxy, M84, was found by STIS. The spectra showed a rotation velocity of 400 km/s which is equivalent to 1.4 million km every hour! Thus, these arguments strongly suggest that the cores of these galaxies contain black holes, but they are not the absolute proof for the existence of black holes.

1.4 Scattering by black holes

One of the most useful and efficient ways to study the properties of black hole is by scattering matter waves off them.[18] By studying how a black hole interacts with its environment one can hope for receiving information of these invisible objects. These studies will be useful for understanding of the signals expected to be received by the new generation of gravitational-wave detectors in the near future,[19] a most challenging task for modern observational astronomy, and they allow us to make detailed observations of physics in the immediate neighborhood of a black hole.[20] Our interest is in the study of the scattering problems involving black holes. Here, the curvature of space-time enters not only at the level of the boundary conditions, but also in the equations describing the propagation of the various wave-fields such as scalar, electromagnetic or gravitational. In the case of a black hole, scattering was done by the curvature of space-time itself. So we begin our discussion with the simplest of scattering

problems involving black holes such as the bending of light rays due to the strong gravitational field of black hole space-time.

1.4.1 Gravitational lensing

With enhanced astronomical observational capabilities, ranging from large radio telescopes to the Hubble space telescope, astronomers have found plenty of evidences for the deflection of light due to strong gravitational field, to be refereed to as gravitational lensing and it is treated as a powerful tool to probe the universe. The first experimental verification of Einstein theory of general relativity, which also considered as the first black-hole scattering experiment (Figure 1.1), was done by Sir Arthur Eddington in 1919, when light from a distant star was seen to bent by the sun during a total solar eclipse.

In 1979, two quasars 6 seconds of arc apart were discovered and they were found to have identical red shifts and spectra. The probability of this happening by accident is exceedingly small. It was postulated that this pair actually corresponds to the same quasar that is lensed so strongly by intervening mass and its image appears double as we view it from Earth. The first observation of gravitational lensing came from this "Twin Quasar" in Ursa Major constellation and is named as Q0957+561.

In a lensing system[21] there is,

- **a Source**: from where the light comes. The source can be a quasar, a galaxy, etc.
- **Lenses**: the one which deflect the path of light. It may be a galaxy, dark matter or a supermassive black hole.
- **Image**: these are the result of gravitational lensing.

Q2237+030 or QSO 2237+0305 is a gravitationally lensed quasar found in Pegasus constellation is quadruply imaged, hence the name Einstein Cross, forming a nearly perfect cross, with the lensing galaxy

at its center. If the lens were perfectly symmetric with respect to the line between source and observer we would see a ring of images and is called Einstein ring.

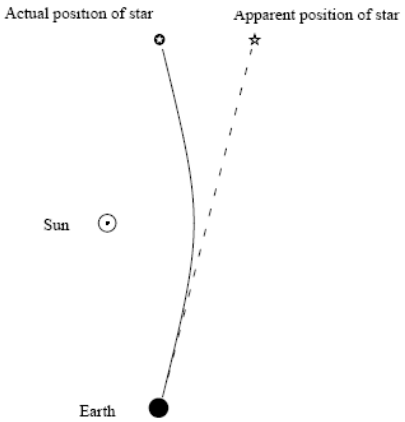

Figure 1.1: The earliest 'black hole scattering' experiment: Defection of starlight by the sun

Since our astronomical observational capability is improving, the list of lensed systems is also growing rapidly. And these new observations provide challenges for the theorists who want to deduce the geometry of the lensing mass distribution as well as to understand the nature of the original light source. Also, one can deduce information about cosmology using lensing observations of distant quasars. Considerable progress in these directions has been made during recent years, and our understanding of the universe should be improving with the observational data.

1.4.2 Wave scattering

The extreme nature of black holes leads to the existence of many complicated diffraction effects. To understand them it is essential to develop a framework for studying the scattering of waves by black holes. To introduce various concepts involving the study of the scat-

tering of waves by black holes, we can consider the relatively simple case of scalar waves. Even though no massless scalar fields have yet been observed in nature, the peculiar choice for this is because the main equations governing a weak electromagnetic field, or gravitational field, in a curved space-time are essentially in the same form as of the scalar field wave equation. Hence, the scalar field serves the purpose.

Scalar field near a spherically symmetric black hole

A massless scalar field Φ evolves according to the Klein-Gordon equation,

$$\frac{1}{\sqrt{-g}}\partial_\kappa\left(\sqrt{-g}g^{\kappa\nu}\partial_\nu\right)\Phi = 0. \tag{1.10}$$

The Schwarzschild line element is:

$$ds^2 = \left(1-\frac{2M}{r}\right)dt^2 - \frac{dr^2}{\left(1-\frac{2M}{r}\right)} - r^2d\theta^2 - r^2\sin^2\theta d\phi^2. \tag{1.11}$$

Since the Schwarzschild metric is spherically symmetric, we can introduce the mode decomposition of Φ as,

$$\Phi_{lm} = \frac{u_l(r,t)}{r}Y_{lm}(\theta,\phi), \tag{1.12}$$

where Y_{lm} are the standard spherical harmonics. The radial part $u_l(r,t)$ satisfy the equation:

$$[\frac{\partial^2}{\partial r_*^2} - \frac{\partial^2}{\partial t^2} - V_l(r)]u_l(r,t) = 0. \tag{1.13}$$

r_* in the above equation refers to the so-called tortoise coordinate which is related to the standard Schwarzschild radial coordinate r by,[22]

$$\frac{d}{dr_*} = (1-\frac{2M}{r})\frac{d}{dr}, \tag{1.14}$$

and integrating the Eq. (1.14) we get,

$$r_* = r + 2M\log(\frac{r}{2M}-1) + C. \tag{1.15}$$

The tortoise coordinate differs from the ordinary radial variable by a logarithmic term. The tortoise coordinate has a special property, i.e., when r is at spatial infinity ($r \to \infty$) r_* is also at infinity ($r_* \to \infty$), but when r is at the event horizon ($r \to 2M$) r_* becomes negative infinity ($r_* \to -\infty$). Thus, the semi-infinite interval $(2M, \infty)$, representing the space-time external to the black hole, is mapped into the infinite interval $(-\infty, \infty)$. In other words "pushing the event horizon of the black hole away to $-\infty$". Now we assume a harmonic time dependence, $u_l(r,t) = \hat{u}_l(r,\omega)\exp^{-\imath\omega t}$, we get an ordinary differential equation from Eq. (1.13) as,

$$[\frac{d^2}{dr_*^2} - \omega^2 - V_l(r)]\hat{u}_l(r,t) = 0, \tag{1.16}$$

which has the same form as was derived by Regge and Wheeler[23] for gravitational perturbations in 1957 and hence, this equation is known as the Regge-Wheeler equation. Here the effective potential can be written as,

$$V_l(r) = 1 - \frac{2M}{r}[\frac{l(l+1)}{r^2} + \frac{2M}{r^3}] \tag{1.17}$$

where M is the mass of the black hole. The effective potential $V_l(r)$ corresponds to a single potential barrier, the maximum of which is at the location of the unstable circular photon orbit (r = 3M) as shown in Figure 1.2. Most of the problems involving perturbed black holes involves familiar elements from potential scattering in quantum mechanics. So, one would expect waves of short wavelength or higher frequency to be easily transmitted through the barrier and waves with low energy will be partly transmitted and partly scattered by the black hole barrier (Figure 1.3).

The scattering problem and governing equations

Let us assume that a plane wave impinges on a black hole. The asymptotic behavior of the resultant field can then be used as a

probe of space-time close to the black hole. The key quantity, that tells us about the effect of the central object on the incident wave, is the scattering amplitude ($f(\theta)$). Since, we are considering massless scalar waves in the Schwarzschild geometry, the scattering amplitude can be extracted from the field at infinity[24]

$$\Phi \sim \Phi_{plane} + \frac{f(\theta)}{r} e^{\imath\omega r_*}, r_* \to \infty. \tag{1.18}$$

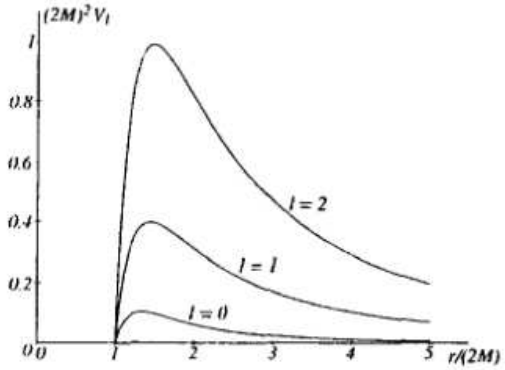

Figure 1.2: The effective potential $V_l(r)$ for $l = 0, 1, 2$ as the function of r

The intensity of the wave scattered into a certain solid angle which is related to the differential cross-section follows from,

$$\frac{d\sigma}{d\Omega} = |f(\theta)|^2 \tag{1.19}$$

where $d\Omega$ is an element of the solid angle. For a massless scalar field, Matzner[25] found the expression for a plane wave at infinity as,

$$\Phi_{plane} \sim \frac{1}{\omega r} \sum_{l=0}^{\infty} \imath^l (2l+1) P_l(\cos\theta) \sin(\omega r_* - \frac{l\pi}{2}), r_* \to \infty \tag{1.20}$$

In scattering theory, it is not only the explicit expressions for the cross section and other scattering parameters are interesting, but

also the general properties satisfied by them. Another phenomenon of obvious importance in black hole scattering is the absorption.

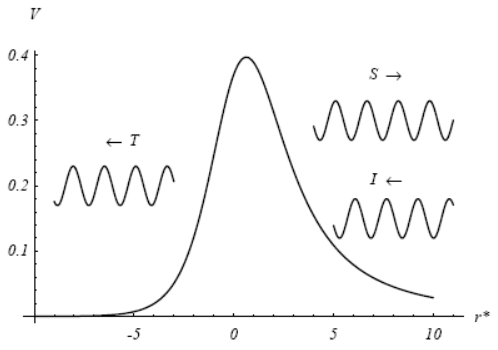

Figure 1.3: The effective potential $V_l(r)$ as the function of r_*. An incident wave I is decomposed into a transmitted component T and a scattered component S

The existence of singularity in a space-time is explicitly related to the presence of non-zero absorption cross section and the expression for total absorption cross-section[26] is given by,

$$\sigma_{abs} = \frac{\pi}{\omega^2} \sum_{l=0}^{\infty} (2l+1)[1 - |S_l|^2] \tag{1.21}$$

where,

$$S_l = (-1)^{l+1} \frac{A_l}{B_l} \exp(2\imath\delta_l), \tag{1.22}$$

A_l represents the amplitude of the incident wave and B_l that of the reflected wave.

1.4.3 Quasi-normal modes

In the early 1970's, numerical investigations of various "physical" scenarios involving black holes were carried out, the basis being the black hole perturbation equations. A black hole can be perturbed in a

variety of ways: wave packets scattering by black holes,[27] small bodies (test particles) falling into - or passing close by - black holes,[28–30] slightly non-spherical gravitational collapse to form a black holes,[31–33] etc. We may expect on general grounds that any initial perturbations will, during its last stages, decay in a manner characteristic of the black hole and independently of the original source. i.e., the black hole oscillates with frequencies and rates of damping, characteristic of itself in the manner of a bell surrounding its last dying notes. The corresponding frequencies are known as the quasi-normal modes of the black hole because they are damped as radiation dissipates to infinity and thus played a dominant role in the evolution of black hole perturbations.

The first indication of this phenomenon was observed by Vishveshwara.[27] He realized that one might be able to observe a solitary black hole by scattering off radiation, provided the black hole left its fingerprint on the scattered wave. So he started pelting the black hole with Gaussian wave packets. By tuning the width of the impinging Gaussian packets Vishveshwara found that the general features of the emitted waves can be divided into three components: First an initial wave burst that contains radiation emitted directly by the source of the perturbation. Second an exponentially damped "ringing" at frequencies that do not depend on the source of the perturbation at all and a power-law "tail" that arises because of backscattering by the long-range gravitational field (Figure 1.4).

1.4.4 Definition and boundary conditions

Mathematically a quasi-normal mode is a formal solution of linearized differential equations (Eq. (1.16)) that satisfy the causal condition of purely ingoing waves crossing the event horizon, while at the same time behaving as purely outgoing waves reaching spatial

infinity. i.e.,

$$\hat{u}_l(r,\omega) \sim \exp(+\imath\omega r_*), r_* \to \infty \tag{1.23}$$

$$\hat{u}_l(r,\omega) \sim \exp(-\imath\omega r_*) r_* \to -\infty \tag{1.24}$$

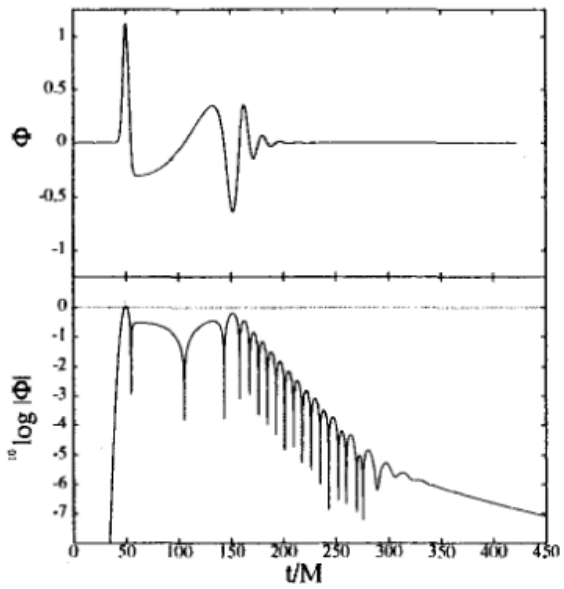

Figure 1.4: The response of a Schwarzschild black hole as a Gaussian wave packet of scalar waves impinges upon it. The first bump (at $t = 50M$) is the initial Gaussian passing by the observer on its way towards the black hole. Quasi-normal-mode ringing clearly dominates the signal after $t \sim 150M$. At very late times (after $t \sim 300M$) the signal is dominated by a power-law fall-off with time.

These are physically motivated boundary conditions. Only, a discrete set of complex frequencies satisfy these boundary conditions. These are the quasi-normal frequencies, and the associated wave functions $\hat{u}_l(r,\omega)$, i.e., the solutions to Eq. (1.16) are the quasi-normal modes (QNMs). If a black hole is to be an astro-physically realistic proposition, solutions to the original wave equation Eq. (1.13) must be damped with time for each value of r_*. Hence, all acceptable

mode solutions to Eq. (1.16) should have $Im\omega < 0$.[34] This means that a quasi-normal mode is distinguished by solutions to the radial equation that grows exponentially as we approach $r_* = \pm\infty$. At spatial infinity the solution is as $u_l(r_*, t) \sim \exp[-\imath\omega(t - r_*)]$, then it is clear that we require solutions that behave as $\exp(-\imath\omega r_*)$ and for $Im\omega < 0$, the solution will diverge as $r_* \to \infty$. In other words, because a mode solution is expected to be damped with time at any fixed value of r_*, it must diverge as $r_* \to \infty$ at any fixed value of t.

Various methods have been implemented to calculate the quasi-normal frequency analytically and numerically. Chandrasekhar and Detweiler[35] have succeeded in finding some of the Schwarzschild QN frequencies numerically in 1975. Thereafter analytical methods have been developed, like WKB technique,[36] later refined to 3rd order,[37,38] and then extended to 6th order[39] and Pöschl-Teller potential method[40] etc to study quasi-normal modes.

1.4.5 Importance of QNMs

The QNMs are crucial for studying the gravitational and electromagnetic perturbations around black hole space-time. They provide valuable help for identifying black hole parameters. Gravitational waves have not yet been detected and is expected to be detected in the near future, with gravitational wave detectors. But the gravitational waves are week and thus for their detection one needs to have a strong source of gravitational waves like stellar collapse or black hole collisions. Numerical simulations have shown that in the final stage of such process, QNMs dominate the black hole response. Thus, these QNMs, seem to have an observational significance in principle, can be used for unambiguous detection of black holes and also about the cosmic string which we are considering. Other motivations to study QNMs are estimating thermalization timescales in connections with the AdS/CFT conjecture and semi-classical attempts to quantize the

black hole area etc.

1.5 Outline of the thesis

This thesis deals with the study of scattering of waves by different black hole space-times. In this study we concentrate to derive the scattering absorption cross sections of different black hole space-times which scatter different types waves. We have also concentrated for obtaining quasi-normal frequencies for various spherically symmetric black hole space-times having cosmic string.

In **Chapter 2**, we have studied the scattering of scalar waves in SdS (Schwarzschild de Sitter) space-time. Radial Klein-Gordon equation is solved in different regions outside the black hole horizon such as in the vicinity of the horizon, sufficiently away from the horizon and at very large distances from the horizon. From the solutions in the 3 regions we find the S-matrix and the absorption cross section for SdS black hole in the low energy limit and studied its dependents on the Hawking temperature. Similar studies are done for RN extremal and SdS extremal space-times also. We have obtained expressions for absorption cross sections of the RN extremal and SdS extremal black holes.

Chapter 3 deals with scattering of charged scalar wave in Reissner-Nordstrom space-time. Here we derive the expression for absorption cross section and find how does it behave when the charge of the RN black hole is increasing. **Chapter 4** describes the scattering of Dirac waves in a Schwarzschild space-time in the low energy limit. The absorption cross section (σ_{abs}) of Schwarzschild black hole in Dirac field for $k = 1$ is found and compared with absorption cross section of Schwarzschild black hole in a scalar field. We also find the absorption cross section for $k = 2$ in Dirac field and plotted emission spectrum for Schwarzschild black hole in Dirac field with and without considering the reflection of waves taking place at the event

horizon.

Chapter 5 gives the influence of cosmic string on the QNMs of various spherical black hole background space-time which are perturbed by a massless Dirac field. Here we have evaluated quasi-normal mode frequencies of Schwarzschild, RN extremal, SdS and near extremal SdS black hole space-times having cosmic string and have studied how the quasi-normal modes are effected by the presence of cosmic string. In **Chapter 6** we study the influence of cosmic string on the QNMs of RN black hole background space-time which are perturbed by positively and negatively charged Dirac fields. QNMs are obtained using the Pöschl-Teller method and compared how the positively charged Dirac field and negatively charged Dirac field decay for the RN black hole with and without cosmic string. The main conclusions of this thesis and future prospects are given in **Chapter 7**.

2

Absorption cross section of SdS, RN extremal and SdS extremal black holes perturbed by scalar fields

2.1 Introduction

A black hole is distinguished by the fact that no information can escape from within the horizon and is believed that they will play a crucial role in the discovery of the laws of a quantum theory of gravity just as the hydrogen atom did in the formulation of quantum mechanics.[41] To obtain a deeper theoretical understanding of these extreme objects, the best method is to study the scattering off waves by them. A considerable effort has taken place in studying the waves scattered off by black holes. Both numerical and analytical methods in solving the various wave equations in black hole scattering have been developed.[18,42] Hawking found, when the laws of quantum field theory is applied, black holes are not truly black. It possesses entropy and temperature and quantum mechanically a black hole with temperature is able to emit radiation, leading to a situation of particle production. When we try to quantize gravitational force, we

have to consider how does quantum mechanics affect the behavior of black holes.

Interest in the absorption of quantum waves by black hole was reignited in the 1970s, following Hawking's discovery that black holes can emit, as well as scatter and absorb radiation.[15] Hawking showed that the evaporation rate is proportional to the total absorption cross section. Unruh[43] found the absorption cross section for massive scalar and Dirac particles scattered off by small non-rotating black holes and Sanchez[44–46] studied the scattering and absorption by black holes for a massless scalar field.

Another quantum effect of interest is that horizons need not be fully absorptive type but can reflect waves falling on it and it is also proposed that the event horizon has a finite energy width. 't Hooft[47] explained the horizon of the black hole as a brick wall so that the black hole horizon r_b spreads into a range of $(r_b - \Delta, r_b + \Delta)$ where $\Delta = \Delta r$. Quantum horizon concepts were introduced by Mu-Lin Yan and Hua Bai.[48] The relevant equation governing a scattering process in a black hole space-time is analogous to the Schrodinger type equations governing scattering phenomena in quantum mechanics. Hence the standard techniques used to study quantum scattering can be used to study scattering problems in black hole space-time.

Recent astronomical observations show that the expansion of our universe is accelerating and our universe may look like de Sitter space-time.[49] Schwarzschild-de Sitter (SdS) black hole described with a positive cosmological constant, having two horizons finds an important place in these types of studies. The size of the black hole is much smaller than that of the cosmological horizon and the radiation coming from the cosmological horizon is negligible compared to that from the black hole horizon. Thus studying the scattering effect of this type of black hole may be of very interesting especially considering the effect near the black hole horizon.

We are also often interested in a different class of black holes -

the extremal one, which is the limiting case of its non-extremal counterpart; when the inner horizon at r_- and outer event horizon r_+ are degenerate, the non-extremal black hole becomes extremal.[50,51] It has been pointed out by many authors[52–56] that at the extremal limit a phase transition and a corresponding scaling law exist. But this traditional viewpoint has been recently challenged by many others.[57–60] Based on an argument of the topological difference between the extremal and the non-extremal Reissner-Nordstrom (RN) black holes, Hawking et al.[57] showed that the entropy of an extremal RN black hole is zero and the formula of Bekenstein-Hawking entropy $S = A/4$, where A is the surface area of the horizon, is not valid and the temperature of the extremal black hole is zero and claimed that the entropy changes discontinuously in the extremal limit. This implies that one should regard non-extremal and extremal black holes as qualitatively different objects. Also what makes an extremal black hole different from a non-extremal black hole have been observed as an area of particular importance in string theory.[61] All these investigations indicate that the entropy and other physical properties are still far from being fully understood in the extremal limit. To clarify this puzzle, it is of importance to study the absorption properties of extremal black holes.

In this chapter we study the scattering off scalar waves in the Schwarzschild-de Sitter, RN extremal and SdS extremal space-time. In section 2.2, we find the absorption cross section for scalar wave scattered off by SdS black hole which depends inversely on the Hawking temperature. Section 2.3 gives an expression for absorption cross section of RN extremal black hole. The absorption cross section of SdS extremal black hole is found in section 2.4 and section 2.5 concludes the chapter.

2.2 Scalar wave on Schwarzschild-de Sitter black hole

The introduction of a non-zero cosmological constant Λ in general relativity, made possible study of black holes known as Schwarzschild-de Sitter black holes which are described by the static and neutral solutions of Einstein-Hilbert action with a positive cosmological constant. The metric of SdS space-time is given by,

$$ds^2 = -f dt^2 + f dr^2 + r^2(d\theta^2 + \sin^2\theta d\varphi^2), \tag{2.1}$$

where

$$f = 1 - \frac{2M}{r} - \frac{r^2}{a^2} = \frac{1}{ra^2}\left(ra^2 - 2Ma^2 - r^3\right), \tag{2.2}$$

with M, denoting the black hole mass and $a^2 = \frac{3}{\Lambda}$, Λ being the cosmological constant. The space-time possesses two horizons: the black hole horizon at $r = r_b$ and the cosmological horizon at $r = r_c$, where $r_c >> r_b$. The function f becomes zero at r_b and r_c and let us put $r_0 = -(r_b + r_c)$. In terms of these quantities we can express f as,

$$f = \frac{1}{a^2 r}(r - r_b)(r_c - r)(r - r_0). \tag{2.3}$$

Expressing M and a^2 as functions of two SdS parameters r_b and r_c, we find :

$$(r - r_b)(r_c - r)(r - r_0) = \left(ra^2 - 2Ma^2 - r^3\right). \tag{2.4}$$

From this, it follows that $r_0 = -(r_b + r_c)$ and,

$$a^2 = r_b^2 + r_c^2 + r_b r_c, \tag{2.5}$$

$$2Ma^2 = r_b r_c (r_b + r_c). \tag{2.6}$$

The action for a massive scalar field in this background is

$$I = \frac{1}{2}\int d^4x\sqrt{-g}\left(g^{\kappa\nu}\partial_\kappa\Psi\partial_\nu\Psi - \mu^2\Psi^2\right). \tag{2.7}$$

Varying the action with Φ we get the equation of motion as

$$\left[\frac{1}{\sqrt{-g}}\partial_\kappa\left(\sqrt{-g}g^{\kappa\nu}\partial_\nu\right)+\mu^2\right]\Psi=0. \tag{2.8}$$

Here μ is the mass of the scalar field. Using spherical polar coordinates this equation can be written as,

$$\begin{aligned}\Bigg[\frac{a^2r}{ra^2-2Ma^2-r^3}\frac{\partial^2}{\partial t^2}-\frac{1}{r^2}\frac{\partial}{\partial r}\left(\frac{r}{a^2}\left(ra^2-2Ma^2-r^3\right)\right)\frac{\partial}{\partial r} \\ -\frac{1}{r^2\sin\theta}\frac{\partial}{\partial\theta}\sin\theta\frac{\partial}{\partial\theta}-\frac{1}{r^2\sin^2\theta}\frac{\partial^2}{\partial\phi^2}+\mu^2\Bigg]\Psi\left(r,\theta\,\phi,t\right)=0,\end{aligned} \tag{2.9}$$

The wave function can be separated out as,

$$\Psi\left(r,t\right)=\exp\left(-\imath\epsilon t\right)Y_{lm}\left(\theta,\phi\right)\Phi_l(r), \tag{2.10}$$

where ϵ, l, m represents energy, angular momentum and its projection respectively, while $\Phi_l(r)$ is the radial function. The radial wave equation will be,

$$\begin{aligned}[\frac{1}{r^2}\frac{\partial}{\partial r}(\frac{r}{a^2}(ra^2-2Ma^2-r^3))\frac{\partial}{\partial r}+\frac{ra^2\epsilon^2}{ra^2-2Ma^2-r^3}- \\ \frac{l(l+1)}{r^2}-\mu^2]\Phi_l(r)=0.\end{aligned} \tag{2.11}$$

Now we will solve the above radial equation in different regions outside the black hole horizon.[43]

2.2.1 Solution of wave equation in the vicinity of black hole horizon: $r \to r_b$ (region 1)

In this region, we use WKB approximation to solve the radial wave equation. We assume that the reflection of scalar waves from the horizon can take place. Reflection from the horizon means that there is a finite probability for a particle approaching the vicinity of horizon to be reflected back to the outside world. Knowing reflection coefficient we can find Hawking temperature of SdS black hole. Using the WKB approximation we can write $\Phi_l(r)=\exp^{-\imath\int k(r)dr}$, we have

the radial wave number $k(r,l,\varepsilon)$ from the corresponding equation of motion, as:

$$\left(\frac{\epsilon^2}{\left(1-\frac{2M}{r}-\frac{r^2}{a^2}\right)}-\frac{l\,(l+1)}{r^2}+\mu^2\right)+\left(-k^2\left(1-\frac{2M}{r}-\frac{r^2}{a^2}\right)\right)=0. \tag{2.12}$$

Therefore,

$$k^2(r,l,\epsilon)=(1-\frac{2M}{r}-\frac{r^2}{a^2})^{-1}\left[\frac{\epsilon^2}{(1-\frac{2M}{r}-\frac{r^2}{a^2})}-\frac{l(l+1)}{r^2}+\mu^2\right]. \tag{2.13}$$

Using Eq. (2.4) we can write

$$k\,(r)=\pm\left[\epsilon^2-\left(\frac{l(l+1)}{r^2}-\mu^2\right)\left(\frac{1}{a^2r}\,(r-r_b)\,(r_c-r)\,(r-r_0)\right)\right]^{\frac{1}{2}} \frac{ra^2}{(r-r_b)\,(r_c-r)\,(r-r_0)}. \tag{2.14}$$

In the region $r\to r_b$,

$$k(r\to r_b)=\pm\frac{\epsilon r_b a^2}{(r-r_b)(r_c-r_b)(r_b-r_0)}=\pm\frac{\xi}{(r-r_b)}, \tag{2.15}$$

where

$$\xi=\frac{\epsilon r_b a^2}{(r_c-r_b)(r_b-r_0)}. \tag{2.16}$$

Therefore the wave function in the region $r\to r_b$ can be written as

$$\Phi_l(r)=\exp^{\mp\imath\int\frac{\xi}{r-r_b}dr}=\exp^{\mp\imath\xi\ln(r-r_b)}, \tag{2.17}$$

i.e.,

$$\Phi_l(r)\propto\exp(\mp\imath\xi\ln(r-r_b)). \tag{2.18}$$

Using Eq. (2.18), the wave function in the vicinity of horizon can be written, assuming that the wave gets reflected at the horizon, as

$$\Phi_l\,(r)=\exp\left(-\imath\xi\ln\left(r-r_b\right)\right)+\mid R\mid\exp\left(+\imath\xi\ln\left(r-r_b\right)\right), \tag{2.19}$$

where R represents the reflection coefficient and the solution represents the interference between the incident and reflected waves. If

$R \neq 0$, there is a definite probability for the incident waves to get reflected on the horizon. Since the wave function is singular at $r = r_b$, we need not consider the events that take place on the black hole horizon $r = r_b$. We now consider a point distant $z = r - r_b$, from the horizon and treat z as a complex variable. The above wave function is analytic in z, except at $z = 0$ which induces a cut emerging from this point on the complex plane z. Let us take r outside black hole horizon, but close to the vicinity of black hole horizon, which means, $0 < z \ll 1$. Now rotate z in the complex z plane over an angle 2π clockwise and examine what happens to the wave function. The validity of semiclassical wave function is justified by keeping $\mid z \mid \ll 1$. This analytical continuation necessarily incorporates a crossing of the cut on the complex plane. Therefore, after finishing this rotation and returning to a real physical value $z > 0$, the wave function acquires a new value on its Riemannian surface. Let it be $\Phi_l^{2\pi}(r)$. Then,

$$\Phi_l^{2\pi}(r) = \rho \exp\left(-\imath\xi \ln\left(r - r_b\right)\right) + \frac{\mid R \mid}{\rho} \exp\left(+\imath\xi \ln\left(r - r_b\right)\right), \quad (2.20)$$

where $\rho = \exp\left(-2\pi\xi\right)$. The analytically continued function $\Phi_l^{2\pi}(r)$ satisfies the same radial differential equation as the initial wave function $\Phi_l(r)$. And one has to expect that $\Phi_l^{2\pi}(r)$ must satisfy the same normalization condition as the initial wave function $\Phi_l(r)$. This implies that one of the coefficients, either ρ or $\frac{|R|}{\rho}$ should have an absolute value equal to unity. Since $\rho < 1$, we deduce that $\frac{|R|}{\rho} = 1$, thus $R = \exp\left(-2\pi\xi\right)$. We see that reflection coefficient is non-zero. In other words black hole horizon is capable of reflection. i.e., reflection from the horizon takes place.

Hawking temperature of Schwarzschild-de Sitter black hole

Using the interesting phenomena of reflection from the horizon we obtain Hawking temperature of the black hole as a byproduct. The

probability of reflection from the horizon can be found as $P = |R|^2 = \exp(-4\pi\xi)$, which depends on the black hole temperature T as $P = \exp\left(-\frac{\epsilon}{T}\right)$, where ϵ is the energy of the particles.[62] Thus we find

$$\frac{\epsilon}{T} = 4\pi\xi = \frac{4\pi\epsilon r_b a^2}{(r_c - r_b)(r_b - r_0)}, \tag{2.21}$$

therefore,

$$T = \frac{(r_c - r_b)(r_b - r_0)}{4\pi r_b a^2}. \tag{2.22}$$

This gives the Hawking temperature of the SdS black hole which agrees with standard result.[63]

2.2.2 Solution of wave equation in the intermediate region: $r > r_b$ (region 2)

This region is sufficiently away from r_b but not very far away from r_b. In the radial equation, the terms in ϵ^2 and μ^2 are much smaller than all other terms. Thus we neglect the low energy and momentum terms in the radial equation and hence Eq. (2.11) now takes the form, for the s wave:

$$\Phi_0''(r) + \left(\frac{2ra^2 - 2Ma^2 - 4r^3}{r(ra^2 - 2Ma^2 - r^3)}\right)\Phi_0'(r) = 0. \tag{2.23}$$

Therefore,

$$\ln \Phi_0'(r) = -\ln r\left(ra^2 - 2Ma^2 - r^3\right) + \ln C, \tag{2.24}$$

can be written as

$$\Phi_0'(r) = \frac{C}{r(ra^2 - 2Ma^2 - r^3)} = \frac{C}{r}\left(\frac{A_1}{(r - r_b)} + \frac{B_1}{(r_c - r)} + \frac{C_1}{(r - r_0)}\right), \tag{2.25}$$

where $A_1 = \frac{1}{a^2 - 3r_b^2}$, $B_1 = \frac{1}{3r_c^2 - a^2}$, $C_1 = \frac{1}{a^2 - 3r_0^2}$. In this region we are far away from r_c and hence the effect of r_c can be neglected. Thus we get,

$$\Phi_0(r) = \int \frac{K}{r(r - r_b)} dr + C_1. \tag{2.26}$$

But,

$$\int \frac{dr}{r\,(r-r_b)} = \frac{1}{r_b}\ln\frac{(r-r_b)}{r} + C_2. \tag{2.27}$$

Thus,

$$\Phi_0(r) = \alpha \ln\frac{(r-r_b)}{r} + \beta, \tag{2.28}$$

represents the wave function in the intermediate region and α and β are the constant of integration.

Comparing solutions of regions 1 and 2

Now we compare solutions given by Eqs. (2.19) and (2.28) in region 1 and 2 at the boundary. We can expand Eq. (2.19) as $\exp(\mp\imath\xi\ln(r-r_b)) \simeq 1 \mp \imath\xi\ln(r-r_b)$ and Eq. (2.19) becomes,

$$\Phi_0(r) = 1 - \imath\xi\ln(r-r_b) + \mid R \mid (1 + \imath\xi\ln(r-r_b)), \tag{2.29}$$

i.e.,

$$\Phi_0(r) = -\imath\xi\,(1- \mid R \mid)\ln(r-r_b) + (1+ \mid R \mid). \tag{2.30}$$

And using the asymptotic relation $\ln\frac{(r-r_b)}{r} \simeq \ln(r-r_b)$ Eq. (2.28) can be written as,

$$\Phi_0(r) = \alpha\ln(r-r_b) + \beta. \tag{2.31}$$

Equating the coefficients of Eq. (2.31) and Eq. (2.30) we get,

$$\alpha = -\imath\xi\,(1- \mid R \mid),\ \beta = (1+ \mid R \mid). \tag{2.32}$$

Thus, we can express α and β in terms of reflection coefficient $|R|$.

2.2.3 Solution of the wave equation at far away from the horizon: $r >> r_b$ (region 3)

In this region we can rearrange the radial equation as,

$$\Phi_l''(r)+(\frac{a^2}{ra^2-2Ma^2-r^3}+\frac{1}{r}-\frac{3r^2}{ra^2-2Ma^2-r^3})\Phi_l'(r)+ \quad (2.33)$$
$$(\frac{\epsilon^2a^4r^2}{(ra^2-2Ma^2-r^3)^2}-\frac{\mu^2ra^2}{ra^2-2Ma^2-r^3}-$$
$$\frac{l(l+1)a^2}{r(ra^2-2Ma^2-r^3)})\Phi_l(r)=0.$$

The above equation can be simplified using partial fraction method. i.e.,

$$\frac{a^2-3r^2}{ra^2-2Ma^2-r^3}=\frac{a^2-3r^2}{(r-r_b)(r_c-r)(r-r_0)}= \quad (2.34)$$
$$\frac{K_1}{(r-r_b)}+\frac{K_2}{(r_c-r)}+\frac{K_3}{(r-r_0)}.$$

From the Eq. (2.34) we find,

$$a^2-3r^2=K_1(r_c-r)(r-r_0)+K_2(r-r_b)(r-r_0)+ \quad (2.35)$$
$$K_3(r-r_b)(r_c-r).$$

Therefore,

$$K_1=\frac{a^2-3r_b^2}{(r_c-r_b)(r_b-r_0)}, \quad (2.36)$$

$$K_2=\frac{a^2-3r_c^2}{(r_c-r_b)(r_c-r_0)}, \quad (2.37)$$

$$K_3=\frac{a^2-3r_0^2}{(r_0-r_b)(r_c-r_0)}. \quad (2.38)$$

We know that $r_0=-(r_b+r_c)$. Thus we obtain $(r_c-r_b)(r_b-r_0)=a^2-3r_b^2$, $(r_c-r_b)(r_c-r_0)=3r_c^2-a^2$ and $(r_0-r_b)(r_c-r_0)=a^2-3(r_b+r_c)^2$. i.e., $K_1=1$, $K_2=-1$ and $K_3=1$. Thus Eq. (2.34) becomes,

$$\frac{a^2-3r^2}{ra^2-2Ma^2-r^3}=\frac{1}{(r-r_b)}+\frac{1}{(r-r_c)}+\frac{1}{(r-r_0)}, \quad (2.39)$$

and the energy and momentum terms in Eq. (2.33) can be written as,

$$\frac{\epsilon^2 a^4 r^2}{(ra^2 - 2Ma^2 - r^3)^2} - \frac{\mu^2 r a^2}{ra^2 - 2Ma^2 - r^3} = \epsilon^2 - \mu^2 + \frac{(2\epsilon^2 - \mu^2)2Ma^2}{ra^2 - 2Ma^2 - r^3} = p^2 + \frac{(\epsilon^2 + p^2)2Ma^2}{ra^2 - 2Ma^2 - r^3}, \tag{2.40}$$

where $p^2 = \epsilon^2 - \mu^2$ is the momentum at infinity. R.H.S of Eq. (2.40) can be written as,

$$p^2 + \frac{(\epsilon^2 + p^2)2Ma^2}{ra^2 - 2Ma^2 - r^3} = p^2 + (\epsilon^2 + p^2)2M(\frac{A}{(r - r_b)} + \frac{B}{(r_c - r)} + \frac{C}{(r - r_0)}). \tag{2.41}$$

Similarly, we can find,

$$\frac{l(l+1)a^2}{ra^2 - 2Ma^2 - r^3} = \frac{l\,(l+1)}{r}\left(\frac{A}{(r - r_b)} + \frac{B}{(r_c - r)} + \frac{C}{(r - r_0)}\right). \tag{2.42}$$

Thus Eq. (2.33) becomes,

$$\Phi_l''(r) + (\frac{1}{(r - r_b)} + \frac{1}{(r - r_c)} + \frac{1}{(r - r_0)} + \frac{1}{r})\Phi_l'(r) + [p^2 + (\epsilon^2 + p^2)2M(\frac{A}{(r - r_b)} + \frac{B}{(r_c - r)} + \frac{C}{(r - r_0)}) + \frac{l(l+1)}{r}(\frac{A}{(r - r_b)} + \frac{B}{(r_c - r)} + \frac{C}{(r - r_0)})]\Phi_l(r) = 0, \tag{2.43}$$

where $A = \frac{a^2}{a^2 - 3r_b^2}$, $B = \frac{a^2}{3r_c^2 - a^2}$, $C = \frac{a^2}{a^2 - 3r_0^2}$. Let us describe with the help of Eq. (2.43), the scattering of the scalar wave by SdS black hole in the region 3, ($r \gg r_b$). At very large distances, the terms in Eq. (2.43) can be written as

$$\frac{A}{(r - r_b)} + \frac{B}{(r_c - r)} + \frac{C}{(r - r_0)} = \frac{(A - B + C)}{r}, \tag{2.44}$$

but

$$A - B + C = \frac{a^2}{a^2 - 3r_b^2} - \frac{a^2}{3r_c^2 - a^2} + \frac{a^2}{a^2 - 3r_0^2} = \frac{a^2 Q}{P}, \tag{2.45}$$

where

$$Q = (3r_c^2 - a^2)(a^2 - 3r_0^2) - (a^2 - 3r_b^2)(a^2 - 3r_0^2) + (a^2 - 3r_b^2)(3r_c^2 - a^2), \tag{2.46}$$

and

$$P = \left(a^2 - 3r_b^2\right)\left(3r_c^2 - a^2\right)\left(a^2 - 3r_0^2\right). \tag{2.47}$$

Using Eq. (2.5) we find that $Q = 0$. Since $r_c \gg r_b$, $r \gg r_b$ we can approximate the coefficient of $\Phi_l'(r)$ as $\frac{2}{r}$. Thus Eq. (2.43) at very large distances becomes,

$$\Phi_l''(r) + \frac{2}{r}\Phi_l'(r) + p^2\Phi_l(r) = 0. \tag{2.48}$$

Solution of Eq. (2.48) is written as a combination of $\sin z$ and $\cos z$ using Frobenius method. Thus the solution can be written as

$$\Phi_l(r) = \frac{1}{r}\left(A_l \exp(\imath z) + B_l \exp(-\imath z)\right), \tag{2.49}$$

where $z = pr$. Here the wave function can be written as a combination of two function $F(r)$ and $G(r)$. Therefore

$$\Phi_l(r) = \frac{1}{r}\left(aF(r) + bG(r)\right), \tag{2.50}$$

but by comparing this with the solution obtained using Frobenius method, we know that $F(r) = \sin pr$ and $G(r) = \cos pr$.

Comparing solutions of regions 2 and 3

This is the boundary between regions 2 and 3. On the other hand, since ϵ is low we can assume $pr \ll 1$ and thus

$$F(r) \simeq pr\,,\ G(r) \simeq 1. \tag{2.51}$$

Thus in the asymptotic region, Eq. (2.50) for the s-wave will become,

$$\Phi_0(r) = ap + \frac{b}{r}. \tag{2.52}$$

For the wave function in region 2, taking $r >> r_b$ Eq. (2.28) becomes,

$$\Phi_0(r) = \alpha \ln\left(1 - \frac{r_b}{r}\right) + \beta, \tag{2.53}$$

but $\ln\left(1 - \frac{r_b}{r}\right) = -\frac{r_b}{r}$, therefore

$$\Phi_0(r) = -\frac{\alpha r_b}{r} + \beta. \tag{2.54}$$

Using Eq. (2.32), Eq. (2.54) becomes,

$$\Phi_0(r) = (1+ \mid R \mid) + \frac{\imath\xi\,(1- \mid R \mid)\, r_b}{r}. \tag{2.55}$$

Thus,

$$a = \frac{(1+ \mid R \mid)}{p},\; b = \imath\xi\,(1- \mid R \mid)\, r_b, \tag{2.56}$$

which is obtained by comparing Eq. (2.52) and Eq. (2.55).

2.2.4 Absorption cross section

Now we calculate the S matrix element, which is given by the ratio of the coefficients of the incoming and outgoing waves. Thus,

$$S_l = (-1)^{l+1}\, \frac{A_l}{B_l} \exp\left(2\imath\partial_l\right). \tag{2.57}$$

We find that, the reflection coefficient $R = \exp(-2\pi\xi)$ decreases exponentially with energy and thus we will consider first the low energy case, i.e., $\epsilon \ll 1$, where reflection from the horizon is prominent and restricted to $l = 0$ and denote s wave as $\Phi_0\,(r)$. In the asymptotic region, $r \to \infty$, we obtain $F\,(r) = \sin z$, $G\,(r) = \cos z$, where $z = pr$. Thus comparing Eq. (2.50) with Eq. (2.49) for $l = 0$ case, we obtain the coefficients A_0, B_0 as,

$$A_0 = \frac{a + \imath b}{2\imath},\; B_0 = \frac{-a + \imath b}{2\imath}. \tag{2.58}$$

Using Eq. (2.56) we get,

$$A_0 = \frac{[1+ \mid R \mid -\xi p\,(1- \mid R \mid)\, r_b]}{2\imath p}, \tag{2.59}$$

$$B_0 = -\frac{[1+\mid R \mid +\xi p\,(1-\mid R \mid) r_b]}{2\imath p}. \tag{2.60}$$

The S-matrix from Eq. (2.57) for the s-wave is given by,

$$S_0 = \frac{1+\mid R \mid -\xi p\,(1-\mid R \mid) r_b}{1+\mid R \mid +\xi p\,(1-\mid R \mid) r_b} \exp\left(2\imath\partial_l\right), \tag{2.61}$$

$$= \frac{1-\xi p r_b \eta}{1+\xi p r_b \eta} \exp\left(2\imath\partial_l\right), \tag{2.62}$$

where,

$$\eta = \frac{1-\mid R \mid}{1+\mid R \mid}. \tag{2.63}$$

The absorption cross section in the low energy limit is given by,[26]

$$\sigma_{abs} = \frac{\pi}{p^2}\left(1-\mid S_o \mid^2\right) = \frac{\pi}{p^2}\frac{4\xi p r_b \eta}{\left(1+\xi p r_b \eta\right)^2}. \tag{2.64}$$

From Eq. (2.16) and putting $p = \epsilon v$, we can write Eq. (2.64) as,

$$\sigma_{abs} = \frac{1}{v}\frac{4\pi r_b a^2}{\left(r_c - r_b\right)\left(r_b - r_0\right)}\frac{r_b\eta}{\left(1+\xi p r_b\eta\right)^2} = \frac{1}{vT}\frac{r_b\eta}{\left(1+\frac{\epsilon^2 v r_b \eta}{4\pi T}\right)^2}. \tag{2.65}$$

Thus we get total absorption cross section for s-wave scattering in the low energy limit for a Schwarzschild-de Sitter black hole and we see that it depends inversely on Hawking temperature. Let us substitute $T = \frac{1}{4\pi r_g}$, $\eta = \frac{1-R}{1+R}$, and we take reflection coefficient as zero , i.e., $R = 0$, which is the classical point of view and also $r_b = r_g$ which corresponds to Schwarzschild black hole,[64] in Eq. (2.65); and r_g is equal to $2GM$. Thus we find,

$$\eta = \frac{1-R}{1+R} = 1. \tag{2.66}$$

Therefore,

$$\sigma_{abs} = \frac{1}{v}\frac{4\pi r_g^2}{\left(1+\epsilon^2 v r_g^2\right)^2} \simeq \frac{4\pi r_g^2}{v} = \frac{16\pi M^2}{v}, \tag{2.67}$$

which agrees with the results of Unruh.[43] If we are taking the effect of reflection we have,

$$R = \exp(-2\pi\xi), \tag{2.68}$$

for $a^2 = 0$, we can write

$$R = \exp(-2\pi\epsilon r_b). \tag{2.69}$$

Therefore,

$$\eta = \frac{1 - \exp(-2\pi\epsilon r_b)}{1 + \exp(-2\pi\epsilon r_b)} = \tanh \pi\epsilon r_b \simeq \pi\epsilon r_b, \tag{2.70}$$

and the absorption cross section for Schwarzschild black hole is given by,

$$\sigma_{abs} = \frac{4\pi r_b^2 \eta}{v\left(1 + \xi p r_b\right)^2} \simeq \frac{4\pi^2 \epsilon r_b^3}{v}, \tag{2.71}$$

which agrees with the result obtained earlier.[64]

2.3 RN black hole - Extremal case

The Reissner-Nordstrom (RN) black hole's (event and inner) horizons are given in terms of the black hole parameters, by $r_\pm = M \pm \sqrt{M^2 - Q^2}$ where M and Q are respectively mass and charge of the black hole. In extreme case these two horizons coincide, when, $M = Q$, and then $r_\pm = M = r_0$. So the metric for RN extremal black hole is given by,

$$ds^2 = \left(1 - \frac{r_o}{r}\right)^2 dt^2 - \frac{1}{\left(1 - \frac{r_o}{r}\right)^2} dr^2 - r^2\left(d\theta^2 + \sin^2\theta d\phi^2\right). \tag{2.72}$$

Klein-Gordon equation in the present case,

$$\begin{aligned}[\frac{1}{(1 - \frac{r_o}{r})^2}\frac{\partial^2}{\partial t^2} - \frac{1}{r^2}\frac{\partial}{\partial r}(r - r_0)^2\frac{\partial}{\partial r} - \frac{1}{r^2\sin\theta}\frac{\partial}{\partial\theta}\sin\theta\frac{\partial}{\partial\theta} \\ -\frac{1}{r^2\sin^2\theta}\frac{\partial^2}{\partial\phi^2} + \mu^2]\Phi(r,\theta,\phi,t) = 0.\end{aligned} \tag{2.73}$$

Separating the wave functions into radial and angular parts: ,

$$\Psi\left(r,\theta,\phi,t\right) = \exp\left(-\imath\epsilon t\right) Y_{lm}\left(\theta,\phi\right)\Phi_l(r), \tag{2.74}$$

where ϵ, l, m are energy, momentum and its projection. Substituting Eq. (2.74) in Eq. (2.73) we get,

$$\Phi_l''(r)+\frac{2}{r-r_0}\Phi_l'(r)+\left(\frac{\epsilon^2 r^4}{(r-r_0)^4}-\frac{\mu^2 r^2}{(r-r_0)^2}-\frac{l\,(l+1)}{(r-r_0)^2}\right)\Phi_l(r)=0. \tag{2.75}$$

To study the scattering problem, we divide the space-time into 3 regions as is done in the case of SdS black hole. We start the three different regions starting from the horizon as given below.

2.3.1 Solution of wave equation in the region 1: $r \to r_0$

Now we solve the wave equation in the vicinity of horizon, i.e., as $r \to r_0$ and using the WKB approximation; $\Phi_l(r) = \exp^{-\imath \int k(r)dr}$, in Eq. (2.75) we find,

$$k\,(r)=\pm\left[\epsilon^2-\left(\frac{L^2}{r^2}-\mu^2\right)\left(1-\frac{r_0}{r}\right)^2\right]^{\frac{1}{2}}\frac{r^2}{(r-r_0)^2}. \tag{2.76}$$

Thus, near the horizon, i.e., as $r \to r_0$,

$$k\,(r\to r_0)=\pm\frac{\epsilon r_0^2}{(r-r_0)^2}. \tag{2.77}$$

Therefore, the wave function in the region $r \to r_b$ can be written as,

$$\Phi_l(r)=\exp^{\mp\imath\int\frac{\epsilon r_0^2 dr}{(r-r_0)^2}}=\exp\left(\mp\imath\frac{\epsilon r_0^2}{r_0-r}\right), \tag{2.78}$$

i.e.,

$$\Phi_l\,(r)=\exp\left(\mp\imath\frac{\epsilon r_0^2}{r_0-r}\right). \tag{2.79}$$

Let us describe the radial motion with the help of the wave function $\Phi_l\,(r)$. Using Eq. (2.78), the wave function in the vicinity of the horizon can be written:

$$\Phi_l\,(r)=\exp\left(-\imath\frac{\epsilon r_0^2}{r_0-r}\right)+\mid R\mid\exp\left(+\imath\frac{\epsilon r_0^2}{r_0-r}\right), \tag{2.80}$$

where we have assumed that the wave gets reflected at the horizon and having a reflection coefficient $|R|$.

2.3.2 Solution of wave equation in the region 2: $r > r_0$

As in SdS case, this region is also considered as sufficiently away from the horizon, but not very far away from $r = r_0$. Thus assuming the terms in energy and momentum in Eq. (2.75) are very small compared to others, the equation can be reduced for the s wave as:

$$\Phi_0''(r) + \frac{2}{r - r_0}\Phi_0'(r) = 0. \tag{2.81}$$

Therefore,

$$\Phi_0'(r) = \frac{C}{(r - r_0)^2}, \tag{2.82}$$

where C is the constant of integration. Thus the wave function will be of the form,

$$\Phi_0(r) = -\frac{\alpha}{(r - r_0)} + \beta, \tag{2.83}$$

where we have to determine α and β.

Comparing solutions of regions 1 and 2

Here, we compare the wave functions in regions 1 and 2. Eq. (2.80) can be written for s wave as,

$$\Phi_0(r) = 1 - \imath\frac{\epsilon r_0^2}{r_0 - r} + \mid R \mid (1 + \imath\frac{\epsilon r_0^2}{r_0 - r}) = 1 + \mid R \mid + \frac{(1 - \mid R \mid)\imath\epsilon r_0^2}{r - r_0}. \tag{2.84}$$

Comparing wave functions in regions 1 and 2 (Eqs. (2.84) & (2.83)),

$$\alpha = -(1 - \mid R \mid)\imath\epsilon r_0^2,\ \beta = 1 + \mid R \mid, \tag{2.85}$$

are obtained by matching the solutions at the boundary.

2.3.3 Solution of wave equation in the region 3: $r >> r_0$

This region is very far away from the horizon. Since r is very large, we rewrite terms containing energy and momentum in Eq. (2.75) as,

$$\frac{\epsilon^2 r^4}{(r - r_0)^4} = \epsilon^2 + \frac{4\epsilon^2 r_0}{r - r_0} + \frac{4\epsilon^2 r_0^2}{(r - r_0)^2} + \frac{\epsilon^2 r_0^2 (r + r_0)}{(r - r_0)^3} + \frac{\epsilon^2 r_0^2 r^2}{(r - r_0)^4}, \tag{2.86}$$

and

$$\frac{\mu^2 r^2}{(r-r_0)^2} = \mu^2 + \frac{2\mu^2 r_0}{(r-r_0)} + \frac{\mu^2 r_0^2}{(r-r_0)^2}. \tag{2.87}$$

Thus,

$$\frac{\epsilon^2 r^4}{(r-r_0)^4} - \frac{\mu^2 r^2}{(r-r_0)^2} = \epsilon^2 - \mu^2 + \frac{(2\epsilon^2-\mu^2)2r_0}{r-r_0} + \frac{(4\epsilon^2-\mu^2)r_0^2}{(r-r_0)^2} + \frac{\epsilon^2 r_0^2(r+r_0)}{(r-r_0)^3} + \frac{\epsilon^2 r_0^2 r^2}{(r-r_0)^4}$$

$$= p^2 + \frac{(p^2+\epsilon^2)2r_0}{r-r_0} + \frac{(p^2+3\epsilon^2)r_0^2}{(r-r_0)^2} + \frac{\epsilon^2 r_0^2(r+r_0)}{(r-r_0)^3} + \frac{\epsilon^2 r_0^2 r^2}{(r-r_0)^4}, \tag{2.88}$$

where $p^2 = \epsilon^2 - \mu^2$. Substituting Eq. (2.88) in Eq. (2.75) we get,

$$\Phi_l''(r) + \frac{2}{r-r_0}\Phi_l'(r) + (p^2 + \frac{(p^2+\epsilon^2)2r_0}{r-r_0} + \frac{(p^2+3\epsilon^2)r_0^2}{(r-r_0)^2} + \frac{\epsilon^2 r_0^2(r+r_0)}{(r-r_0)^3} + \frac{\epsilon^2 r_0^2 r^2}{(r-r_0)^4} - \frac{l(l+1)}{(r-r_0)^2})\Phi_l(r) = 0. \tag{2.89}$$

At $r \gg r_0$ we get,

$$\Phi_l''(r) + \frac{2}{r}\Phi_l'(r) + \left(p^2 + \frac{\left(p^2+\epsilon^2\right)2r_0}{r} - \frac{l\,(l+1)}{r^2}\right)\Phi_l(r) = 0. \tag{2.90}$$

Treating this equation as a Coulomb problem with Coulomb charge $Z = \left(p^2+\epsilon^2\right) r_0$ then, solution to this equation can be written as,

$$\Phi_l(r) = \frac{1}{r}\left(A_l \exp\left(\imath z\right) + B_l \exp\left(-\imath z\right)\right), \tag{2.91}$$

where $z = pr - \frac{l\pi}{2} + \nu \ln 2pr + \delta_t^{(c)}$, $\delta_t^{(c)} = \arg\Gamma\left(l+1-\nu\right)$ and $\nu = \frac{Z}{p}$. Introducing regular $F\left(r\right)$ and singular $G\left(r\right)$ solution of Coulomb problem, one can present the wave function as a linear combination:

$$\Phi_l(r) = \frac{1}{r}\left(aF_l\left(r\right) + bG_l\left(r\right)\right). \tag{2.92}$$

In the asymptotic limit, $r \to \infty$, the Coulomb functions takes the forms, $F_l(r) = \sin z$, $G_l(r) = \cos z$ where $z = pr - \frac{l\pi}{2} + \nu \ln 2pr + \delta_t^{(c)}$, thus Eq. (2.92) will be in the form:

$$\Phi_l(r) = \frac{1}{r}(a \sin z + b \cos z), \tag{2.93}$$

But we know that for l=0,[26]

$$F_0(r) = cpr\,,\; G_0(r) = \frac{1}{c}, \tag{2.94}$$

where,

$$c^2 = \frac{2\pi\nu}{1 - 2\pi\nu}. \tag{2.95}$$

Thus, Eq. (2.92) for s wave becomes,

$$\Phi_0(r) = acp + \frac{b}{cr}, \tag{2.96}$$

where a and b are obtained by comparing the wave functions in the regions 2 and 3.

Comparing the solutions in regions 2 and 3

Neglecting higher powers of $\frac{1}{r}$, Eq. (2.83) can be written as,

$$\Phi_0(r) = -\frac{\alpha}{r\left(1 - \frac{r_0}{r}\right)} + \beta \simeq -\frac{\alpha}{r} + \beta, \tag{2.97}$$

and using Eq. (2.96), Eq. (2.97) and Eq. (2.85) we get,

$$a = \frac{1 + \mid R \mid}{pc}, b = (1 - \mid R \mid)\, \imath\epsilon r_0^2 c. \tag{2.98}$$

Eq. (2.98) gives a and b in terms of reflection coefficient $|R|$.

2.3.4 Absorption cross section of RN extremal black hole

Eq. (2.91) represents the incoming and outgoing waves. Here also we limit to low energy absorption cross section for $l = 0$ case (s wave).

Thus from Eq. (2.91) and Eq. (2.93), we find coefficients A_0 and B_0 as,

$$A_0 = \frac{a + \imath b}{2\imath},\ B_0 = \frac{-a + \imath b}{2\imath}. \tag{2.99}$$

Using Eq. (2.98) we get,

$$A_0 = \frac{\left[1+ \mid R \mid -\epsilon c^2 p \left(1- \mid R \mid\right) r_o^2\right]}{2\imath p c}, \tag{2.100}$$

and

$$B_0 = -\frac{\left[1+ \mid R \mid +\epsilon c^2 p \left(1- \mid R \mid\right) r_0^2\right]}{2\imath p c}. \tag{2.101}$$

Thus the S-matrix for the s-wave is given by,

$$\begin{aligned} S_0 = -\frac{A_0}{B_0} \exp\left(2\imath\partial_0\right) &= \frac{1+ \mid R \mid -\epsilon c^2 p \left(1- \mid R \mid\right) r_o^2}{1+ \mid R \mid +\epsilon c^2 p \left(1- \mid R \mid\right) r_o^2} \exp\left(2\imath\partial_0\right) \\ &= \frac{1 - \epsilon c^2 p r_o^2 \eta}{1 + \epsilon c^2 p r_o^2 \eta} \exp\left(2\imath\partial_0\right), \end{aligned} \tag{2.102}$$

where $\eta = \frac{1+|R|}{1-|R|}$. Thus the absorption cross section is given by,

$$\sigma_{abs} = \frac{\pi}{p^2}\left(1- \mid S_o \mid^2\right) = \frac{\pi}{p^2} \frac{4c^2 \epsilon p r_0^2 \eta}{\left(1 + \epsilon c^2 p r_0^2 \eta\right)^2}, \tag{2.103}$$

taking $p = \epsilon v$, we get Eq. (2.103) as,

$$\sigma_{abs} = \frac{4\pi c^2 r_0^2 \eta}{v\left(1 + \epsilon^2 c^2 v r_0^2 \eta\right)^2}. \tag{2.104}$$

Eq. (2.129) gives the expression for absorption cross section of RN extremal black holes perturbed by scalar field.

2.4 Schwarzschild-de Sitter black hole - Extremal case

Eq. (2.2) represents the metric of a SdS space-time where $a^2 = \frac{3}{\Lambda}$ with $\Lambda > 0$ and $m > 0$. For $0 < 9\Lambda m^2 < 1$, there exist two positive roots r_b and r_c of $f(r)$ such that $0 < 2m < r_b < 3m < r_c$.

The roots $r_b = \frac{2}{\sqrt{\Lambda}}\cos\left(\frac{\alpha}{3}+\frac{4\pi}{3}\right)$ with $\cos\alpha = -3m\sqrt{\Lambda}$, describes the black hole horizon, and the root $r_c = \frac{2}{\sqrt{\Lambda}}\cos\left(\frac{\alpha}{3}\right)$ localizes the cosmological horizon. As Λ approaches its extremal value, i.e., $\Lambda \to \frac{1}{9m^2}$, the position of the black hole horizon r_b monotonically increases and the cosmological horizon r_c decreases to a common value at $r = 3m$. Here we analyze this extreme case of the SdS black hole which is characterized by the condition $9\Lambda m^2 = 1$. In this case, $f(r)$ becomes,[65]

$$f(r) = -\frac{1}{27m^2r}(r-3m)^2(r+6m). \tag{2.105}$$

Applying this in Klein-Gordon equation we will get,

$$\begin{aligned}[\frac{-27m^2r}{(r-3m)^2(r+6m)}\frac{\partial^2}{\partial t^2} + \frac{1}{27m^2r^2}\frac{\partial}{\partial r}r(r-3m)^2(r+6m)\frac{\partial}{\partial r} \\ -\frac{1}{r^2\sin\theta}\frac{\partial}{\partial\theta}\sin\theta\frac{\partial}{\partial\theta} - \frac{1}{r^2\sin^2\theta}\frac{\partial^2}{\partial\phi^2} + \mu^2]\psi(r,\theta,\phi,t) = 0.\end{aligned} \tag{2.106}$$

Separating the wave equation into radial and angular components by,

$$\Psi(r,\theta,\phi,t) = \exp(-\imath\epsilon t)\, Y_{lm}(\theta,\phi)\, \Phi_l(r). \tag{2.107}$$

where ϵ, l, m are energy, momentum and its projection, while $\Phi_l(r)$ is the radial function. Substituting Eq. (2.107) in Eq. (2.106) we get,

$$\begin{aligned}\Phi_l''(r) + (\frac{1}{r} + \frac{2}{r-3m} + \frac{1}{r+6m})\Phi_l'(r) + (\frac{\epsilon^2 27^2 m^4 r^2}{(r-3m)^4(r+6m)^2} \\ +\frac{\mu^2 27m^2 r}{(r-3m)^2(r+6m)} - \frac{l(l+1)27m^2r}{(r-3m)^2(r+6m)})\Phi_l(r) = 0.\end{aligned} \tag{2.108}$$

Let us describe the scattering of scalar waves by SdS extremal black hole with the help of Eq. (2.108). We will find solution of the wave equation in different regions outside the horizon.

Solution of wave equation in the vicinity of horizon, region 1: $r \to 3m$

This region is very near to the horizon and is the limit for a wave to reflect from the horizon. i.e., the wave function $\Phi_l(r)$ in this region (i.e., as $r \to 3m$) will contain incident and reflected waves. To find $\Phi_l(r)$ we use WKB approximation and write $\Phi = \exp(-\imath \int k(r)dr)$, which will lead to,

$$k\,(r \to 3m) = \pm\frac{\epsilon 27m^2 \times 3m}{(r-3m)^2(3m+6m)} = \pm\frac{9m^2\epsilon}{(r-3m)^2} = \pm\frac{\xi}{(r-3m)^2}. \tag{2.109}$$

Therefore the wave function in the region $r \to 3m$ can be written as,

$$\Phi_l(r) = \exp^{\mp\imath\int\frac{\epsilon 9m^2 dr}{(r-3m)^2}} = \exp(\pm\imath\frac{\epsilon 9m^2}{(r-3m)^2}), \tag{2.110}$$

where $\xi = \epsilon 9m^2$. The wave function in the vicinity of horizon is written, assuming that the wave gets reflected at the horizon, as

$$\Phi_l\,(r) = \exp\left(-i\frac{\xi}{3m-r}\right) + \mid R \mid \exp\left(+i\frac{\xi}{3m-r}\right), \tag{2.111}$$

where $|R|$ represents the reflection coefficient.

Solution of wave equation in region 2: $r > 3m$

Now we consider the second region, $r > 3m$. As in sections 2.2.2 and 2.3.2 we neglect the energy and momentum terms in Eq. (2.108) and for the s wave the resulting equation will be,

$$\Phi_0''(r) + (\frac{1}{r} + \frac{2}{r-3m} + \frac{1}{r+6m})\Phi_0'(r) = 0, \tag{2.112}$$

i.e.,

$$\ln\Phi_0'(r) = -2\ln(r-3m) - \ln r - \ln(r+6m). \tag{2.113}$$

Therefore,

$$\Phi_0(r) = -\frac{\alpha}{r-3m} + \beta, \tag{2.114}$$

gives the wave function in region 2.

Comparing solutions in regions 1 and 2

We compare the solutions in the regions 1 and 2 as before. Eq. (2.111) for s wave, can be written as

$$\Phi_0(r) = 1 - i\frac{\xi}{3m-r} + \mid R \mid \left(1 + i\frac{\xi}{3m-r}\right) = 1 + \mid R \mid + \frac{i\xi(1 - \mid R \mid)}{r-3m}. \tag{2.115}$$

Comparing Eq. (2.115) with Eq. (2.114) we get,

$$\alpha = -(1 - \mid R \mid) i\xi,\ \beta = 1 + \mid R \mid . \tag{2.116}$$

The above equation (Eq. (2.116)) gives the dependence of α and β on $|R|$.

Solution of wave equation far away from the horizon, region 3: $r >> 3m$

In this region, the terms containing energy and momentum in Eq. (2.108) can be simplified as,

$$\frac{27^2\epsilon^2 m^4 r^2}{(r-3m)^4(r+6m)^2} + \frac{27\mu^2 m^2 r}{(r-3m)^2(r+6m)} \simeq \epsilon^2 - \mu^2$$
$$+\frac{27 \times 2m^3(2\epsilon^2 - \mu^2)}{(r-3m)^2(r+6m)} = p^2 + \frac{27 \times 2m^3(p^2+\epsilon^2)}{(r-3m)^2(r+6m)}, \tag{2.117}$$

where p is the momentum and is given by $p^2 = \epsilon^2 - \mu^2$. Thus Eq. (2.108) becomes,

$$\Phi_l''(r) + (\frac{1}{r} + \frac{2}{r-3m} + \frac{1}{r+6m})\Phi_l'(r) + (p^2 +$$
$$\frac{27 \times 2m^3(p^2+\epsilon^2)}{(r-3m)^2(r+6m)} - \frac{27m^2 r(l+1)}{(r-3m)^2(r+6m)})\Phi_l(r) = 0. \tag{2.118}$$

Now at region $r >> 3m$ we can neglect higher powers of $\frac{1}{r}$ and we get the equation for the s-wave as,

$$\Phi_0''(r) + (\frac{1}{r} + \frac{2}{r-3m} + \frac{1}{r+6m})\Phi_0'(r) + p^2\Phi_0(r) = 0. \tag{2.119}$$

Since $r + 6m > r > r - 3m$, we can approximate the coefficient of $\Phi_0'(r)$ as $\frac{2}{r}$. Therefore at large distances we can write the equation as,

$$\Phi_0''(r) + \frac{2}{r}\Phi_0'(r) + p^2\Phi_0(r) = 0. \tag{2.120}$$

Here the solution is,

$$\Phi_0(r) = \frac{1}{r}(A_0 \exp iz + B_0 \exp -iz), \tag{2.121}$$

where $z = pr$. As in section 2.2.3 here also solution of Eq. (2.120) is obtained as a combination of $\sin z$ and $\cos z$ using Frobenius method. Thus following the earlier procedure solution, for low ϵ case,

$$\Phi_0(r) = ap + \frac{b}{r}. \tag{2.122}$$

Thus, wave function in region 3 can be represented by Eq. (2.122).

Comparing solutions of regions 2 and 3

By neglecting higher powers of $\frac{1}{r}$, Eq. (2.114) can also be written as,

$$\Phi_0(r) = -\frac{\alpha}{r\left(1 - \frac{3m}{r}\right)} + \beta \simeq -\frac{\alpha}{r} + \beta, \tag{2.123}$$

Thus Eq. (2.123) has the same form as Eq. (2.122). Therefore comparing the coefficients of wave functions in regions 2 and 3, we will get,

$$a = \frac{1+ \mid R \mid}{p},\ b = i\,(1- \mid R \mid)\,\xi. \tag{2.124}$$

Thus a and b depend on $|R|$.

2.4.1 Absorption cross section of SdS extremal black hole

Now we will find the expression for absorption cross section of SdS extremal black hole. From Eq. (2.95) and Eq. (2.124) we will get,

$$A_0 = \frac{[1+ \mid R \mid -(1- \mid R \mid)\,\xi p]}{2\imath pc}, \tag{2.125}$$

and

$$B_0 = -\frac{[1+ \mid R \mid + (1- \mid R \mid) \xi p]}{2\imath pc}. \tag{2.126}$$

S-matrix for the s-wave is given by,

$$\begin{aligned} S_0 = -\frac{A_0}{B_0} \exp(2\imath\partial_0) &= \frac{[1+ \mid R \mid - (1- \mid R \mid) \xi p]}{[1+ \mid R \mid + (1- \mid R \mid) \xi p]} \exp(2\imath\partial_0) \\ &= \frac{1 - \xi p\eta}{1 + \xi p\eta} \exp(2\imath\partial_0), \end{aligned} \tag{2.127}$$

where $\eta = \frac{1-|R|}{1+|R|}$. The expression for absorption cross section in the low energy limit will be,

$$\sigma_{abs} = \frac{\pi}{p^2} \left(1- \mid S_o \mid^2\right) = \frac{\pi}{p} \frac{4\xi\eta}{(1 + \xi p\eta)^2}, \tag{2.128}$$

i.e.,

$$\sigma_{abs} = \frac{4\pi 9m^2\eta}{v\left(1 + 9m^2\epsilon^2c^2v\eta\right)^2}. \tag{2.129}$$

Thus the absorption cross section of SdS extremal black hole which has depends on reflection coefficient $|R|$ is also obtained.

2.5 Conclusion

We have found the radial wave function $\Phi_l(r)$ in the vicinity of black hole horizon of Schwarzschild-de Sitter black hole (i.e., at $r \to r_b$) using WKB approximation. Assuming that reflection of scalar wave can take place at the horizon of black holes, we have obtained the expression for the Hawking temperature of Schwarzschild-de Sitter black hole. We have also studied the behavior of scattered scalar waves in the regions $r > r_b$ and $r \gg r_b$ in low energy limit. By comparing the solutions in the 3 regions, viz, $r \to r_b$, $r > r_b$ and $r \gg r_b$, we have found the S-matrix and the absorption cross section for SdS black hole in the low energy limit. The absorption cross section is found to be inversely depending on the Hawking temperature. From σ_{abs} of SdS, we can deduce the absorption cross section of

Schwarzschild black hole considering and neglecting the effect of of reflection from the horizon, which agree with the results obtained earlier. These calculations are extended to the cases of RN extremal and SdS extremal black holes and we have evaluated the S-matrix and the absorption cross section for RN extremal and SdS extremal black hole in the low energy limit.

3

Absorption cross section of RN black hole

3.1 Introduction

Even though the Kerr solution is the most relevant one from an astrophysical point of view, the solution of the coupled Einstein-Maxwell equation that describes an electrically charged, non-rotating black hole - Reissner Nordstrom (RN)- is of less direct importance because it seems unlikely that black holes with a considerable charge will exist in the Universe. Nevertheless, these solutions have several interesting features that need a closer inspection. The most intriguing one concerns the possible conversion of electromagnetic energy into gravitational energy and vice versa: In a charged environment an electromagnetic wave will inevitably give rise to gravitational waves. The Reissner-Nordstrom metric provides the simplest framework for studies of this effect.

The perturbation theory for a weak (massless) field in the geometry of an electrically charged black hole were first derived by Zerilli[66] and Moncrief[67–69] and further devolvements done by Chandrasekhar,[70] Xanthopoulos[71] and other authors. But we know that a charged black hole is formed by the collapse of a charged matter.

Thus the evolution of a charged scalar field outside the RN black hole is a most relevant thing. The late time behavior of a charged scalar field was considered by S.Hod and T.Piran.[72]

In this chapter we study the scattering of charged scalar waves in the Reissner-Nordstorm (RN) space-time. In section 3.2, we explain the nature of radial wave functions in different regions of RN space-time. Here we use WKB approximation for finding the solution of wave equation in the vicinity of event horizon of black holes. Section 3.3 contains calculation of absorption cross section for charged scalar wave scattered off by RN black hole, wherein we take into consider both reflection and absorption properties of the black hole horizon. Here we have found the effect of charge on the absorption cross section of RN black hole. Section 3.4 gives the conclusion.

3.2 Nature of radial wave functions in different regions of RN space-time

The Reissner-Nordstrom geometry describes the geometry of empty space surrounding a charged black hole. The metric describing a charged spherically symmetric black hole, written in spherical polar coordinates, is given by

$$ds^2 = (1 - \frac{1}{r} + \frac{q^2}{r^2})dt^2 - \frac{1}{(1 - \frac{1}{r} + \frac{q^2}{r^2})}dr^2 - r^2(d\theta^2 + \sin^2\theta d\phi^2). \quad (3.1)$$

If the charge of the black hole is less than its mass (G=c=M=1), then the geometry contains two horizons, an outer horizon and an inner horizon and are given by,

$$r_\pm = \frac{1}{2} \pm \sqrt{\frac{1}{4} - q^2}. \quad (3.2)$$

The dynamical behavior of a massive charged scalar field under RN background is,[73]

$$\Psi_{;ab}g^{ab} + \imath eA_a g^{ab}[2\Psi_{;b} + \imath eA_b\Psi] + \imath eA_{a;b}g^{ab}\Psi + \mu^2\Psi = 0. \quad (3.3)$$

For Reissner-Nortstrom metric we have, $g^{tt} = \frac{1}{(1-\frac{1}{r}+\frac{q^2}{r^2})} = \frac{1}{f(r)}$, $g^{rr} = -f(r) = -\frac{1}{h(r)}$, $g^{\theta\theta} = -\frac{1}{r^2}$ and $g^{\phi\phi} = -\frac{1}{r^2\sin^2\theta}$. Thus we find,

$$\Psi_{;tt} = \frac{\partial^2\Psi}{\partial t^2} - \frac{1}{2h(r)}f'(r)\frac{\partial\Psi}{\partial r}$$
$$\Psi_{;rr} = \frac{\partial^2\Psi}{\partial r^2} - \frac{1}{2h(r)}h'(r)\frac{\partial\Psi}{\partial r}$$
$$\Psi_{;\theta\theta} = \frac{\partial^2\Psi}{\partial\theta^2} + \frac{r}{h(r)}\frac{\partial\Psi}{\partial r}$$
$$\Psi_{;\phi\phi} = \frac{\partial^2\Psi}{\partial\phi^2} + \frac{r\sin^2\theta}{h(r)}\frac{\partial\Psi}{\partial r} + \sin\theta\cos\theta\frac{\partial\Psi}{\partial\theta}. \tag{3.4}$$

also,

$$A_{a;b} = \frac{\partial A_a}{\partial t} - \Gamma^{\kappa}_{ab}A_{\kappa}. \tag{3.5}$$

But A_a takes the values, $(A_t, 0, 0, 0)$. Now Substituting Eqs (3.4) and (3.5) in Eq. (3.3), we get,

$$[\frac{1}{f(r)}\frac{\partial^2\Psi}{\partial t^2} - \frac{1}{2h(r)f(r)}f'(r)\frac{\partial\Psi}{\partial r} - \frac{1}{h(r)}\frac{\partial^2\Psi}{\partial r^2} - \frac{1}{2h^2(r)}h'(r)\frac{\partial\Psi}{\partial r}$$
$$-\frac{2}{rh(r)}\frac{\partial\Psi}{\partial r} + \frac{2\imath eA_t}{f(r)} - \frac{e^2A_t^2}{f(r)} + \frac{1}{r^2}(\frac{\partial^2\Psi}{\partial\theta^2} + \frac{1}{\sin^2\theta}\frac{\partial^2\Psi}{\partial\phi^2} +$$
$$\cot\theta\frac{\partial\Psi}{\partial\theta})]\Psi = 0 \tag{3.6}$$

The radial part is separated out by putting, $\Psi = \exp(-\imath\epsilon t)\Phi_l(r)Y_{lm}(\theta,\phi)$, where ϵ, l, and m are energy, momentum and its projection, while $\Phi_l(r)$ is radial function. Thus, we find

$$\Phi_l''(r) + (\frac{f'(r)}{2f(r)} - \frac{h'(r)}{2h(r)} + \frac{2}{r})\Phi_l'(r) + [\frac{h(r)}{f(r)}(\epsilon - eA_t)^2 -$$
$$\mu^2h(r) - \frac{l(l+1)}{r^2}h(r)]\Phi_l(r) = 0. \tag{3.7}$$

Now putting $f(r) = \frac{1}{h(r)} = \frac{\Delta}{r^2}$, where Δ is given by $r^2 - r + q^2 = (r - r_+)(r - r_-)$. Thus Eq. (3.2) becomes,

$$\Delta\Phi_l''(r) + (2r-1)\Phi_l'(r) + (\frac{(\epsilon - eA_t)^2r^4}{\Delta} - \mu^2r^2 - l(l+1))\Phi_l(r) = 0, \tag{3.8}$$

where e is the electric charge, $A_t = \frac{q}{r}$ is the electric potential and therefore Eq. (3.8) will be,

$$(r^2 - r + q^2)\Phi_l''(r) + (2r-1)\Phi_l'(r) + (\frac{(\epsilon - eA_t)^2 r^4}{r^2 - r + q^2} \\ -\mu^2 r^2 - l(l+1))\Phi_l(r) = 0. \tag{3.9}$$

The radial equation can also be written as

$$\frac{d}{dr}(r^2 - r + q^2)\Phi_l'(r) + (\frac{(\epsilon - eA_t)^2 r^2}{(1 - \frac{1}{r} + \frac{q^2}{r^2})} - \mu^2 r^2 - l(l+1))\Phi_l(r) = 0. \tag{3.10}$$

To study the scattering problem we divide the space-time into 3 regions.[43] We consider the three different regions starting from the event horizon as shown below.

Solution of wave equation in the vicinity of horizon: $r \to r_+$ ***(region 1)***

We solve the wave equation near the horizon and also evaluate Hawking temperature using WKB approximation. By using WKB approximation $\Phi = \exp^{-\imath \int k(r) dr}$ in Eq. (3.9), we get

$$k^2(r) = \left(1 - \frac{1}{r} + \frac{q^2}{r^2}\right)^{-1} \left[\frac{(\epsilon - eA_t)^2}{\left(1 - \frac{1}{r} + \frac{q^2}{r^2}\right)} - \frac{l(l+1)}{r^2} - \mu^2\right], \tag{3.11}$$

which gives,

$$k(r) = \pm[(\epsilon - eA_t)^2 r^4 - (l(l+1) + \mu^2 r^2)(r^2 - r + q^2)]^{\frac{1}{2}} \frac{1}{(r^2 - r + q^2)}. \tag{3.12}$$

Thus near the outer horizon $r \to r_+$, we will get $k\,(r \to r_+) = \pm\frac{\xi}{(r - r_+)}$, where $\xi = \frac{(\epsilon - eA_t)r_+^2}{(r_+ - r_-)}$. Therefore the wave function in the region $r \to r_+$ can be written as,

$$\Phi_l(r) \sim \exp(\pm\imath \int \frac{\xi}{(r - r_+)} dr) = \exp\left(\pm\imath\xi \ln\left(r - r_+\right)\right), \tag{3.13}$$

i.e.,

$$\Phi_l(r) \sim \exp\left(\pm\imath\xi \ln\left(r - r_+\right)\right). \tag{3.14}$$

Let us describe its radial motion with the help of the wave function $\Phi_l\left(r\right)$. Assuming the wave gets reflected at the horizon and using Eq. (3.14), the wave function in the vicinity of horizon can be written as,

$$\Phi_l\left(r\right) \sim \exp\left(-\imath\xi \ln\left(r - r_+\right)\right) + \mid R \mid \exp\left(+\imath\xi \ln\left(r - r_+\right)\right). \tag{3.15}$$

Following the method described in chapter 2, the new wave function $\Phi_l^{2\pi}\left(r\right)$ in the Riemannian surface is given by,

$$\Phi_l^{2\pi}\left(r\right) = \rho \exp\left(-\imath\xi \ln\left(r - r_+\right)\right) + \frac{\mid R \mid}{\rho} \exp\left(+\imath\xi \ln\left(r - r_+\right)\right), \tag{3.16}$$

where $\rho = \exp\left(-2\pi\xi\right)$. And since $\rho < 1$, we assume that $\frac{|R|}{\rho} = 1$, thus $R = \exp\left(-2\pi\xi\right)$. Thus outer horizon is capable of reflection and the probability of reflection from the horizon can be found as $P = |R|^2 = \exp\left(-4\pi\xi\right)$. Since the reflection is taking place against the background of a black hole with temperature T, we see that $P = \exp\left(-\frac{(\epsilon - eA_t)}{T}\right)$, where ϵ is the energy of the particles, e the electric charge and $A_t = \frac{q}{r}$ is the electric potential. Therefore,

$$T = \frac{r_+ - r_-}{4\pi r_+^2}, \tag{3.17}$$

represents the Hawking temperature of RN black hole.

Solution of wave equation in the intermediate region: $r > r_+$ ***(region 2)***

This region is away from r_+ but not very far away from r_+. Here the terms in $(\epsilon - eA_t)^2$ and μ^2 are much smaller than all other terms and hence neglecting, Eq. (3.9) can be reduced to,

$$\Phi_0''(r) + \frac{2r - 1}{r^2 - r + q^2}\Phi_0'(r) = 0. \tag{3.18}$$

Therefore $\ln \Phi_0'(r) = -\ln\left(r^2 - r + q^2\right) + \ln C$ and it can be written as,

$$\Phi_0'(r) = \frac{C}{r^2 - r + q^2} = \frac{A}{r - r_+} + \frac{B}{r - r_-}. \tag{3.19}$$

Since $r > r_+$ we neglect the effect of r_-, and the above equation can be written as,

$$\Phi_0(r) = \int \frac{K}{(r - r_+)\, r} dr, \tag{3.20}$$

i.e.,

$$\Phi_0(r) = \alpha \ln \frac{(r - r_+)}{r} + \beta, \tag{3.21}$$

is the wave function in region 2.

Comparing solutions in regions 1 and 2

The definitions of the above two regions do not really lead to any overlap region. However, near the point r_+ one can approximate the solutions by linear combinations of constant terms and terms proportional to $\ln(r - r_+)$. To obtain this, consider Eq. (3.15) which is the wave function in the region $r \to r_+$,

$$\Phi_l(r) = \exp\left(-\imath\xi \ln(r - r_+)\right) + \mid R \mid \exp\left(+\imath\xi \ln(r - r_+)\right). \tag{3.22}$$

We can take $\exp\left(\pm\imath\xi \ln(r - r_+)\right) = 1 \pm \left(\imath\xi \ln(r - r_+)\right)$, therefore the above equation becomes,

$$\Phi(r) = 1 + \mid R \mid - (1 - \mid R \mid)\, \imath\xi \ln(r - r_+). \tag{3.23}$$

Also Eq. (3.21) can be approximated as,

$$\Phi_0(r) = \alpha \ln(r - r_+) + \beta. \tag{3.24}$$

Comparing Eq. (3.24) with Eq. (3.23) we get,

$$\alpha = -\imath\xi\,(1 - \mid R \mid),\ \beta = 1 + \mid R \mid. \tag{3.25}$$

As in Chapter 2 here also α and β are functions of $|R|$.

Solution of wave equation at far away from the horizon (region 3) : $r >> r_+$

Now in the region $r >> r_+$, we can write $2r - 1 = 2r - (r_+ + r_-) = (r - r_+) + (r - r_-)$. Therefore Eq. (3.9) becomes:

$$\Phi_l''(r) + (\frac{1}{r - r_+} + \frac{1}{r - r_-})\Phi_l'(r) + (\frac{(\epsilon - eA_t)^2 r^4}{(r^2 - r + q^2)^2} - \frac{\mu^2 r^2}{r^2 - r + q^2} - \frac{l(l+1)}{r^2 - r + q^2})\Phi_l(r) = 0. \tag{3.26}$$

In the above equation the terms containing energy and mass can be simplified as,

$$\frac{(\epsilon - eA_t)^2 r^4}{(r^2 - r + q^2)^2} = (\epsilon - eA_t)^2 + \frac{2(\epsilon - eA_t)^2 r}{(r^2 - r + q^2)} + \frac{(\epsilon - \frac{eq}{r})^2 (r^2 - 2r^2 q^2 - q^4)}{(r^2 - r + q^2)^2}, \tag{3.27}$$

and

$$\frac{\mu^2 r^2}{r^2 - r + q^2} = \mu^2 + \frac{\mu^2 r}{r^2 - r + q^2} - \frac{\mu^2 q^2}{r^2 - r + q^2}. \tag{3.28}$$

Thus,

$$\frac{(\epsilon - eA_t)^2 r^4}{(r^2 - r + q^2)^2} - \frac{\mu^2 r^2}{r^2 - r + q^2} = (\epsilon - eA_t)^2 - \mu^2 + \frac{(2(\epsilon - eA_t)^2 - \mu^2) r}{(r^2 - r + q^2)} = p^2 + \frac{(p^2 + (\epsilon - eA_t)^2) r}{(r^2 - r + q^2)}, \tag{3.29}$$

where p is the momentum and is given by $p^2 = (\epsilon - eA_t)^2 - \mu^2$. Since r is very large and since we are considering for the low energy case, only terms up to $\frac{1}{r}$ is taken. Substituting Eq. (3.29) in Eq. (3.26) we get,

$$\Phi_l''(r) + \frac{2}{r}\Phi_l'(r) + \left(p^2 + \frac{\left(p^2 + (\epsilon - eA_t)^2\right)}{2r} - \frac{l\,(l+1)}{r^2} \right) \Phi_l(r) = 0. \tag{3.30}$$

This equation is of Coulomb type where the Coulomb charge is $Z = \frac{(\epsilon - eA_t)^2 + p^2}{2}$ and the solution to this equation can be written,

$$\Phi_l(r) = \frac{1}{r}\left(A_l \exp(\imath z) + B_l \exp(-\imath z)\right), \tag{3.31}$$

where $z = pr - \frac{l\pi}{2} + \nu \ln 2pr + \delta_t^{(c)}$, $\delta_t^{(c)}$ is defined as $\delta_t^{(c)} = \arg\Gamma(l + 1 - \nu)$ and $\nu = \frac{Z}{p}$.[26] The Coulomb wave function has a regular singularity at $r = 0$ and it has an irregular singularity at $r = \infty$. And we know that $F_l(r)$ be the regular Coulomb wave function and $G_l(r)$ be the irregular Coulomb wave function as discussed in section 2.3.3. Thus for s wave,

$$\Phi_0(r) = acp + \frac{b}{cr}, \tag{3.32}$$

where

$$c^2 = \frac{2\pi\nu}{1 - \exp(2\pi\nu)}. \tag{3.33}$$

Thus Eq. (3.32) represents the wave function in the region of large separations $r \gg r_+$ for the s wave.

Comparing solutions in regions 2 and 3

To compare the wave function in the regions 2 and 3, we write Eq. (3.21) as,

$$\Phi_0(r) = \alpha \ln\left(1 - \frac{r_+}{r}\right) + \beta \simeq -\frac{\alpha r_+}{r} + \beta, \tag{3.34}$$

since $\ln\left(1 - \frac{r_+}{r}\right) = -\frac{r_+}{r}$. Thus from Eq. (3.32) and Eq. (3.34) we get,

$$a = \frac{1 + |R|}{pc},\ b = \imath\xi r_+ c\,(1 - |R|). \tag{3.35}$$

Thus a and b depend on the reflection coefficient.

3.3 Absorption cross section

Now we will find an expression for the absorption cross section of RN black hole. The two terms in Eq. (3.31) represent the incoming

and outgoing waves. The S matrix can be written as the ratio of coefficient of the incoming and outgoing waves. We will consider first the low energy region $\epsilon \ll 1$, where reflection from the horizon is prominent and restricted to $l = 0$ case and denoting s wave $\Phi_0(r)$, and we will find the coefficients A_0, B_0. From chapter 2 we can deduce,

$$A_0 = \frac{a + \imath b}{2\imath},\ B_0 = \frac{-a + \imath b}{2\imath}. \tag{3.36}$$

Employing Eq. (3.35) we can find,

$$A_0 = \frac{\left[1+ \mid R \mid -\xi c^2 p\,(1- \mid R \mid) r_+\right]}{2\imath pc}, \tag{3.37}$$

and

$$B_0 = -\frac{\left[1+ \mid R \mid +\xi c^2 p\,(1- \mid R \mid) r_+\right]}{2\imath pc}. \tag{3.38}$$

Corresponding S-matrix for the s-wave is given by,

$$S_0 = -\frac{A_0}{B_0}\exp(2\imath\delta_0) = \frac{1+ \mid R \mid -\xi c^2 p\,(1- \mid R \mid) r_+}{1+ \mid R \mid +\xi c^2 p\,(1- \mid R \mid) r_+}\exp(2\imath\delta_0), \tag{3.39}$$

which can be written as,

$$S_0 = \frac{1 - \xi c^2 p r_+ \eta}{1 + \xi c^2 p r_+ \eta}\exp(2\imath\delta_0), \tag{3.40}$$

where $\eta = \frac{1-|R|}{1+|R|}$. The absorption cross section in the low energy limit is given by,

$$\sigma_{abs} = \frac{\pi}{p^2}\left(1- \mid S_o \mid^2\right) = \frac{\pi}{p^2}\frac{4c^2\xi p r_+ \eta}{(1 + \xi c^2 p r_+ \eta)^2}. \tag{3.41}$$

Taking $p = (\epsilon - eA_t)\,v$, we write Eq. (3.41) as,

$$\sigma_{abs} = \frac{4\pi c^2 r_+^3 \eta}{v\,(r_+ - r_-)\,(1 + \xi c^2 p r_+ \eta)^2}. \tag{3.42}$$

We know that Hawking temperature is given by,

$$T = \frac{r_+ - r_-}{4\pi r_+^2}. \tag{3.43}$$

Therefore

$$\sigma_{abs} = \frac{c^2 r_+ \eta}{vT\left(1+\xi c^2 p r_+ \eta\right)^2}. \tag{3.44}$$

In the expression for absorption cross section we have to substitute for c^2 and η. We know that $\nu = \frac{Z}{p}$, where $Z = \frac{(\epsilon - eA_t)^2 + p^2}{2}$ and therefore $\nu = \frac{(\epsilon - eA_t)^2 + p^2}{2p} = \frac{(\epsilon - eA_t)v}{2}\left(1 + \frac{1}{v^2}\right)$. Hence,

$$c^2 = \frac{\pi\left(\epsilon - eA_t\right) v \left(1+\frac{1}{v^2}\right)}{1 - \exp\left(-\pi\left(\epsilon - eA_t\right) v \left(1+\frac{1}{v^2}\right)\right)}, \tag{3.45}$$

and for low energy,

$$c^2 = \frac{\pi\left(\epsilon - eA_t\right) v \left(1+\frac{1}{v^2}\right)}{1 - \left(1 - \pi\left(\epsilon - eA_t\right) v \left(1+\frac{1}{v^2}\right)\right)} \simeq 1, \tag{3.46}$$

and

$$\eta = \frac{1 - \exp\left(-2\pi\xi\right)}{1 + \exp\left(-2\pi\xi\right)} = \tanh \pi\xi \simeq \pi\xi. \tag{3.47}$$

Substituting Eqs. (3.46) and (3.47) in Eq. (3.44) we find,

$$\sigma_{abs} = \frac{r_+ \pi \xi}{vT\left(1 + \frac{(\epsilon - eA_t)^2 r_+}{16\pi^2 T^2}\right)^2} \simeq \frac{\left(\epsilon - eA_t\right) r_+}{4vT^2}. \tag{3.48}$$

i.e., the absorption cross section of RN black hole is found to depend inversely on square of the Hawking temperature. Now, if $q = 0$, the metric becomes of the Schwarzschild type. Thus if we substitute $T = \frac{1}{4\pi r}$ and $r_+ = r$ we will get the result

$$\sigma_{abs} = \frac{4\pi^2 r^3 \epsilon}{v}, \tag{3.49}$$

derived earlier.[64] And in the absence of reflection we arrive at the result obtained by Unruh.[43] Now using Eq. (3.42) we plot σ_{abs} versus ϵ. The curve is plotted for RN black hole with reflection and taking charges q=0.1, 0.2, 0.3, 0.4. And we found that absorption cross section decreases when charge is increased from 0.1 to 0.4, i.e., there is more possibility of reflection. It is shown in Figure 3.1. In Figure 3.2 we plot σ_{abs} versus ε for RN black hole with and without reflection

and for Schwarzschild black hole with and without reflection. From the plot it is clear that absorption cross section is decreased by the presence of charge. And also found that for RN case the graph is shifted to right.

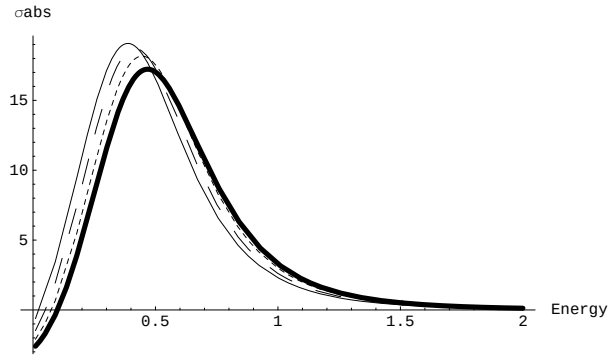

Figure 3.1: σ_{abs} versus ϵ for RN black hole with reflection, is plotted for different charges. The solid curve is for $q = 0.1$, dashed curve is for $q = 0.2$, dotted curve is for $q = 0.3$, and bold curve is for $q = 0.4$.

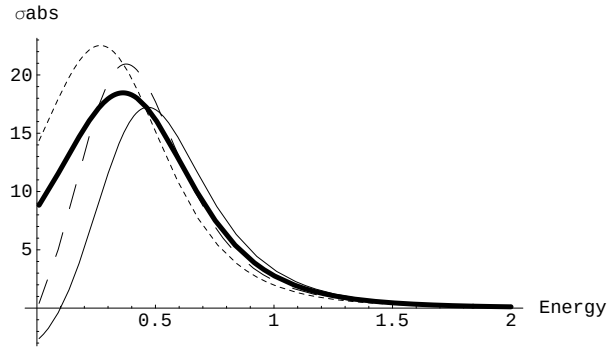

Figure 3.2: σ_{abs} versus ϵ for RN black hole with (solid curve) and without (bold curve) reflection and for Schwarzschild black hole with (dashed curve) and without reflection (dotted curve).

3.4 Conclusion

We have found the wave function $\Phi_l(r)$ in the vicinity of outer horizon of RN black hole i.e., at $r \to r_+$, for charged scalar field using WKB approximation. We have also studied the behavior of scattered charged scalar waves in the regions $r > r_+$ and $r \gg r_+$ in low energy limit. By comparing the solutions in the 3 regions we find the S-matrix and the absorption cross section for RN black hole in the low energy limit. The absorption cross section is found to be inversely depending on the square of the Hawking temperature. From σ_{abs} of RN, we deduce the absorption cross section of Schwarzschild black hole in the presence of reflection and in the absence of reflection, which agree with the results obtained earlier.[43,64] By plotting σ_{abs} versus ϵ plot it is found that absorption cross section is decreased by increasing the of charge in RN black hole.

4

Absorption cross section and emission spectra of Schwarzschild black hole in Dirac field

4.1 Introduction

The no-hair theorem in General Relativity asserts that the metrics of stationary black holes can be uniquely described by three parameters: mass M, charge Q and angular momentum per unit mass a and these parameters become parameters of the field equation when we write matter field equation in a black hole background. The Dirac equation and its separability properties on black hole metrics have been investigated in many complicated contexts. The pioneering work was done in the neutrino field equation on the Schwarzschild metric by Brill and Wheeler[74] and Teukolsky[75] solved for massles spin 0, 1 and 2 cases and the spin 1/2 case is independently shown by Teukolsky and Unruh.[76] The separation of radial and angular part of massive Dirac equation came from Chandrasekhar.[70,77,78]

Later Finster and collaborators[79–88] have shown renewed interests in the interaction of the Dirac field with gravity in a series of

papers. They found stable particle like solutions in the Einstein-Dirac-Maxwell system[79,80] and also proved the nonexistence of time-periodic solutions in various black hole space-times.[82,83] This means that Dirac particles, including electrons and neutrinos, cannot remain on a periodic orbit around a black hole and this is quite surprising. This indicates that if a cloud of Dirac particles collapses gravitationally, the particles must eventually vanish inside the event horizon of a black hole or escape to infinity and therefore it is interesting to see how Dirac fields evolve in curved background space-times. To understand this, we have to consider the scattering solutions of the radial equations of massive Dirac fields in spherically symmetric black hole space-times.

One reason for getting additional importance for wave scattering and absorption by black holes,[89] after Hawking realized that black holes should evaporate thermally,[14,15] is that the power emitted by the black hole is related to the rate of absorption. After Hawking published his results, the power spectrum of black holes was largely analyzed. Page[90–92] computed Hawking emission for different kinds of black holes and particles. Nevertheless, until recently the absorption spectrum of black holes has not been studied so extensively as the black hole emission spectrum. The Schwarzschild black hole absorption cross section for arbitrary frequencies is known for fields with spin 0, 1, and 2. The results for the fermion case were first obtained by Doran et al.[93] Fermionic Hawking radiation is also expected to exist[94–97] (eg. neutrino radiation), and has recently been shown to arise as a tunnelling effect.[98]

Also the computation of low energy absorption cross section is important in the context of string theories and brane-world scenario. In the context of the brane-world scenario the most remarkable fact is that fundamental Planck mass can be low as a TeV scale. One of the striking consequences arising due to TeV-scale gravity is that, if the Large Hadron Collider in CERN may become a black hole

factory,[99–101] and if so one can examine the quantum gravity effects such as Hawking radiation and information loss problem[102,103] of black hole in the laboratory. Thus in this context it is important to investigate the absorption and emission problems.

In the present chapter, we study the scattering of Dirac waves in a Schwarzschild space-time in the low energy limit. Earlier, several authors have studied scattering of scalar and Fermi fields under different black hole space-time and calculated absorption cross sections. In all these calculations, the black hole is assumed to be capable of absorbing the radiation falling on it, but here we consider that both absorption and reflection could take place at the horizon of black holes.[3,104] In this work we consider Spin-1/2 particles in 4 dimensional Schwarzschild background using the traditional Dirac equation. Here, WKB approximation is used for finding the solution of wave equation in the vicinity of event horizon of black hole. Section 4.2 deals with familiarization of the Dirac equation for a general metric. In section 4.3, we explain the nature of radial wave functions in different regions of Schwarzschild space-time. Section 4.4 contains calculation of absorption cross section wherein we take into consider reflection, absorption and emission properties of the black hole horizon. Section 4.5 concludes the chapter.

4.2 General metric of a black hole space-time perturbed by a Dirac field

The Dirac equation in a general background space-time is given by ,

$$(\imath\gamma^a e_a^\mu(\partial_\mu + \Gamma_\mu) - m)\,\Psi = 0, \tag{4.1}$$

where m is the the mass of the Dirac field and e_a^μ is the tetrad given by,[105]

$$e_a^\mu = \begin{pmatrix} f^{-\frac{1}{2}} & 0 & 0 & 0 \\ 0 & f^{\frac{1}{2}}\sin\theta\cos\phi & r^{-1}\cos\theta\cos\phi & -r^{-1}\csc\theta\sin\phi \\ 0 & f^{\frac{1}{2}}\sin\theta\sin\phi & r^{-1}\cos\theta\sin\phi & r^{-1}\csc\theta\cos\phi \\ 0 & f^{\frac{1}{2}}\cos\theta & -r^{-1}\sin\theta & 0 \end{pmatrix}. \tag{4.2}$$

The rows of this matrix are specified by the index a and the columns by the index is μ. The inverse of the tetrad e_a^μ defined by,

$$g_{\mu\nu} = \eta_{ab} e_\mu^a e_\nu^b, \tag{4.3}$$

with $\eta_{ab} = diag(1,-1,-1,-1)$, being Minkowski metric. γ^a are the Dirac matrices. Γ_μ is the spin connection given by

$$\Gamma_\mu = \frac{1}{2}[\gamma^a,\gamma^b]e_a^\nu e_{b\nu;\mu}, \tag{4.4}$$

where $e_{b\nu;\mu} = \partial_\mu e_{b\nu} - \Gamma^\kappa_{\nu\mu} e_{b\kappa}$ is the covariant derivative of $e_{b\nu}$ with $\Gamma^\kappa_{\nu\mu}$ being the Christoffel symbols. Substituting Eq. (4.4) in Eq. (4.1) for a general spherically symmetric metric we find,

$$\left(\frac{\gamma^0}{f^{\frac{1}{2}}}\partial_t + \frac{\widetilde{\gamma} f^{\frac{1}{2}}}{r}\partial_r\left(r f^{\frac{1}{4}}\right) - \frac{\widetilde{\gamma}}{r}\left(\overrightarrow{\Sigma}.\overrightarrow{L}+1\right) + \imath m\right)\Psi = 0, \tag{4.5}$$

with,

$$\widetilde{\gamma} \equiv \gamma^1\sin\theta\cos\phi + \gamma^2\sin\theta\sin\phi + \gamma^3\cos\theta, \tag{4.6}$$

where, in the Dirac representation,

$$\overrightarrow{\Sigma} = \begin{pmatrix} \overrightarrow{\sigma} & 0 \\ 0 & \overrightarrow{\sigma} \end{pmatrix}, \tag{4.7}$$

and $\overrightarrow{L}$ is the angular momentum operator with components

$$\begin{aligned} L_1 &= \sin\phi\partial_\theta + \cot\theta\cos\phi\partial_\phi, \\ L_1 &= -\cos\phi\partial_\theta + \cot\theta\sin\phi\partial_\phi, \\ L_1 &= -\partial_\phi. \end{aligned} \tag{4.8}$$

Using separation of variables,[106] we write

$$\Psi(t,r,\theta,\phi)=\frac{e^{-\imath\epsilon t}}{rf^{\frac{1}{4}}}\begin{pmatrix}G^{(\pm)}(r)\,\psi^{\pm}_{j\tilde{m}}(\theta,\phi)\\ -\imath F^{\pm}(r)\psi^{\mp}_{j\tilde{m}}(\theta,\phi)\end{pmatrix}, \tag{4.9}$$

where for $j=l+\frac{1}{2}$, we have

$$\psi^{+}(\theta,\phi)=\begin{pmatrix}\sqrt{\frac{l+\frac{1}{2}-\tilde{m}}{2l+1}}Y_l^{\tilde{m}-\frac{1}{2}}\\ \sqrt{\frac{l+\frac{1}{2}+\tilde{m}}{2l+1}}Y_l^{\tilde{m}+\frac{1}{2}}\end{pmatrix}, \tag{4.10}$$

and for $j=l-\frac{1}{2}$

$$\psi^{-}(\theta,\phi)=\begin{pmatrix}\sqrt{\frac{l+\frac{1}{2}+\tilde{m}}{2l+1}}Y_l^{\tilde{m}-\frac{1}{2}}\\ -\sqrt{\frac{l+\frac{1}{2}-\tilde{m}}{2l+1}}Y_l^{\tilde{m}+\frac{1}{2}}\end{pmatrix}. \tag{4.11}$$

Eq. (4.5) now takes the form,

$$f^{\frac{1}{2}}\frac{\partial G}{\partial r}+\frac{k}{r}G=\left(\frac{\epsilon}{f^{\frac{1}{2}}}+m\right)F, \tag{4.12}$$

$$f^{\frac{1}{2}}\frac{\partial F}{\partial r}-\frac{k}{r}F=\left(-\frac{\epsilon}{f^{\frac{1}{2}}}+m\right)G, \tag{4.13}$$

where k is a positive or a negative non-zero integer with $l=|k+\frac{1}{2}|-\frac{1}{2}$. Here l is the total angular momentum, $\tilde{m}$ is the angular momentum in the z direction and $j=|k|-\frac{1}{2}$ is the total angular momentum. We define $\lambda=\frac{m}{\epsilon}$. Substituting Eq. (4.12) in Eq. (4.13) we get a second order differential equation,

$$\begin{aligned}\frac{f}{1+\lambda f^{\frac{1}{2}}}\frac{d}{dr}\left(\frac{f}{1+\lambda f^{\frac{1}{2}}}\frac{dG}{dr}\right)+\frac{f}{1+\lambda f^{\frac{1}{2}}}G\frac{d}{dr}\left(\frac{f}{1+\lambda f^{\frac{1}{2}}}\frac{k}{r}\right)+\\ -\frac{k^2}{r^2}\frac{f}{\left(1+\lambda f^{\frac{1}{2}}\right)^2}G=-\epsilon^2\left(\frac{1-\lambda f^{\frac{1}{2}}}{1+\lambda f^{\frac{1}{2}}}\right)G.\end{aligned} \tag{4.14}$$

Defining

$$\frac{dr}{dx}=\frac{f}{1+\lambda f^{\frac{1}{2}}}, \tag{4.15}$$

Eq. (4.14) becomes,

$$\frac{d^2G}{dx^2}+\left[\frac{d}{dx}\left(\frac{f^{\frac{1}{2}}}{1+\lambda f^{\frac{1}{2}}}\frac{k}{r}\right)-\frac{f}{\left(1+\lambda f^{\frac{1}{2}}\right)^2}\frac{k^2}{r^2}+\epsilon^2\left(\frac{1-\lambda f^{\frac{1}{2}}}{1+\lambda f^{\frac{1}{2}}}\right)\right]G=0. \tag{4.16}$$

This is the Dirac radial equation for a general metric. Substituting Eq. (4.13) in Eq. (4.12) we can get a coupled second order differential equation in F.

4.3 Radial solutions of Dirac field in Schwarzschild space-time

Schwarzschild space-time metric is given by,

$$ds^2=\left(1-\frac{1}{r}\right)dt^2-\frac{dr^2}{\left(1-\frac{1}{r}\right)}-r^2d\theta^2-r^2\sin^2\theta d\phi^2. \tag{4.17}$$

For this metric Eq. (4.16) takes the form,

$$\frac{d^2G}{dx^2}+\left[\frac{d}{dx}\left(\frac{\rho}{1+\lambda\rho}\frac{k}{r}\right)-\frac{\rho^2}{(1+\lambda\rho)^2}\frac{k^2}{r^2}+\epsilon^2\left(\frac{1-\lambda\rho}{1+\lambda\rho}\right)\right]G=0. \tag{4.18}$$

where $f=\rho^2$. For the metric given by Eq. (4.17), the singularity is at $r=1$ which is considered as the Schwarzschild horizon. We will find solution of the equation in different regions outside the horizon.[43]

Solution of wave equation in the vicinity of horizon (region 1): $r\to 1$

This is the region very near to the horizon and is the last limit for a wave to reflect from the horizon. While solving the wave equation in this region we will get the incident and reflected waves. Here we solve the wave equation near the horizon and also evaluate Hawking temperature using WKB approximation. From Eq. (4.15) we have, $dx=\frac{1+\lambda\rho}{\rho^2}dr$, Eq. (4.18), then becomes,

$$\frac{\rho^2}{1+\lambda\rho}\frac{d^2G}{dr^2}+\frac{d}{dr}(\frac{\rho^2}{1+\lambda\rho})\frac{dG}{dr}+[\frac{d}{dr}(\frac{\rho}{1+\lambda\rho}\frac{k}{r})-$$
$$\frac{\rho^2}{(1+\lambda\rho)^2}\frac{k^2}{r^2}+\epsilon^2\frac{(1-\lambda\rho)}{\rho^2}]G=0. \tag{4.19}$$

Since $\lambda=\frac{\mu}{\epsilon}$, Eq. (4.3) becomes

$$\frac{d^2G}{dr^2}+\frac{1}{\rho^2}\frac{d\rho^2}{dr}\frac{dG}{dr}+(1+\lambda\rho)\frac{d}{dr}\left(\frac{1}{(1+\lambda\rho)}\right)\frac{dG}{dr}+ \tag{4.20}$$
$$\left[\frac{1}{\rho^2}\frac{k}{r}\frac{d\rho}{dr}+\frac{(1+\lambda\rho)}{\rho}\frac{k}{r}\frac{d}{dr}\frac{(1+\lambda\rho)}{\rho}+\frac{1}{\rho}\frac{d}{dr}\frac{k}{r}-\frac{k^2}{r^2\rho}+\frac{\epsilon^2}{\rho^4}-\frac{\mu^2}{\rho^2}\right]G=0.$$

G_I will contain both incident and reflected waves. To find G_I, we use WKB approximation and write $G_I=\exp(\pm\imath\int\kappa(r)dr)$ which will lead to,

$$\kappa\left(r\to 1\right)=\pm\frac{\epsilon}{(r-1)}. \tag{4.21}$$

Using Eq. (4.21), the radial wave function G_I in the vicinity of horizon can be written as,

$$G_I\left(r\right)\sim\exp\left(-\imath\epsilon\ln\left(r-1\right)\right)+\mid R\mid\exp\left(+\imath\epsilon\ln\left(r-1\right)\right), \tag{4.22}$$

where R represents the reflection coefficient and the solution represents the interference between the incident and reflected waves. From previous chapters we know that the wave function acquires a new value $G_I^{2\pi}\left(r\right)$ on its Riemannian surface, after finishing the rotation in the complex z plane over an angle 2π and returning to a real physical value $z>0$. Thus,

$$G_I^{2\pi}\left(r\right)=\varrho\exp\left(-\imath\epsilon\ln\left(r-1\right)\right)+\frac{\mid R\mid}{\varrho}\exp\left(+\imath\epsilon\ln\left(r-1\right)\right), \tag{4.23}$$

where $\varrho=\exp\left(-2\pi\varepsilon\right)$. The new wave function $G_I^{2\pi}\left(r\right)$ and the initial wave function satisfies the same differential equation. But $\varrho<1$, so we get $\frac{|R|}{\varrho}=1$. i.e., the black hole horizon can reflect because it have a non-zero reflection coefficient $R=\exp\left(-2\pi\epsilon\right)$.

Therefore the probability of reflection from the horizon can be obtained as $P =\mid R \mid^2 = \exp(-4\pi\varepsilon)$. Here also reflection is taking place against the background of a black hole with temperature T, we see that $P = \exp\left(-\frac{(\epsilon)}{T}\right)$, where ϵ is the energy of the particles. Therefore the Hawking temperature of Schwarzschild black hole with the Schwarzschild radius r_g is,

$$T = \frac{1}{4\pi r_g}. \tag{4.24}$$

Thus the property of reflection from horizon helps us to find the expression for Hawking temperature of Schwarzschild black hole.

Solution of wave equation in the intermediate region: $r > 1$ ***(region2)***

This region is considered to be sufficiently away from the horizon, but not very far away from $r = 1$. Thus it is considered as the intermediate region between regions 1 and 3. Assuming the terms in ϵ^2, m^2 are much smaller than all other terms, Eq. (4.18) becomes,

$$\frac{d^2G}{dx^2} + \left[\frac{d}{dx}\left(\frac{\rho}{1+\lambda\rho}\frac{k}{r}\right) - \frac{\rho^2}{(1+\lambda\rho)^2}\frac{k^2}{r^2}\right]G = 0. \tag{4.25}$$

This equation is solved by breaking it into a pair of coupled first order equations by defining a new function,

$$H = \frac{dG}{dx} + \frac{k\rho}{1+\lambda\rho}\frac{G}{r}. \tag{4.26}$$

From Eq. (4.15) we know that $dr = \left(\frac{1+\lambda\rho}{\rho^2}\right)dx$. So using this and Eq. (4.26), Eq. (4.25) will be transformed as,

$$\frac{dH}{dr} - \frac{k}{\rho r}H = 0. \tag{4.27}$$

We know that $\rho = \left(1 - \frac{1}{r}\right)^{\frac{1}{2}}$, thus $\rho r = \left(r^2 - r\right)^{\frac{1}{2}}$. Now to get the solution of Eq. (4.27) we use $\int \frac{dr}{(r^2-r)^{\frac{1}{2}}} = \ln(2(r^2-r)^{\frac{1}{2}} + 2r - 1)$. Thus,

$$\ln H = k\ln(2\sqrt{r^2 - r} + 2r - 1) + \ln\beta_{II}, \tag{4.28}$$

where β_{II} is a constant of integration. This can be rearranged as,

$$H = \beta_{II} \left(\frac{(1+\sqrt{1-\frac{1}{r}})^2}{\frac{1}{r}} \right)^k . \tag{4.29}$$

So we can write,

$$H = \beta_{II} \left(\frac{(1-\sqrt{1-\frac{1}{r}})}{(1+\sqrt{1-\frac{1}{r}})} \right)^{-k} = \beta_{II} \left(\frac{1-\rho}{1+\rho} \right)^{-k} . \tag{4.30}$$

Substituting the equation for H in Eq. (4.26), we will get a first order differential equation in G:

$$\frac{dG}{dx} + \frac{k\rho}{1+\lambda\rho}\frac{G}{r} = \beta_{II} \left(\frac{1-\rho}{1+\rho} \right)^{-k} . \tag{4.31}$$

The above equation can also be written as,

$$\frac{dG}{dr} + \frac{k}{\rho r} G = \beta_{II} \left(\frac{1-\rho}{1+\rho} \right)^{-k} \frac{1+\lambda\rho}{\rho^2}, \tag{4.32}$$

where variable x is changed to r.

Solution for $k > 0$

For $k > 0$, Eq. (4.32) becomes,

$$\frac{dG}{dr} + \frac{k}{\rho r} G = \beta_{II} g, \tag{4.33}$$

where the particular integral is obtained from,

$$\frac{dg}{dr} + \frac{k}{\rho r} g = \left(\frac{1-\rho}{1+\rho} \right)^{-k} \frac{1+\lambda\rho}{\rho^2}. \tag{4.34}$$

This equation is of the form $Y'' + P(x)Y = Q(x)$ and its solution will be $Y = e^{-\int P(x)dx}[\int e^{\int P(x)dx} Q(x)dx]$. Thus solution for Eq. (4.34) will be,

$$g = e^{-\int \frac{k}{r\rho} dr} \left[\int e^{\int \frac{k}{r\rho} dr} \left(\frac{1-\rho}{1+\rho} \right)^{-k} (\frac{1+\lambda\rho}{\rho^2}) dr \right], \tag{4.35}$$

i.e.,

$$g = \left(\frac{1-\rho}{1+\rho}\right)^k \left[\ln\rho^2 + \int_0^\rho \frac{2}{\rho}\left[\frac{1+\lambda\rho}{(1-\rho^2)^2}\left(\frac{1+\rho}{1-\rho}\right)^{2k} - 1\right] d\rho\right]. \tag{4.36}$$

The general solution will be a linear combination of complementary function and particular integral. The complementary function will be found out by following the procedure described to find H. Therefore the solution of Eq. (4.33) at $k > 0$ is,

$$G_{II} = \alpha_{II}(\frac{1-\rho}{1+\rho})^k + \beta_{II}(\frac{1-\rho}{1+\rho})^k[\ln\rho^2 + \int_0^\rho \frac{2}{\rho}[\frac{1+\lambda\rho}{(1-\rho^2)^2}(\frac{1+\rho}{1-\rho})^{2k} - 1]d\rho]. \tag{4.37}$$

Thus Eq. (4.37) represents the wave function in the intermediate region when the value of k is positive.

Solution for $k < 0$

In this case Eq. (4.32) can be written as,

$$\frac{dG}{dr} - \frac{k}{\rho r}G = \beta_{II}\left(\frac{1-\rho}{1+\rho}\right)^k \frac{1+\lambda\rho}{\rho^2}, \tag{4.38}$$

i.e.,

$$\frac{dG}{dr} - \frac{k}{\rho r}G = \beta_{II}g, \tag{4.39}$$

where the particular integral is obtained from,

$$\frac{dg}{dr} - \frac{k}{\rho r}g = \left(\frac{1-\rho}{1+\rho}\right)^k \frac{1+\lambda\rho}{\rho^2}, \tag{4.40}$$

i.e.,

$$g = \left(\frac{1-\rho}{1+\rho}\right)^{-k} \int_0^\rho \frac{2}{\rho}(1+\lambda\rho)\frac{(1+\rho)^{2k-2}}{(1-\rho)^{2k+2}}d\rho. \tag{4.41}$$

Therefore,

$$G_{II} = \alpha_{II}(\frac{1-\rho}{1+\rho})^k + \beta_{II}(\frac{1-\rho}{1+\rho})^{-k}\int_0^\rho \frac{2}{\rho}(1+\lambda\rho)\frac{(1+\rho)^{2k-2}}{(1-\rho)^{2k+2}}d\rho. \tag{4.42}$$

represents the general solution of Eq. (4.39) for $k < 0$.

Solution of the wave equation at far away from the horizon: $r >> 1$ ***(region 3)***

Since $r >> 1$ and also for low energy value, we can neglect the energy terms containing $\frac{1}{r^2}$ in Eq. (4.20) and the equation becomes,

$$\frac{d^2G}{dr^2} + (\frac{1}{r-1} - \frac{1}{r})\frac{dG}{dr} + \left[2\epsilon^2 - m^2 + \frac{2\epsilon^2 - m^2}{r} - \frac{k\,(k+1)}{r^2}\right] G = 0, \tag{4.43}$$

where $\epsilon^2 - m^2 = p^2 = (\epsilon v)^2$ represents momentum. Since $r >> 1$, we will get

$$\frac{d^2G}{dr^2} + \left[p^2 + \frac{\epsilon^2 + p^2}{r} - \frac{k\,(k+1)}{r^2}\right] G = 0. \tag{4.44}$$

Solution of the above equation is given by,

$$G_{III} = \alpha_{III} F_l^c \left(-\frac{\epsilon\left(1+v^2\right)}{2v}, \epsilon v r\right) + \beta_{III} G_l^c \left(-\frac{\epsilon\left(1+v^2\right)}{2v}, \epsilon v r\right). \tag{4.45}$$

In the asymptotic region, Eq. (4.45) can be written as,

$$G_{III} = \alpha_{III} C_l\,(-\eta)\,(\epsilon v r)^{l+1} + \beta_{III} \frac{(\epsilon v r)^{-l}}{(2l+1)\,C_l\,(\eta)}, \tag{4.46}$$

where $\eta = \frac{\epsilon\left(1+v^2\right)}{2v}$ and

$$|C_l\,(-\eta)\,|^2 = \frac{2^{2l+1}\pi\eta}{(2l+1)!^2\,(1-e^{-2\pi\eta})} \prod_{s=1}^{l} \left(s^2 + \eta^2\right), \tag{4.47}$$

where we define $l = k$ for $k > 0$ and $l = -k - 1$ for $k < 0$. We will now compare solutions in different regions.

Comparing solutions in regions 1 and 2

The two regions 1 and 2 do not really lead to any overlap region. However, near the point $r = 1$, but not very close, i.e., $r - 1 << 1$,

we can approximate G_I as $\exp(\imath\epsilon \ln(r-1)) = 1 + \imath\epsilon \ln(r-1)$. Eq. (4.22) now becomes,

$$G_I = (1+|R|) - \imath\epsilon\,(1-|R|)\ln(r-1), \tag{4.48}$$

In the limit $r \to 1$, $\rho \to 0$ and the wave function for region 2 in this limit, becomes,

$$G_{II} = \alpha_{II} + \beta_{II} \ln(r-1)\,, \tag{4.49}$$

Thus matching the solutions at the boundary of regions 1 and 2 :

$$\alpha_{II} = 1 + |R|, \beta_{II} = -\imath\epsilon\,(1-|R|)\,. \tag{4.50}$$

The Eq. (4.50) gives the connection of α, β with $|R|$

Comparing solutions in regions 2 and 3

For $k > 0$, Eq. (4.37) can be written as,

$$G_{II} = \alpha_{II}(\frac{1-\rho^2}{(1+\rho)^2})^k + \beta_{II}(\frac{1-\rho^2}{(1+\rho)^2})^k[\ln\rho^2 + \int_0^r \frac{2}{\rho}[\frac{1+\lambda\rho}{(1-\rho^2)^2}(\frac{1+\rho}{1-\rho})^{2k} - 1](\frac{(1-\rho^2)^2}{2\rho})dr], \tag{4.51}$$

when $r >> 1$, $\rho \simeq 1$ so, $1+\rho \simeq 2$ and $1-\rho^2 = \frac{1}{r}$. Therefore,

$$G_{II} = \alpha_{II}\left(\frac{1}{4r}\right)^k + \beta_{II}\left(\frac{1}{4r}\right)^k \int_0^r (1+\lambda)\,(4r)^{k+1}\,dr, \tag{4.52}$$

i.e.,

$$G_{II} = \frac{\alpha_{II}}{(4r)^k} + \frac{\beta_{II}\,(1+\lambda)}{4\,(2k+1)}\,(4r)^{2k}\,. \tag{4.53}$$

For $k < 0$, Eq. (4.37) can be written as,

$$G_{II} = \alpha_{II}(\frac{1-\rho^2}{(1+\rho)^2})^{-k} + \beta_{II}(\frac{1-\rho^2}{(1+\rho)^2})^{-k} \int_\infty^r \frac{1+\lambda\rho}{\rho^2}(\frac{1-\rho^2}{(1+\rho)^2})dr. \tag{4.54}$$

For $r >> 1$, above equation becomes,

$$G_{II} = \alpha_{II}\left(\frac{1}{4r}\right)^{-k} + \beta_{II}\left(\frac{1}{4r}\right)^{-k} \int_\infty^r \frac{(1+\lambda)}{(4r)^{2k}}\,dr, \tag{4.55}$$

i.e.,

$$G_{II} = \alpha_{II} (4r)^k + \frac{\beta_{II} (1+\lambda)}{4 (2k-1)} \frac{1}{(4r)^{k-1}}. \tag{4.56}$$

Eq. (4.46) for $k > 0$ becomes,

$$G_{III} = \alpha_{III} C_k (-\eta) (\epsilon v r)^{k+1} + \beta_{III} \frac{(\epsilon v r)^{-k}}{(2k+1) C_k (\eta)}, \tag{4.57}$$

and for $k < 0$ we get,

$$G_{III} = \alpha_{III} C_{k-1} (-\eta) (\epsilon v r)^{k} + \beta_{III} \frac{(\epsilon v r)^{-k+1}}{(2k-1) C_{k-1} (\eta)}, \tag{4.58}$$

Here also the two solutions in regions 2 and 3 for $k > 0$ and $k < 0$ have same form in the limit $r >> 1$. Thus on comparing Eq. (4.53) with Eq. (4.57), we will get for $k > 0$,

$$\frac{\alpha_{II}}{(4)^k} = \beta_{III} \frac{(\epsilon v)^{-k}}{(2k+1) C_k (\eta)}, \tag{4.59}$$

and

$$\frac{\beta_{II} (1+\lambda)}{4 (2k+1)} (4)^{k+1} = \alpha_{III} C_k (-\eta) (\epsilon v)^{k+1}. \tag{4.60}$$

Substituting the values of α_{II} and β_{II} from Eq. (4.50) we will get, for $k > 0$,

$$\frac{\beta_{III}}{\alpha_{III}} = \frac{\frac{(2k+1) C_k (\eta) (\epsilon v)^k (1+R)}{4^k}}{-\imath \frac{4^{k+1} (1+\lambda)(1-R)}{C_k (-\eta) \epsilon^k v^{k+1}}} = \imath \frac{(2k+1)^2 |C_k (\eta)|^2 \epsilon^{2k} v^{2k+1}}{4^{2k} (1+\lambda) \xi}, \tag{4.61}$$

where $\xi = \frac{1-R}{1+R}$. Now comparing Eq. (4.56) with Eq. (4.58) we will get (for $k < 0$),

$$\frac{\beta_{II} (1+\lambda)}{4 (2k-1)} \frac{1}{(4)^{k-1}} = \beta_{III} \frac{(\epsilon v)^{-k+1}}{(2k-1) C_{k-1} (\eta)}, \tag{4.62}$$

and

$$\alpha_{II} (4)^k = \alpha_{III} C_{k-1} (-\eta) (\epsilon v)^k. \tag{4.63}$$

For $k < 0$, we find

$$\frac{\beta_{III}}{\alpha_{III}} = \frac{\frac{-\imath\frac{(1+\lambda)C_{k-1}(\eta)\epsilon^k v^{k-1}(1-R)}{4^k}}{\frac{(4r)^k(1-R)}{C_{k-1}(-\eta)(\epsilon v)^k}}}{} = \frac{-\imath(1+\lambda)|C_{k-1}(\eta)|^2\epsilon^{2k}v^{2k-1}\xi}{4^{2k}}. \tag{4.64}$$

Thus for positive and negative values of k, $\frac{\beta_{III}}{\alpha_{III}}$ depends on the reflection coefficient R through ξ.

4.4 Absorption cross section and emission spectra

We will find expressions for the absorption cross section and the emission spectra of Schwarzschild black hole perturbed by Dirac fields.[26] Absorption cross section is defined as:

$$\sigma_{\alpha bs} = \frac{\pi}{p^2}\sum k\Gamma_j, \tag{4.65}$$

where

$$\Gamma_j = \frac{2i\left(\frac{\beta^*_{III}}{\alpha^*_{III}} - \frac{\beta_{III}}{\alpha_{III}}\right)}{|1+\imath\frac{\beta_{III}}{\alpha_{III}}|^2}. \tag{4.66}$$

From Eq. (4.61) (for $k > 0$) we get,

$$\Gamma_{k>0} = \frac{\pi\epsilon^{2k+1}v^{2k}\left(1+v^2\right)}{\xi 2^{2k-2}\left(1+\lambda\right)(2k)!^2\left(1-e^{\frac{-\pi\epsilon\left(1+v^2\right)}{v}}\right)}\prod_{s=1}^{k}(s^2+(\frac{\epsilon(1+v^2)}{2v})^2), \tag{4.67}$$

for $k < 0$, we get from Eq. (4.64),

$$\Gamma_{k<0} = \frac{\pi\epsilon^{2k+1}v^{2k-2}\left(1+\lambda\right)\xi\left(1+v^2\right)}{2^{2k}\left(2k-1\right)!^2\left(1-e^{\frac{-\pi\epsilon\left(1+v^2\right)}{v}}\right)}\prod_{s=1}^{k-1}\left(s^2+\left(\frac{\epsilon\left(1+v^2\right)}{2v}\right)^2\right). \tag{4.68}$$

Therefore, the expression for absorption cross section becomes,

$$\sigma_{abs} = \frac{\pi}{(\epsilon v)^2} \sum |k| \left(|\Gamma_{k>0}| + |\Gamma_{k<0}| \right). \tag{4.69}$$

and

$$\sigma_{abs}(k=1) = \frac{\pi}{(\epsilon v)^2} \left(\Gamma_{1>0} + \Gamma_{1<0} \right), \tag{4.70}$$

Substituting expression for $\Gamma_{1>0}$ and $\Gamma_{1<0}$ from Eqs.(4.67) and (4.68),

$$\sigma_{abs}(k=1) = \frac{\pi}{(\epsilon v)^2} \frac{\pi\epsilon^3 \left(1+v^2\right)}{4\left(1 - e^{\frac{-\pi\epsilon\left(1+v^2\right)}{v}}\right)} \left(\frac{v^2}{(1+\lambda)\,\xi} + (1+\lambda)\,\xi \right). \tag{4.71}$$

Substituting $v^2 = 1 - \frac{m_o^2}{\epsilon^2} = 1 - \lambda^2$, the expression for σ_{abs} becomes

$$\sigma_{abs}(k=1) = \frac{\pi^2\epsilon \left(1+v^2\right)}{4v^2\left(1 - e^{\frac{-\pi\epsilon\left(1+v^2\right)}{v}}\right)\xi} \left((1-\lambda) + (1+\lambda)\,\xi^2 \right). \tag{4.72}$$

We know that,

$$\xi = \frac{1 - e^{-2\pi\epsilon}}{1 + e^{-2\pi\epsilon}} = \tanh \pi\epsilon. \tag{4.73}$$

For low energy case we can approximate $\xi \simeq \pi\epsilon$ then, $1 + \xi^2 \simeq 1 + 2\pi^2\epsilon^2$ and $\xi^2 - 1 \simeq -1$. Therefore Eq. (4.72) becomes,

$$\sigma_{abs}(k=1) = \frac{\pi^2\epsilon \left(1+v^2\right)}{4v^2\left(1 - e^{\frac{-\pi\epsilon\left(1+v^2\right)}{v}}\right)} \left(\frac{2\pi^2\epsilon^2}{\pi\epsilon} + \frac{1-\lambda}{\pi\epsilon} \right). \tag{4.74}$$

On simplification we get

$$\sigma_{abs}(k=1) \simeq \frac{\pi^3\epsilon^2 \left(1+v^2\right)}{2v^2\left(1 - e^{\frac{-\pi\epsilon\left(1+v^2\right)}{v}}\right)} \simeq \frac{\pi^2\epsilon}{2v}. \tag{4.75}$$

When the effect of reflection is neglected, i.e., when $R = 0$ then $\xi = 1$, then Eq. (4.72) becomes,

$$\sigma_{abs}(k=1) = \frac{\pi^2\epsilon \left(1+v^2\right)}{4v^2\left(1 - e^{\frac{-\pi\epsilon\left(1+v^2\right)}{v}}\right)} 2 = \frac{\pi^2\epsilon \left(1+v^2\right)}{2v^2\left(1 - e^{\frac{-\pi\epsilon\left(1+v^2\right)}{v}}\right)}, \tag{4.76}$$

which agrees with the results obtained earlier.[43] Now for $k = 2$,

$$\sigma_{abs}\left(k=2\right) = \frac{\pi^2}{8*\left(3!\right)^2}\frac{\epsilon^3\left(1+v^2\right)}{\left(1-e^{\frac{-\pi\epsilon\left(1+v^2\right)}{v}}\right)}\left(1+\left(\frac{\epsilon\left(1+v^2\right)}{2v}\right)^2\right)$$
$$\left(\frac{v^2}{4\left(1+\lambda\right)\xi}\left(4+\left(\frac{\epsilon\left(1+v^2\right)}{2v}\right)^2\right)+\left(1+\lambda\right)\xi\right)$$
$$= \frac{\pi^2}{288}\frac{\epsilon^3\left(1+v^2\right)}{\left(1-e^{\frac{-\pi\epsilon\left(1+v^2\right)}{v}}\right)}\left(1+\left(\frac{\epsilon\left(1+v^2\right)}{2v}\right)^2\right)$$
$$\left(\frac{1}{\xi}\left(1-\lambda)+\left(1+\lambda\right)\xi^2+\frac{\epsilon^2\left(1+v^2\right)^2}{16v^2}\right)\right). \qquad (4.77)$$

For low energy case total absorption cross section is,

$$\sigma_{abs} \simeq \frac{\pi^2\epsilon}{2v}+\frac{\pi^2\epsilon^3 v}{144}\left(1+\left(\frac{\epsilon\left(1+v^2\right)}{2v}\right)^2\right). \qquad (4.78)$$

For a static black hole, the quantum particle emission rate $H(\epsilon)$ and the absorption cross section σ_{abs} are related by Hawking's formula,[15]

$$H\left(\epsilon\right) = \frac{\sigma_{abs}\left(\epsilon\right)}{\exp(\frac{\epsilon}{T})+1}, \qquad (4.79)$$

where T is the Hawking temperature. The emission spectrum is obtained from the above formula and is shown in Figure 4.2. By studying the emission spectra it was found that the effect of higher modes are negligible when compared with $k = 1$.

4.5 Conclusion

We have found the wave functions $G_I(r)$ in the vicinity of event horizon of Schwarzschild black hole i.e., $r \to 1$, $G_{II}(r)$ in the region $r > 1$ and $G_{III}(r)$ in the asymptotic region for Dirac field.

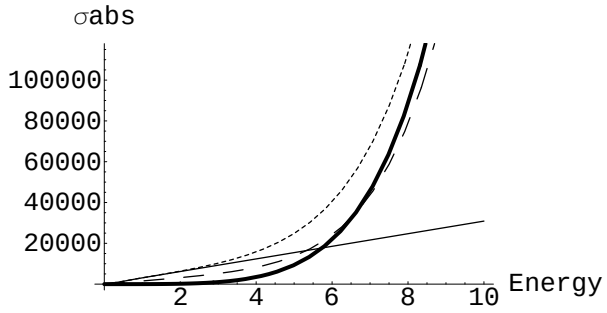

Figure 4.1: σ_{abs} versus ϵ for Schwarzschild black hole in Dirac field is plotted. The solid curve is absorption cross for $k = 1$, dotted curve is absorption cross for $k = 2$, and the bold curve is the absorption cross section for $k = 1 + k = 2$ of Dirac waves which undergo reflection in the presence of Schwarzschild black hole. The dashed curve is the same for the Dirac wave which don't undergo reflection.

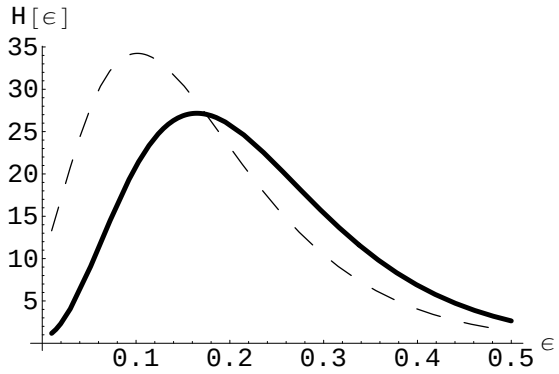

Figure 4.2: Emission spectrum for Schwarzschild black hole in Dirac field is plotted. The bold curve is the emission spectrum for Dirac waves which undergo reflection in the presence of Schwarzschild black hole. The dotted curve is the same for the Dirac wave which don't undergo reflection.

We have also studied the behavior of scattered Dirac waves in

all these regions in low energy limit. By comparing the solutions in the 3 regions viz., $r \to 1$, $r > 1$ and $r \gg 1$, the absorption cross section of Schwarzschild black hole in Dirac field for $k = 1$ is found to be $\frac{1}{8}$ of absorption cross section of Schwarzschild black hole in scalar field, which agrees with the results obtained earlier.[43,64] We also found the absorption cross section for $k = 2$ in Dirac field. We have plotted the absorption cross section for $k = 1$ and for $k = 2$ separately and combined absorption cross section of Schwarzschild black hole in Dirac field with and without reflection and is shown in Figure 4.1. Emission spectrum for Schwarzschild black hole in Dirac field with and without reflection is plotted in Figure 4.2 and found that higher modes have negligible effect when compared to $k = 1$.

5

Quasi-normal modes of spherically symmetric black hole space-times with cosmic string in a Dirac field

5.1 Introduction

The question of stability of black hole was first studied by Regge and Wheeler[107] who investigated linear perturbations of the exterior Schwarzschild space-time. Further work[34] on this problem led to the study of quasi-normal modes which is believed as a characteristic sound of black holes. Quasi-normal modes (QNMs) describe the damped oscillations under perturbations in the surrounding geometry of a black hole with frequencies and damping times of oscillations entirely fixed by the black hole parameters. The study of QNMs has become an intriguing subject of discussion during the last few decades,[108–111] and references therein. QNMs carry unique finger prints of black holes and it is well known that they are crucial in studying the gravitational and electromagnetic perturbations around black hole space-times. They are also seem to have an observational significance as the gravitational waves produced by the

perturbations, in principle, can be used for unambiguous detection of black holes. This motivates us to study the quasi-normal mode spectra of black holes.

The motivation of the present work is to study the signature of cosmic strings on QNMs. Although the study of black-hole quasi-normal modes has a long history, most works are concentrated on the wave fields with spins 0, 1 and 2. We know that the field of spin 1/2 is of great importance in quantum physics and thus it is very necessary to investigate its quasi-normal modes in a black-hole space-time. Cho,[112] Wu[113] and Jing[114] evaluated respectively the Dirac fields quasi-normal frequencies in the Schwarzschild, Reissner-Nordstrom and Reissner-Nordstrom-de Sitter space-times recently. However, the question of how the dilation field affects the Dirac quasi-normal modes of a black hole having string still remains open.

The QNMs of scalar perturbations around a Schwarzschild black hole pierced by a cosmic string was studied earlier.[115] In the present work we study the influence of cosmic string on the QNMs of various black hole background space-times which are perturbed by a massless Dirac field. Section 5.2 gives a detailed description of cosmic string. In section 5.3, we study the Dirac equation in a general spherically symmetric space-time with a cosmic sting and its deduction into a set of second order differential equations. In section 5.4, we evaluate the Dirac quasi-normal frequencies for the massless case using WKB scheme for Schwarzschild, RN extremal, SdS and near extremal SdS black hole space-times. Conclusion of the chapter is given in section 5.5

5.2 Cosmic string

Cosmic string is considered to be 1-dimensional topological defect in the fabric of space-time. Such defects are stable configurations of matter formed during the phase transition at the end of the grand

unification era. These topological defects, may come in with different structures such as monopoles, strings, domain walls etc and among them, cosmic string has been proved to be the most potential one for cosmic structure formation.[116] Cosmic string is a line like relic of high energy density or in otherwise empty space that contain energy field, the Higgs field, etc.

A string can be either of infinite in length or a close loop and in either case, the string tension will generally cause it to oscillate at velocities close to the speed of light, which yield an asymmetric, highly dynamic structure whose gravitational field cannot be easily calculated. Vilenkin[117] has taken an important first step in studying the gravitational effects of strings. He found that the gravitational field of a straight string in the linear approximation to general relativity has the peculiar property that the Newtonian potential vanishes, yet there are nontrivial gravitational effects. He also described the space-time exterior to a string as conical in nature, with the deficit angle of the cone equal to $8\pi\breve{\mu}$, to first order in $\breve{\mu}$, where $\breve{\mu}$ is the linear density of the string and the conical nature of the space outside the string produces observable effects such as light deflection.

The unusual gravitational field of a string is due to a negative pressure. The equation of state of the matter in the interior of the string is[118]

$$p_1 = \rho_E, p_2 = p_3 = 0, \tag{5.1}$$

where ρ_E is the energy density, p_1 is the pressure along the axis of the string, and p_2 and p_3 are the pressure perpendicular to this axis, averaged over a cross section. Thus the source for the Newtonian potential $\rho_E + p_1 + p_2 + p_3$ in the linearized gravity theory vanishes which explains the absence of Newtonian gravitational effects. This applies only for straight stings. A non-zero gravitational potential will exist for a curved infinite string or for a closed loop.

5.2.1 Importance of cosmic string

The possibility of having strings in the early universe has been suggested by Kibble in 1976.[119] Cosmic strings seem to be of particular interest because they provide a unique tool to learn the physics of the very early universe and are considered as a possible "seed" for galaxy formation[120,121] and as a possible gravitational lens.[117] The cosmic strings are very important in the study of black holes because they may sometimes act as "hairs" for black holes. A black hole with cosmic string could be formed in a phase transition. A flux tube of a confined gauge field consists of a possible string. Above the transition temperature, a spherically symmetric Coulomb type field will possess a black hole containing a non-zero magnetic charge. If the above system is cooled below the transition temperature, then the field becomes confined and strings emanating from the black hole would be formed. The total flux carried by the strings must be equal to the net flux across the black hole horizon before the transition according to Gauss theorem. Field such as the electromagnetic and Yang-Mills field that are associated with Gauss law do not violate the dictum that "black holes have no hair". Nonetheless a black hole may have "hairs" in the form of strings and thus it is important.

5.3 General metric for a black hole with cosmic string space-time perturbed by a Dirac field

The metric describing a spherically symmetric black hole with a cosmic string can be written as,[118]

$$ds^2 = -f(r)dt^2 + \frac{dr^2}{f\,(r)} + r^2 d\theta^2 + b^2 r^2 \sin^2\theta d\phi^2. \qquad (5.2)$$

It can be constructed by removing a wedge, which is done by requiring that the azimuthal angle around the axis runs over the range

$0 < \phi' < 2\pi b$, with $\phi' = b\phi$ where ϕ runs over zero to 2π. Here $b = 1 - 4\check{\mu}$ with $\check{\mu}$ being the linear mass density of the string. Here we are following the procedure adopted in reference[74] and develop the Dirac equation in a general background space-time. We start with the Dirac equation;

$$(\gamma^{\mu}(\partial_{\mu} - \Gamma_{\mu}) + m)\,\Psi = 0, \tag{5.3}$$

where m is the the mass of the Dirac field. Here

$$\gamma^{\mu} = g^{\mu\nu}\gamma_{\nu}, \tag{5.4}$$

and

$$\gamma_{\nu} = e^{a}_{\nu}\gamma_{a}, \tag{5.5}$$

where γ^{a} are the Dirac matrices,

$$\gamma_0 = \begin{bmatrix} \imath & 0 \\ 0 & -\imath \end{bmatrix}, \gamma_i = \begin{bmatrix} 0 & \sigma_i \\ \sigma_i & 0 \end{bmatrix}, \tag{5.6}$$

and σ_i are the Pauli matrices. e^{a}_{ν} is the tetrad given by,

$$e^{t}_{t} = f^{\frac{1}{2}}, e^{r}_{r} = \frac{1}{f^{\frac{1}{2}}}, e^{\theta}_{\theta} = r, e^{\phi}_{\phi} = br\sin\theta. \tag{5.7}$$

The inverse of the tetrad e^{a}_{ν} is defined by,

$$g^{\mu\nu} = \eta^{ab}e^{\mu}_{a}e^{\nu}_{b}, \tag{5.8}$$

with $\eta^{ab} = diag(-1, 1, 1, 1)$, the Minkowski metric. The spin connection Γ_{μ} is given by

$$\Gamma_{\mu} = -\frac{1}{2}[\gamma_a, \gamma_b]e^{a}_{\nu}e^{b\nu}_{;\mu}, \tag{5.9}$$

where $e^{b\nu}_{;\mu} = \partial_{\mu}e^{b\nu} + \Gamma^{\nu}_{\kappa\mu}e^{b\kappa}$ is the covariant derivative of $e^{b\nu}$. The spin connections for the above metric are obtained as,

$$\Gamma_t = \frac{1}{4}\gamma_1\gamma_0\frac{\partial f(r)}{\partial r}, \tag{5.10}$$

$$\Gamma_r = 0, \tag{5.11}$$

$$\Gamma_{\theta} = \frac{1}{2}\gamma_1\gamma_2 f^{\frac{1}{2}}(r), \tag{5.12}$$

$$\Gamma_{\phi} = \frac{1}{2}\gamma_2\gamma_3 b\cos\theta + \frac{1}{2}\gamma_1\gamma_3 b\sin\theta f^{\frac{1}{2}}(r). \tag{5.13}$$

Substituting the spin connections in Eq. (5.3) we will get ,

$$[\frac{-\gamma_0}{f^{\frac{1}{2}}}\frac{\partial}{\partial t}+\gamma_1 f^{\frac{1}{2}}(\frac{\partial}{\partial r}+\frac{1}{r}+\frac{1}{4f(r)}\frac{\partial f}{\partial r})+\frac{\gamma_2}{r}(\frac{\partial}{\partial\theta}+\frac{1}{2}\cot\theta) + \frac{\gamma_3}{br\sin\theta}\frac{\partial}{\partial\phi}+m]\Psi(t,r,\theta,\phi)=0, \tag{5.14}$$

Using the transformation $\Psi(t,r,\theta,\phi)=\frac{\exp(-\imath Et)}{rf^{\frac{1}{4}}\sin\theta^{\frac{1}{2}}}\chi(r,\theta,\phi)$, Eq. (5.14) becomes,

$$[\frac{-E}{f^{\frac{1}{2}}}\frac{\partial}{\partial t}+\frac{1}{\imath}\gamma_0\gamma_1 f^{\frac{1}{2}}(\frac{\partial}{\partial r})+\frac{\gamma_1}{\imath r}\gamma_1\gamma_0(\gamma_2\frac{\partial}{\partial\theta} + \frac{\gamma_3}{b\sin\theta}\frac{\partial}{\partial\phi})-\imath\gamma_0 m]\chi(r,\theta,\phi)=0. \tag{5.15}$$

Dirac equation can be separated out into radial and angular parts by the following substitution,

$$\chi(r,\theta,\phi)=R(r)\Omega(\theta,\phi). \tag{5.16}$$

The angular momentum operator is introduced as,[74]

$$\mathbf{K}_{(b)}=-\imath\gamma_1\gamma_0\left(\gamma_2\partial_\theta+\gamma_3\left(b\sin\theta\right)^{-1}\partial_\phi\right), \tag{5.17}$$

such that,

$$\mathbf{K}_{(b)}\Omega(\theta,\phi)=k_b\Omega(\theta,\phi), \tag{5.18}$$

where $k_b=\frac{k}{b}$ are the eigenvalues of $\mathbf{K}_{(b)}$. Here k is a positive or a negative non-zero integer with $l=|k+\frac{1}{2}|-\frac{1}{2}$, where l is the total orbital angular momentum. The presence of cosmic string is codified in the eigenvalues of the angular momentum operator.[122] Substituting Eqs.(5.16) and (5.18) in Eq. (5.15), we will get radial equation which contains γ_0 and γ_1. As γ_0 and γ_1 can be represented by 2×2 matrices, we write the radial factor $R(r)$ by a two component spinor notation,

$$R(r)=\begin{bmatrix}F\\G\end{bmatrix}. \tag{5.19}$$

Then the radial equation in F and G are given by,

$$f\frac{dG}{dr} + f^{\frac{1}{2}}\frac{k_b}{r}G + f^{\frac{1}{2}}mF = EF, \tag{5.20}$$

$$f\frac{dF}{dr} - f^{\frac{1}{2}}\frac{k_b}{r}F + f^{\frac{1}{2}}mG = -EG. \tag{5.21}$$

Introducing a co-ordinate change as,

$$dr_* = \frac{dr}{f}, \tag{5.22}$$

Eq. (5.20) and Eq. (5.21) can be combined into a single equation as,

$$\frac{\partial}{\partial r_*}\begin{bmatrix} G \\ F \end{bmatrix} + f^{\frac{1}{2}}\begin{bmatrix} \frac{k_b}{r} & m \\ m & -\frac{k_b}{r} \end{bmatrix}\begin{bmatrix} G \\ F \end{bmatrix} = \begin{bmatrix} 0 & E \\ -E & 0 \end{bmatrix}\begin{bmatrix} G \\ F \end{bmatrix}. \tag{5.23}$$

Defining,

$$\begin{bmatrix} \hat{G} \\ \hat{F} \end{bmatrix} = \begin{bmatrix} \cos\frac{\theta}{2} & -\sin\frac{\theta}{2} \\ \sin\frac{\theta}{2} & \cos\frac{\theta}{2} \end{bmatrix}\begin{bmatrix} G \\ F \end{bmatrix}, \tag{5.24}$$

where for positive value of k,

$$\theta = \tan^{-1}(\frac{mr}{|k_b|}). \tag{5.25}$$

Eq. (5.23) now becomes,

$$\frac{\partial}{\partial r_*}\begin{bmatrix} \hat{G} \\ \hat{F} \end{bmatrix} + f^{\frac{1}{2}}\sqrt{\left(\frac{k_b}{r}\right)^2 + m^2}\begin{bmatrix} 1 & 0 \\ 0 & -1 \end{bmatrix}\begin{bmatrix} \hat{G} \\ \hat{F} \end{bmatrix} = \tag{5.26}$$
$$-E\left[1 + \frac{1}{2E}\frac{fm|k_b|}{{k_b}^2 + m^2r^2}\right]\begin{bmatrix} 0 & -1 \\ 1 & 0 \end{bmatrix}\begin{bmatrix} \hat{G} \\ \hat{F} \end{bmatrix}.$$

By making another change of the variable;

$$d\hat{r}_* = \frac{dr_*}{\left[1 + \frac{1}{2E}\frac{fm|k_b|}{k_b^2 + m^2r^2}\right]}. \tag{5.27}$$

Eq. (5.27) can be simplified to,

$$\frac{\partial}{\partial \hat{r}_*}\begin{bmatrix} \hat{G} \\ \hat{F} \end{bmatrix} + \frac{f^{\frac{1}{2}}\sqrt{\left(\frac{k_b}{r}\right)^2 + m^2}}{\left[1 + \frac{1}{2E}\frac{fm|k_b|}{k_b^2 + m^2r^2}\right]}\begin{bmatrix} 1 & 0 \\ 0 & -1 \end{bmatrix}\begin{bmatrix} \hat{G} \\ \hat{F} \end{bmatrix}$$
$$= E\begin{bmatrix} 0 & 1 \\ -1 & 0 \end{bmatrix}\begin{bmatrix} \hat{G} \\ \hat{F} \end{bmatrix}, \tag{5.28}$$

i.e.,

$$\frac{\partial}{\partial \hat{r}_*}\begin{bmatrix}\hat{G}\\ \hat{F}\end{bmatrix}+W\begin{bmatrix}\hat{G}\\ -\hat{F}\end{bmatrix}=E\begin{bmatrix}\hat{F}\\ -\hat{G}\end{bmatrix}, \tag{5.29}$$

where

$$W=\frac{f^{\frac{1}{2}}\sqrt{\left(\frac{k_b}{r}\right)^2+m^2}}{\left[1+\frac{1}{2E}\frac{fm|k_b|}{k_b^2+m^2r^2}\right]}. \tag{5.30}$$

Thus from Eq. (5.29), we will get two coupled equations for $\hat{G}$ and $\hat{F}$ which are given bellow,

$$-\frac{\partial^2\hat{F}}{\partial\hat{r}_*^2}+V_1\hat{F}=E^2\hat{F}, \tag{5.31}$$

$$-\frac{\partial^2\hat{G}}{\partial\hat{r}_*^2}+V_2\hat{G}=E^2\hat{G}, \tag{5.32}$$

where

$$V_{1,2}=\pm\frac{\partial W}{\partial\hat{r}_*}+W^2. \tag{5.33}$$

From Eq. (5.31) and Eq. (5.32), we can evaluate the quasi-normal mode frequencies for various black hole space-times. Here V_1 and V_2 are the super symmetric partners derived from the same super potential W and these potentials give same spectra of quasi-normal mode frequencies.[123]

5.4 Quasi-normal mode frequencies

We shall now evaluate the quasi-normal frequencies for various black hole space-times perturbed by a massless Dirac field using WKB approximation. As V_1 and V_2 give same spectra of quasi-normal mode frequencies we avoid the subscripts and write V for the potential function. Thus, for massless case the equation for the potential given by Eq. (5.33) becomes,

$$V=f\frac{\partial\left(f^{\frac{1}{2}}\frac{k_b}{r}\right)}{\partial r}+f\left(\frac{k_b}{r}\right)^2. \tag{5.34}$$

Thus, the effective potential for various black hole space-times is obtained by substituting the corresponding f in Eq. (5.34).

5.4.1 Schwarzschild black hole

We first consider the most simple black hole, viz., the Schwarzschild black hole for which,

$$f(r) = \left(1 - \frac{2M}{r}\right). \tag{5.35}$$

Substituting the above f in Eq. (5.34) we get,

$$V = \left(1 - \frac{2M}{r}\right) \frac{\partial}{\partial r} \left(\left(1 - \frac{2M}{r}\right)^{\frac{1}{2}} \frac{k_b}{r} \right) + \left(1 - \frac{2M}{r}\right) \left(\frac{k_b}{r}\right)^2, \tag{5.36}$$

where M is the mass of the Schwarzschild black hole. The effective potential V which depends on the absolute value of k_b, is in the form of a barrier. The peak of the barrier gets higher and higher as $|k|$ increases for fixed b values. We repeat the calculation for different b values ($b = 1, 0.5, 0.1$), and find that the height of the potential increases with b values decreasing. i.e., the presence of the cosmic string, causes an increase in the height of the potential (Figure 5.1).

To evaluate the quasi-normal mode frequencies, we use the WKB approximation.[36–38] This method can be accurate for both real and imaginary parts of the frequencies for low lying modes with $n \prec k$, where n is the mode number and k is the angular momentum quantum number.

The formula for complex quasi-normal mode frequencies E in the WKB approximation, carried out to third order is,

$$E^2 = \left[V_0 + \left(-2V_0''\right)^{\frac{1}{2}} \Lambda\right] - i\left(n + \frac{1}{2}\right)\left(-2V_0''\right)^{\frac{1}{2}} (1 + \Omega), \tag{5.37}$$

where

$$\Lambda = \frac{1}{(-2V_0'')^{1/2}}\left[\frac{1}{8}\left(\frac{V_0^{(4)}}{V_0''}\right)\left(\frac{1}{4}+\alpha^2\right) - \frac{1}{288}\left(\frac{V_0'''}{V_0''}\right)^2\left(7+60\alpha^2\right)\right], \tag{5.38}$$

$$\Omega = \frac{1}{(-2V_0'')}\left\{\begin{array}{c} \frac{5}{6912}\left(\frac{V_0'''}{V_0''}\right)^4\left(77+188\alpha^2\right) \\ -\frac{1}{384}\left(\frac{V_0'''^2 V_0^{(4)}}{V_0''^3}\right)\left(51+100\alpha^2\right) \\ +\frac{1}{2304}\left(\frac{V_0^{(4)}}{V_0''}\right)^2\left(67+68\alpha^2\right) \\ +\frac{1}{288}\left(\frac{V_0''' V_0^{(5)}}{V_0''^2}\right)\left(19+28\alpha^2\right) \\ -\frac{1}{288}\left(\frac{V_0^{(6)}}{V_0''}\right)\left(5+4\alpha^2\right) \end{array}\right\}. \tag{5.39}$$

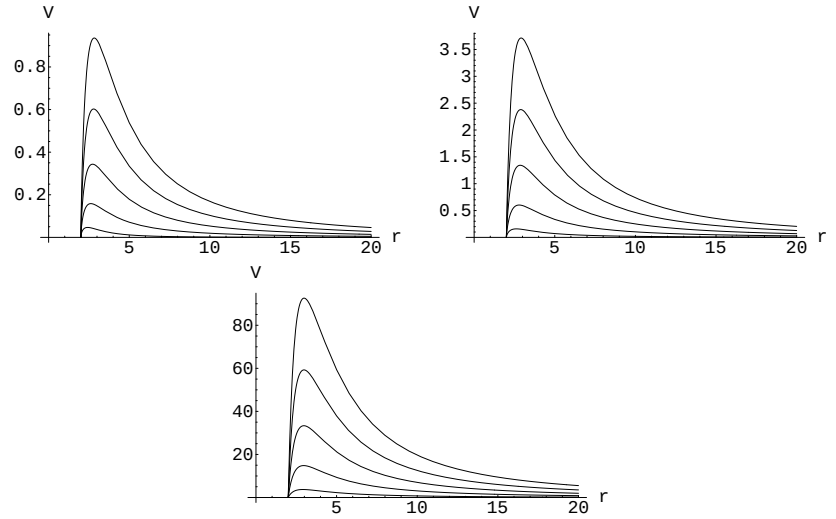

Figure 5.1: Potential versus r for Schwarzschild black hole with cosmic string in Dirac field is plotted for different values of b ($b = 1, 0.5, 0.1$) for $k = 0$ to $k = 5$.

Here

$$\alpha = n + \frac{1}{2}, n = \{\begin{array}{c} 0, 1, 2, ..., Re(E) > 0 \\ -1, -2, -3, ..., RE(E) < 0, \end{array} \tag{5.40}$$

$$V_0^{(n)} = \frac{d^n V}{dr_*^n} \mid_{r_*=r_*(r_{\max})}, \tag{5.41}$$

where the values of n lie in the range: $0 \leq n < k$.

Table 5.1: Quasi-normal frequencies of Schwarzschild black hole with cosmic string.

b	k	n	ReE	ImE
0.1	1	0	1.92351	-0.0962324
	2	0	3.84851	-0.0962269
		1	3.84584	-0.288768
	3	0	5.77297	-0.0966667
		1	5.77131	-0.290031
		2	5.768	-0.483485
	4	0	7.69776	-0.0962255
		1	7.69642	-0.288698
		2	7.69375	-0.481236
		3	7.68976	-0.673882
	5	0	9.62231	-0.0962253
		1	9.62124	-0.28869
		2	9.6191	-0.481196
		3	9.6159	-0.673772
		4	9.61165	-0.866445
0.5	1	0	0.378627	-0.0965424
	2	0	0.767194	-0.096276
		1	0.753957	0.291048
	3	0	1.15303	-0.0962463
		1	1.14416	-0.289714
		2	1.12741	-0.485759
	4	0	1.53836	-0.0962367
		1	1.5317	-0.289257
		2	1.51881	-0.483803
		3	1.50043	-0.680554
	5	0	1.92351	-0.0962324
		1	1.91818	-0.289047
		2	1.90773	- 0.482862
		3	1.89259	- 0.678198
		4	1.87327	- 0.87539

Plugging the effective potential in Eq. (5.36) in to the formula given above, we obtain the complex quasi-normal mode frequencies for Schwarzschild black hole having cosmic string perturbed by a massless Dirac field. The values of $Re(E)$ and $Im(E)$ calculated for different values of b are given in Table (5.1 & 5.2).

For a fixed b value, $Re(E)$ decreases as the mode number n increases for the same angular momentum quantum number k and $|Im(E)|$ increases with n. This indicates that quasi-normal modes with higher mode numbers decay faster than the low-lying one. The variation of mode frequencies for a fixed k and changing the b values are shown in Figure 5.2. When the cosmic string effect is large, i.e., when b is small, $Re(E)$ increases and $|Im(E)|$ decreases for a fixed k [Table (5.1 & 5.2)].

Table 5.2: Quasi-normal frequencies of Schwarzschild black hole without cosmic string.

b	k	n	ReE	ImE
1	1	0	0.176452	- 0.100109
	2	0	0.378627	- 0.0965424
		1	0.353604	- 0.298746
	3	0	0.573685	- 0.0963242
		1	0.556185	- 0.292981
		2	0.527289	- 0.497187
	4	0	0.767194	- 0.096276
		1	0.753957	- 0.291048
		2	0.73045	- 0.49088
		3	0.699918	- 0.695711
	5	0	0.960215	- 0.0962564
		1	0.949593	- 0.290179
		2	0.929979	- 0.487634
		3	0.903578	- 0.689241
		4	0.872052	- 0.894412

This implies that the decay is less in the case of Schwarzschild

black hole having cosmic string compared to the case of black hole without string. For $b = 1$ case, we obtain the same results given in Reference[112] where the quasi-normal modes of Schwarzschild black hole perturbed by a massless Dirac field was calculated.

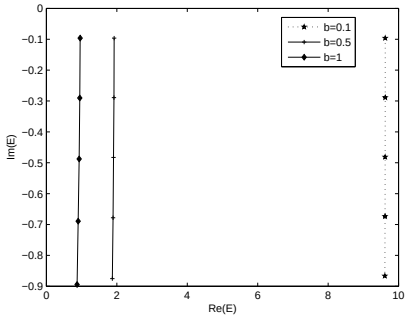

Figure 5.2: Quasi-normal modes of Schwarzschild black hole with cosmic string perturbed by a massless Dirac field is plotted for different values of b ($b = 0.1, 0.5$, and 1) for $k = 5$.

5.4.2 RN extremal black hole

Now we will consider RN extremal black hole for which,

$$f(r) = \left(1 - \frac{r_0}{r}\right)^2. \tag{5.42}$$

Substituting the above f in Eq. (5.34) we will get,

$$V = \left(1 - \frac{r_0}{r}\right)^2 \frac{\partial}{\partial r}\left(\left(1 - \frac{r_0}{r}\right)\frac{k_b}{r}\right) + \left(1 - \frac{r_0}{r}\right)^2 \left(\frac{k_b}{r}\right)^2. \tag{5.43}$$

Here the barrier potential V depends on the absolute value of k_b and for a fixed b value, the peak of the barrier gets higher and higher as $|k|$ increases. We now take 3 different values for b ($b = 1, 0.5, 0.1$) and from Figure 5.3 it is found that the presence of the cosmic string causes an increase in the peak of the potential. When the effective potential given in Eq. (5.43) is substituted in Eq. (5.37), we will get

the complex quasi-normal mode frequencies of RN extremal black hole perturbed by a massless Dirac field [Table (5.3 & 5.4)].

Here also we find that, for a fixed b value, $Re(E)$ decreases while $|Im(E)|$ increases with the mode number n increasing for the same angular momentum eigenvalue k. This means that quasi-normal modes with higher mode numbers decay faster than the low-lying ones. For a fixed k, the variation of mode frequencies with b values are shown in Figure 5.4.

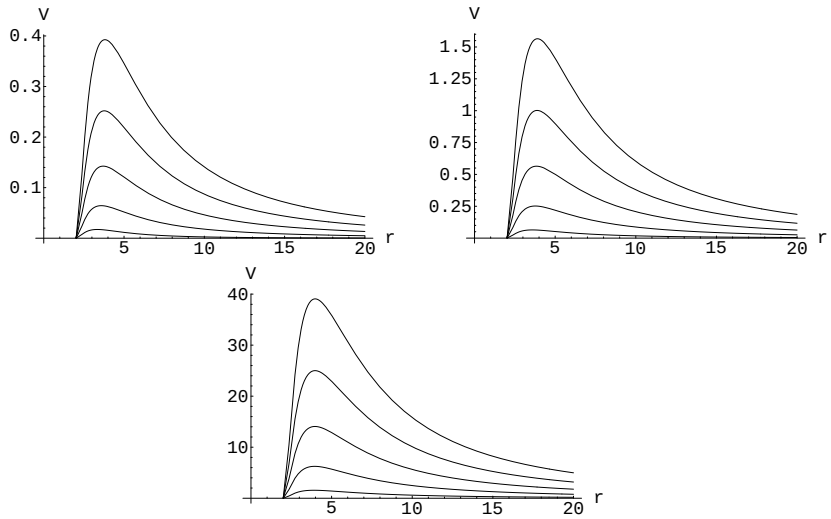

Figure 5.3: Potential versus r for RN extremal black hole with cosmic string in Dirac field is plotted for different values of b ($b = 1, 0.5, 0.1$) for $k = 0$ to $k = 5$.

When $b < 1$, i.e., when the cosmic string is present, $Re(E)$ increases and $|Im(E)|$ decreases for a fixed k, compared to $b = 1$ case [Table (5.3 & 5.4)]. Thus compared to RN extremal black hole, the decay is less in the case of RN extremal black hole having cosmic string.

Table 5.3: Quasi-normal frequencies of RN extremal black hole having Cosmic string

b	k	n	ReE	ImE
0.1	1	0	1.24941	-0.0441915
	2	0	2.49971	-0.0441935
		1	2.49853	-0.132603
	3	0	3.7498	-0.0441939
		1	3.74902	-0.132591
		2	3.74746	-0.221018
	4	0	4.99985	-0.044194
		1	4.99927	-0.132588
		2	4.9981	-0.220998
		3	4.99634	-0.309435
	5	0	6.24988	-0.0441941
		1	6.24941	-0.132586
		2	6.24848	-0.220988
		3	6.24707	-0.309408
		4	6.2452	-0.397852
0.5	1	0	0.246679	-0.044139
	2	0	0.498474	-0.0441761
		1	0.492516	-0.133115
	3	0	0.749004	-0.0441865
		1	0.745065	-0.132812
		2	0.737355	-0.222156
	4	0	0.999259	-0.0441899
		1	0.996315	-0.13271
		2	0.990498	-0.221638
		3	0.981942	-0.311209
	5	0	1.24941	-0.0441915
		1	1.24706	-0.132664
		2	1.24239	-0.221398
		3	1.23548	-0.310554
		4	1.22643	-0.400269

Table 5.4: Quasi-normal frequencies of RN extremal black hole without cosmic string.

b	k	n	ReE	ImE
1	1	0	0.117481	-0.0444736
	2	0	0.246679	-0.0441391
		1	0.234639	-0.135043
	3	0	0.37291	-0.0441622
		1	0.364905	-0.133573
		2	0.350195	-0.225651
	4	0	0.498474	-0.0441761
		1	0.492516	-0.133115
		2	0.481162	-0.481162
		3	0.465287	-0.316232
	5	0	0.623796	-0.0441828
		1	0.619053	-0.132916
		2	0.609859	-0.222676
		3	0.596707	-0.313914
		4	0.580161	-0.406822

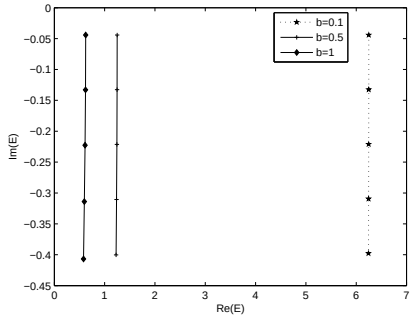

Figure 5.4: Quasi-normal modes of RN extremal black hole with cosmic string perturbed by a massless Dirac field is plotted for different values of b ($b = 0.1, 0.5$, and 1) for $k = 5$.

5.4.3 Schwarzschild-de Sitter black hole

We will now take the case of SdS black hole and see how the quasi-normal modes are effected when the cosmic string pierces a SdS black hole. The metric is,

$$f(r) = 1 - \frac{2M}{r} - \frac{r^2}{a^2}, \tag{5.44}$$

where M denotes the black hole mass and $a^2 = \frac{3}{\Lambda}$, Λ being the cosmological constant. The space-time possesses two horizons: the black-hole horizon at $r = r_b$ and the cosmological horizon at $r = r_c$. The function f has zeros at r_b, r_c and $r_0 = -(r_b + r_c)$. Substituting the above f in Eq. (5.34), we will get

$$V = (1 - \frac{2M}{r} - \frac{r^2}{a^2})\frac{\partial}{\partial r}((1 - \frac{2M}{r} - \frac{r^2}{a^2})^{\frac{1}{2}}\frac{k_b}{r}) + (1 - \frac{2M}{r} - \frac{r^2}{a^2})(\frac{k_b}{r})^2. \tag{5.45}$$

We consider three values of b ($b = 1, 0.5, 0.1$) and from Figure 5.5 we can see that the height of the potential increases with b decreasing.

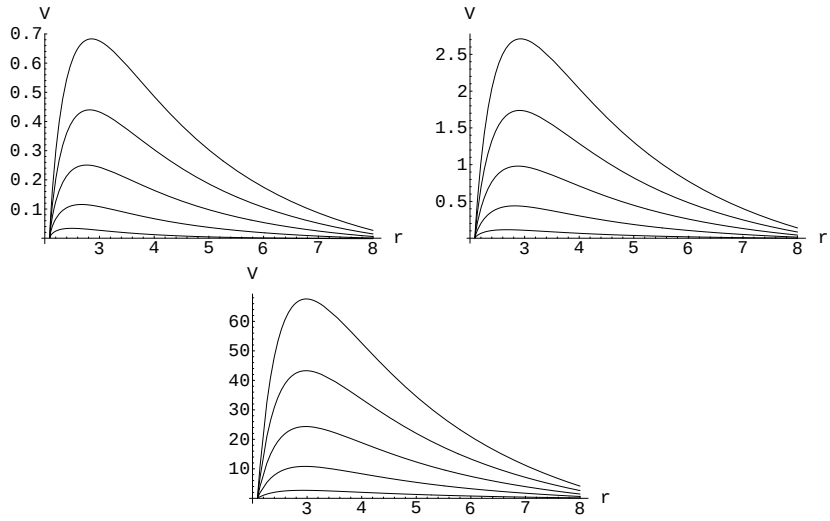

Figure 5.5: Potential versus r for SdS black hole with cosmic string in Dirac field is plotted for different values of b ($b = 1, 0.5, 0.1$) for $k = 0$ to $k = 5$.

Table 5.5: Quasi-normal frequencies of SdS black hole with cosmic string

b	k	n	ReE	ImE
0.1	1	0	1.62881	-0.193788
	2	0	3.28115	-0.193023
		1	3.26217	-0.57955
	3	0	4.92798	-0.192659
		1	4.91537	-0.578183
		2	4.89017	-0.964325
	4	0	6.57352	-0.192473
		1	6.56408	-0.577532
		2	6.5452	-0.962932
		3	6.51691	-1.3489
	5	0	8.21856	-0.192351
		1	8.211	-0.577126
		2	8.19591	-0.962118
		3	8.17328	-1.34747
		4	8.14313	-1.73333
0.5	1	0	0.184451	-0.179973
	2	0	0.611882	-0.191711
		1	0.506702	-0.602245
	3	0	0.959022	-0.193731
		1	0.891965	-0.589723
		2	0.768017	-1.00536
	4	0	1.29563	-0.19389
		1	1.2466	-0.585655
		2	1.15204	-0.98806
		3	1.01702	-1.40482
	5	0	1.62881	-0.193748
		1	1.59011	-0.583538
		2	1.51421	-0.979819
		3	1.40371	-1.38574
		4	1.26152	-1.80321

Table 5.6: Quasi-normal frequencies of SdS black hole without cosmic string.

b	k	n	ReE	ImE
1	1	0	0.118178	0.329652
	2	0	0.18445	-0.179973
		1	0.0172463	-0.686957
	3	0	0.423791	-0.187411
		1	0.283273	-0.623849
		2	0.0808308	-1.10559
	4	0	0.611882	-0.191711
		1	0.5067	-0.602246
		2	0.335459	-1.05152
		3	0.108969	-1.52834
	5	0	0.787788	-0.193209
		1	0.705661	-0.593841
		2	0.560701	-1.02226
		3	0.365525	-1.47586
		4	0.124334	-1.95241

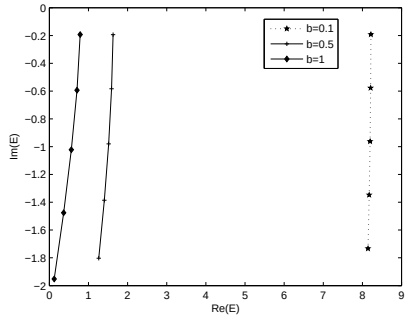

Figure 5.6: Quasi-normal modes of SdS black hole with cosmic string perturbed by a massless Dirac field is plotted for different values of b ($b = 0.1, 0.5$, and 1) for $k = 5$.

By substituting Eq. (5.45) in Eq. (5.37), we obtain the complex quasi-normal modes for SdS black hole with cosmic string perturbed

by a massless Dirac field. Quasi-normal modes of SdS black hole with cosmic string for various b values are shown in Table (5.5 & 5.6).

Here for a fixed b value, $Re(E)$ and $|Im(E)|$ show similar behavior as those of Schwarzschild and RN extremal black holes having cosmic string. The variation of mode frequencies for a fixed k with different b values are shown in Figure 5.6. From Table (5.5 & 5.6), we can see that the behavior of $|Im(E)|$ for $n = 0$ mode is different from the behavior of $|Im(E)|$ for non-zero values of n. From this table we can see that the decay is less in the case of SdS black hole having cosmic string.

5.4.4 Near extremal Schwarzschild-de Sitter black hole.

As a last example, we consider near extremal SdS black hole, which is defined as the space-time for which the cosmological horizon r_c is very close to black hole horizon r_b, i.e., $\frac{r_c - r_b}{r_b} << 1$. For this space-time, one can make the following approximations,

$$r_0 \sim 2r_b; a^2 \sim 3r_b^2; M \sim \frac{r_b}{3}. \tag{5.46}$$

Furthermore, since r is constrained to vary between r_b and r_c, we get $r - r_0 \sim r_b - r_0 \sim 3r_b$ and thus

$$f \sim \frac{(r - r_b)\,(r_c - r)}{r_b^2}. \tag{5.47}$$

Substituting Eq. (5.47) in Eq. (5.34), we get,

$$V = \frac{(r - r_b)(r_c - r)}{r_b^2} \frac{\partial}{\partial r}((\frac{(r - r_b)(r_c - r)}{r_b^2})^{\frac{1}{2}} \frac{k_b}{r}) + (\frac{(r - r_b)(r_c - r)}{r_b^2})(\frac{k_b}{r})^2. \tag{5.48}$$

From Figure 5.7 we can see that the height of the potential increases when the effect of cosmic string increases. By substituting Eq. (5.48) in Eq. (5.37), we obtain the quasi-normal modes of near extremal

SdS black hole with cosmic string perturbed by a massless Dirac field.

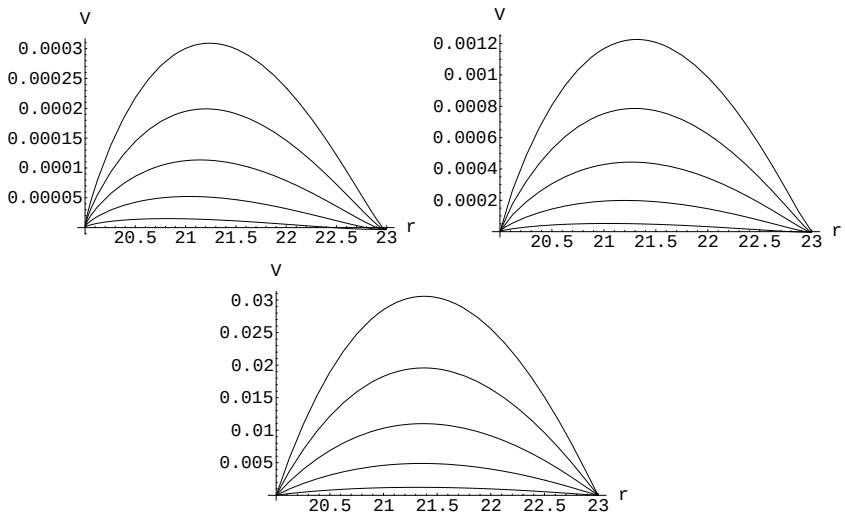

Figure 5.7: Potential versus r for SdS near extremal black hole with cosmic string in Dirac field is plotted for different values of b ($b = 1, 0.5, 0.1$) for $k = 0$ to $k = 5$.

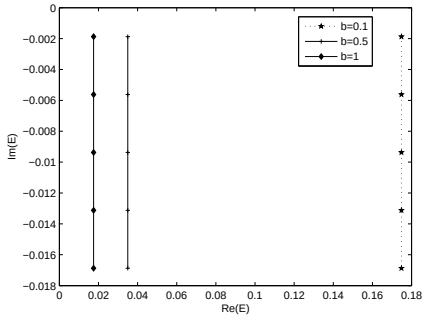

Figure 5.8: Quasi-normal modes of near extremal SdS black hole with cosmic string perturbed by a massless Dirac field is plotted for different values of b ($b = 0.1, 0.5$, and 1) for $k = 5$.

Table 5.7: Quasi-normal frequencies of SdS near extremal black hole with cosmic string

b	k	n	ReE	ImE
0.1	1	0	0.0349689	- 0.001875
	2	0	0.0699379	- 0.001875
		1	0.0699379	- 0.005625
	3	0	0.104907	- 0.001875
		1	0.104907	- 0.005625
		2	0.104907	- 0.009375
	4	0	0.139876	- 0.001875
		1	0.139876	- 0.005625
		2	0.139876	- 0.009375
		3	0.139876	- 0.013125
	5	0	0.174845	-0.001875
		1	0.174845	- 0.005625
		2	0.174845	- 0.009375
		3	0.174845	- 0.013125
		4	0.174845	- 0.016875
0.5	1	0	0.0069931	0.00187594
	2	0	0.0139875	- 0.00187507
		1	0.0139876	- 0.00562519
	3	0	0.0209814	-0.00187501
		1	0.0209814	-0.00562504
		2	0.0209814	-0.00937506
	4	0	0.0279751	- 0.001875
		1	0.0279751	- 0.00562501
		2	0.0279752	- 0.00937502
		3	0.0279752	- 0.013125
	5	0	0.0349689	- 0.001875
		1	0.0349689	- 0.00562501
		2	0.0349689	- 0.00937501
		3	0.0349689	- 0.013125
		4	0.0349689	- 0.016875

Table 5.8: Quasi-normal frequencies of SdS near extremal black hole without cosmic string.

b	k	n	ReE	ImE
1	1	0	0.00348641	- 0.00188365
	2	0	0.0069931	- 0.00187594
		1	0.00699432	- 0.00562683
	3	0	0.0104906	- 0.00187521
		1	0.0104908	- 0.00562551
		2	0.0104911	- 0.00937561
	4	0	0.0139875	- 0.00187507
		1	0.0139876	- 0.00562519
		2	0.0139877	- 0.00937525
		3	0.0139878	- 0.0131253
	5	0	0.0174845	- 0.00187503
		1	0.0174845	- 0.00562508
		2	0.0174845	- 0.00937512
		3	0.0174846	- 0.0131251
		4	0.0174846	- 0.0168751

For a near extremal SdS black hole also the quasi-normal frequencies are obtained for different values of b [Table (5.7 & 5.8)]. We can see that for a fixed b value, $Re(E)$ remains same and $|Im(E)|$ increases as the mode number n increases, for the same k value. The behavior of mode frequencies by changing the b values for a fixed k are shown in Figure 5.8.

When b is small, i.e., when the effect of cosmic string is high, $Re(E)$ increases while $|Im(E)|$ have almost same but with very small decreases for a mode of fixed k value [Table (5.7 & 5.8)]. The decay is less in the case of near extremal SdS black hole having cosmic string.

5.5 Conclusion

We have evaluated the quasi-normal mode frequencies for Schwarzschild, RN extremal, SdS and near extremal SdS black hole space-

times having cosmic string perturbed by a massless Dirac field. In all these cases, we have found that quasi-normal modes with higher mode numbers decay faster than the low-lying ones. We have also found that, when the effect of cosmic string is high, $|Im(E)|$ decreases while $Re(E)$ increases for fixed k implying that the decay is less when cosmic string is present.

6

Quasi-normal modes of RN black hole space-time with cosmic string in a Dirac field

6.1 Introduction

The quasi-normal spectrum of black holes has been extensively investigated during recent years for a great variety of black hole backgrounds and fields, because it is an important characteristic signature of black holes which can be used for observation of the gravitational waves,[109] stability analysis,[124] and AdS/CFT calculations of temperature Greenfunctions.[103,125–127] As a simplest model, when the influence of the spin of the field is neglected, special attention has been given to perturbations due to a scalar field.[128–131] Considering the charged black hole, the scalar electrodynamic can model the interaction of the charged field with the electromagnetic background of the black hole. Quasi-normal modes of charged scalar field in the Reissner-Nordstrom has been calculated earlier.[110,132–135]

In this chapter we study the influence of cosmic string on the QNMs of RN black hole background space-time perturbed by a massless Dirac field. In the previous chapter we have evaluated quasi-normal mode frequencies for Schwarzschild, RN extremal, SdS and

near extremal SdS black hole space-times with cosmic string perturbed by a massless Dirac field. In section 6.2, we consider the Dirac equation in a RN black hole space-time with a cosmic sting and its deduction into a set of second order differential equations. In section **??** we evaluate quasi-normal frequencies for the massless case using Pöschl-Teller potential method for RN black holes. Section 6.4 concludes the chapter.

6.2 RN black hole with cosmic string space-time for a Dirac field

The metric describing a charged spherically symmetric RN black hole with a cosmic string can be written as,[118]

$$ds^2 = f(r)dt^2 - \frac{dr^2}{f\,(r)} - r^2 d\theta^2 - b^2 r^2 \sin^2\theta d\phi^2. \tag{6.1}$$

Here $f(r) = 1 - \frac{2M}{r} + \frac{Q^2}{r^2}$, Q and M represent the electric charge and the mass of the black hole respectively, and ϕ' runs over the range $0 < \phi' < 2\pi b$, with $\phi' = b\phi$ where ϕ runs over zero to 2π. Here $b = 1 - 4\breve{\mu}$ with $\breve{\mu}$ being the linear mass density of the string. The Dirac equation in the presence of an electromagnetic interaction can be written as,

$$\left(\gamma^\mu(\partial_\mu - \Gamma_\mu - \imath e A_\mu) + m\right)\Psi = 0, \tag{6.2}$$

where m and e are the the mass and charge of the Dirac field, A_μ is the electro magnetic potential which can be written as,

$$A_\mu = \left(\frac{Q}{r}, 0, 0, 0\right). \tag{6.3}$$

Here

$$\gamma^\mu = g^{\mu\nu}\gamma_\nu, \tag{6.4}$$

and

$$\gamma_\nu = e^a_\nu \gamma_a, \tag{6.5}$$

where γ^a are the Dirac matrices and e^a_ν is the tetrad given by,

$$e^t_t = f^{\frac{1}{2}}; e^r_r = \frac{1}{f^{\frac{1}{2}}}; e^\theta_\theta = r, e^\phi_\phi = br\sin\theta. \tag{6.6}$$

The spin connection Γ_μ is given by

$$\Gamma_\mu = -\frac{1}{2}[\gamma_a, \gamma_b]e^a_\nu e^{b\nu}_{;\mu}, \tag{6.7}$$

where $e^{b\nu}_{;\mu} = \partial_\mu e^{b\nu} + \Gamma^\nu_{\kappa\mu}e^{b\kappa}$ is the covariant derivative of $e^{b\nu}$. The spin connections for the above metric are obtained as,

$$\Gamma_t = \frac{1}{4}\gamma_1\gamma_0\frac{\partial f(r)}{\partial r}, \tag{6.8}$$

$$\Gamma_r = 0, \tag{6.9}$$

$$\Gamma_\theta = \frac{1}{2}\gamma_1\gamma_2 f^{\frac{1}{2}}(r), \tag{6.10}$$

$$\Gamma_\phi = \frac{1}{2}\gamma_2\gamma_3 b\cos\theta + \frac{1}{2}\gamma_1\gamma_3 b\sin\theta f^{\frac{1}{2}}(r). \tag{6.11}$$

Substituting the spin connections in Eq. (6.2) we will get ,

$$[\frac{-\gamma_0}{f^{\frac{1}{2}}}(\frac{\partial}{\partial t} - \imath\frac{eQ}{r}) + \gamma_1 f^{\frac{1}{2}}(\frac{\partial}{\partial r} + \frac{1}{r} + \frac{1}{4f(r)}\frac{\partial f}{\partial r}) + \frac{\gamma_2}{r}(\frac{\partial}{\partial\theta} + \frac{1}{2}\cot\theta) + \frac{\gamma_3}{br\sin\theta}\frac{\partial}{\partial\phi} + m]\Psi(t,r,\theta,\phi) = 0, \tag{6.12}$$

Using the transformation $\Psi(t,r,\theta,\phi) = \frac{\exp(-\imath Et)}{rf^{\frac{1}{4}}\sin\theta^{\frac{1}{2}}}\chi(r,\theta,\phi)$, Eq. (6.12) becomes,

$$[\frac{-E - \frac{eQ}{r}}{f^{\frac{1}{2}}}\frac{\partial}{\partial t} + \frac{1}{\imath}\gamma_0\gamma_1 f^{\frac{1}{2}}(\frac{\partial}{\partial r}) + \frac{\gamma_1}{\imath r}\gamma_1\gamma_0(\gamma_2\frac{\partial}{\partial\theta} + \frac{\gamma_3}{b\sin\theta}\frac{\partial}{\partial\phi}) - \imath\gamma_0 m]\chi(r,\theta,\phi) = 0. \tag{6.13}$$

Radial part of the Dirac equation can be separated out by the substitution,

$$\chi(r,\theta,\phi) = R(r)\Omega(\theta,\phi). \tag{6.14}$$

As in chapter 5 here also we introduce the angular momentum operator,[74]

$$\mathbf{K}_{(b)} = -\imath\gamma_1\gamma_0\left(\gamma_2\partial_\theta + \gamma_3(b\sin\theta)^{-1}\partial_\phi\right), \tag{6.15}$$

such that,

$$\mathbf{K}_{(b)}\Omega(\theta,\phi) = k_b\Omega(\theta,\phi), \tag{6.16}$$

where the eigenvalues of $\mathbf{K}_{(b)}$ are $k_b = \frac{k}{b}$. Here k is a positive or a negative non-zero integer. Thus, the presence of cosmic string is codified in the eigenvalues of the angular momentum operator.[122] Substituting Eqs.(6.14) and (6.16) in Eq. (6.13), we will get radial equation which contains γ_0 and γ_1 which can be represented by 2×2 matrices. So we write the radial factor $R(r)$ by a two component spinor notation,

$$R(r) = \begin{bmatrix} F \\ G \end{bmatrix}. \tag{6.17}$$

Then the radial equation in F an G are given by,

$$f\frac{dG}{dr} + f^{\frac{1}{2}}\frac{k_b}{r}G + f^{\frac{1}{2}}mF = (E + \frac{eQ}{r})F, \tag{6.18}$$

$$f\frac{dF}{dr} - f^{\frac{1}{2}}\frac{k_b}{r}F + f^{\frac{1}{2}}mG = -(E + \frac{eQ}{r})G. \tag{6.19}$$

Let us have a co-ordinate change given by,

$$dr_* = \frac{dr}{f}. \tag{6.20}$$

Eq. (6.18) and Eq. (6.19) then become,

$$\begin{aligned} &\frac{\partial}{\partial r_*}\begin{bmatrix} G \\ F \end{bmatrix} + f^{\frac{1}{2}}\begin{bmatrix} \frac{k_b}{r} & m \\ m & -\frac{k_b}{r} \end{bmatrix}\begin{bmatrix} G \\ F \end{bmatrix} \\ &= \begin{bmatrix} 0 & E+\frac{eQ}{r} \\ -E-\frac{eQ}{r} & 0 \end{bmatrix}\begin{bmatrix} G \\ F \end{bmatrix}. \end{aligned} \tag{6.21}$$

Defining,

$$\begin{bmatrix} \hat{G} \\ \hat{F} \end{bmatrix} = \begin{bmatrix} \cos\frac{\theta}{2} & -\sin\frac{\theta}{2} \\ \sin\frac{\theta}{2} & \cos\frac{\theta}{2} \end{bmatrix}\begin{bmatrix} G \\ F \end{bmatrix}, \tag{6.22}$$

where

$$\theta = \tan^{-1}(\frac{mr}{|k_b|}). \tag{6.23}$$

Eq. (6.21) becomes,

$$\frac{\partial}{\partial r_*}\begin{bmatrix}\hat{G}\\ \hat{F}\end{bmatrix}+f^{\frac{1}{2}}\sqrt{\left(\frac{k_b}{r}\right)^2+m^2}\begin{bmatrix}1 & 0\\ 0 & -1\end{bmatrix}\begin{bmatrix}\hat{G}\\ \hat{F}\end{bmatrix}$$
$$=-E\left[1+\frac{1}{2E}\frac{fm|k_b|+}{{k_b}^2+m^2r^2}++\frac{eQ}{r}\right]\begin{bmatrix}0 & -1\\ 1 & 0\end{bmatrix}\begin{bmatrix}\hat{G}\\ \hat{F}\end{bmatrix}. \tag{6.24}$$

By making another change of the variable;

$$d\hat{r}_*=\frac{dr_*}{\left[1+\frac{1}{2E}\frac{fmk_b}{k_b^2+m^2r^2}+e\frac{Q}{Er}\right]}. \tag{6.25}$$

Eq. (6.24) can be simplified to,

$$\frac{\partial}{\partial \hat{r}_*}\begin{bmatrix}\hat{G}\\ \hat{F}\end{bmatrix}+\frac{f^{\frac{1}{2}}\sqrt{\left(\frac{k_b}{r}\right)^2+m^2}}{\left[1+\frac{1}{2E}\frac{fm|k_b|}{k_b^2+m^2r^2}+e\frac{Q}{Er}\right]}\begin{bmatrix}1 & 0\\ 0 & -1\end{bmatrix}\begin{bmatrix}\hat{G}\\ \hat{F}\end{bmatrix}$$
$$=E\begin{bmatrix}0 & 1\\ -1 & 0\end{bmatrix}\begin{bmatrix}\hat{G}\\ \hat{F}\end{bmatrix}, \tag{6.26}$$

i.e.,

$$\frac{\partial}{\partial \hat{r}_*}\begin{bmatrix}\hat{G}\\ \hat{F}\end{bmatrix}+W\begin{bmatrix}\hat{G}\\ -\hat{F}\end{bmatrix}=E\begin{bmatrix}\hat{F}\\ -\hat{G}\end{bmatrix}, \tag{6.27}$$

where

$$W=\frac{f^{\frac{1}{2}}\sqrt{\left(\frac{k_b}{r}\right)^2+m^2}}{\left[1+e\frac{Q}{Er}+\frac{1}{2E}\frac{fmk_b}{k_b^2+m^2r^2}\right]}. \tag{6.28}$$

Thus from Eq. (6.27), we will get coupled equations for $\hat{G}$ and $\hat{F}$ which are given bellow,

$$-\frac{\partial^2\hat{F}}{\partial\hat{r}_*^2}+V_1\hat{F}=E^2\hat{F}, \tag{6.29}$$

$$-\frac{\partial^2\hat{G}}{\partial\hat{r}_*^2}+V_2\hat{G}=E^2\hat{G}, \tag{6.30}$$

where

$$V_{1,2}=\pm\frac{\partial W}{\partial\hat{r}_*}+W^2. \tag{6.31}$$

From Eqs (6.29) and (6.30), we can evaluate the corresponding quasi-normal mode frequencies for Reissner-Nordstrom black hole. V_1 and V_2 represent the super symmetric partners derived from the same super potential W.[123] It is seen that potentials related in this way possess the same spectra of quasi-normal mode frequencies.

6.3 Quasi-normal mode frequencies

We shall evaluate the quasi-normal frequencies for RN black hole space-times perturbed by a massless Dirac field. For massless case, i.e., $m = 0$, the equation for the potential (Eq. (6.31)) becomes,

$$V = f\left(1 + e\frac{Q}{Er}\right)\frac{\partial}{\partial r}\left(f^{\frac{1}{2}}\frac{k_b}{r\left(1 + e\frac{Q}{Er}\right)}\right) + f\left(\frac{k_b}{r}\right)^2\frac{1}{\left(1 + e\frac{Q}{Er}\right)^2}, \tag{6.32}$$

where the subscript has been avoided. Here we take Q as always positive and the sign of e can be positive or negative so that the positive sign of e actually means that the product $eQ > 0$ and the negative sign of e means $eQ < 0$. The effective potential as a function of r is plotted in Figure 6.1. We can see that the dependence of V on Q is strong and the peak of the potential increases faster and faster with Q. When the value of b is changed from $b = 1$ to $b = 0.5$ and to 0.1 the peak of the potential is increased, i.e., the presence of cosmic string causes an increase in the height of the potential barrier.

Now we shall evaluate the QNMs using Pöschl-Teller potential approximation proposed by Ferrari and Mashhoon, the Pöschl-Teller potential[40] is given by,

$$V_{PT} = \frac{V_0}{\cosh^2\left(\frac{r^\star}{b}\right)}. \tag{6.33}$$

The quantity V_0 and b are given by the height and curvature of the potential at its maximum($r = r_{max}$).

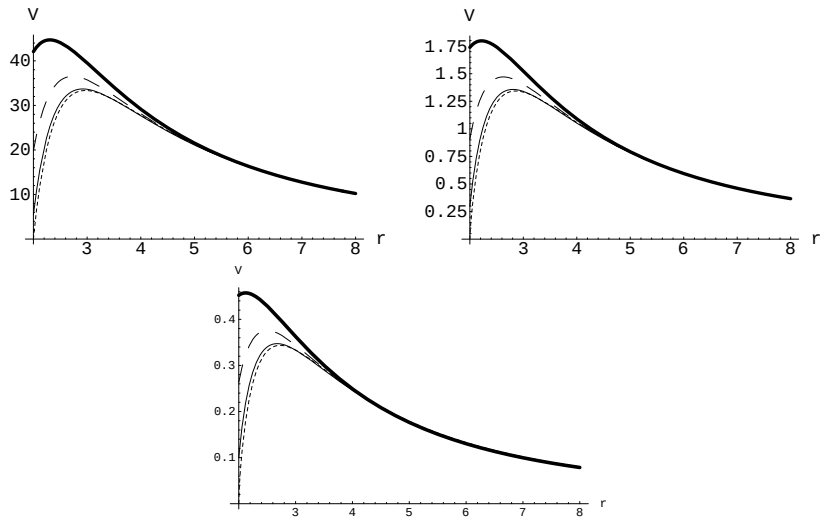

Figure 6.1: Variation of effective potential for Dirac field with m=0 k=3, e=0.1, E=1 and Q=0(doted line), 0.3(solid line), 0.6(dashed line)and 0.9(bold line), for each b value(0.1, 0.5 and 1)

Thus

$$V_0 = V_{r_{max}}, \frac{1}{b^2} = -\frac{1}{2V_0}\left[\frac{d^2V}{dr^2}\right]_{r=r_{max}}. \tag{6.34}$$

The QNMs of the Pöschl-Teller potential can be evaluated analytically;

$$E = \frac{1}{b}\left[\sqrt{V_0 - \frac{1}{4}} - \imath\left(n + \frac{1}{2}\right)\right]. \tag{6.35}$$

In this case the effective potential depends both on Q and E. So we calculate the quasi-normal modes. Here, we first find QNMs for the case $Q = 0$ in which the potential is independent of E and let it be E_0. We take this as the initial value E_0 for a fixed n, l(or k) and e and is used to evaluate the corresponding QNMs for $Q \neq 0$. i.e., we use E_0 as real to modify the potential and find E_1 and repeat the process successfully to get E_2, E_3, E_4....[113]

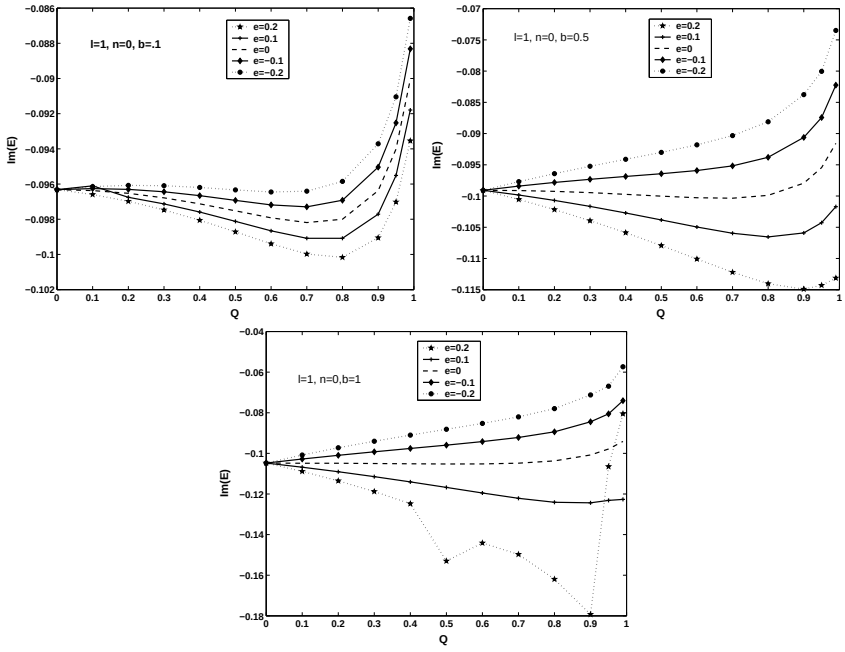

Figure 6.2: Im(E) vs Q for l=1 and n=0 for each b value(0.1, 0.5 and 1)

We first check the effect of positive and negative Dirac field charges $'e'$ on a positively charged RN black hole for a fixed b value. For that we plot the the imaginary part of the QNMs, $Im(E)$, with black hole charge Q for different values of field charge e for each b values. Figure 6.2 shows the behavior of $Im(E)$ versus Q for the mode $l = 1(k = 1)$ and $n = 0$ case. And it is clear that as black hole charge Q increases from 0 to 0.99, at first there is a small increase of $|Im(E)|$ and then it decreases with increase of the charge Q. Also, for a fixed b value, $|Im(E)|$ is small for negatively charged Dirac field compared to positively charged ones. For $b = 0.1$ case, that is, when the effect of cosmic string is high we get very good curves compared to others. When the l value increases the behavior is similar to that of $l = 1$ case.

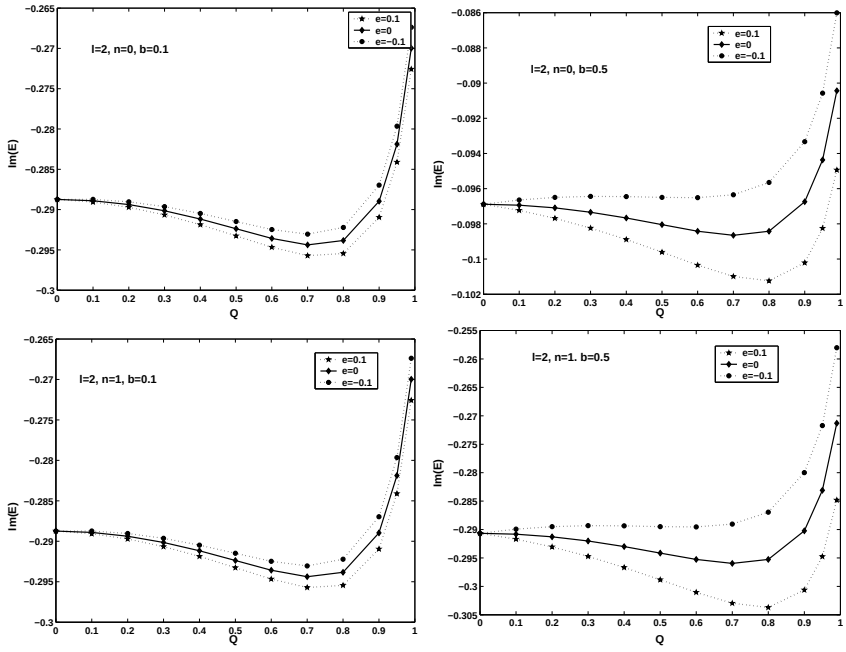

Figure 6.3: Im(E) vs Q for b=0.1 and 0.5 for l=2, n=0 and n=1

Figure 6.3 shows the behavior of $Im(E)$ versus Q for $l = 2$ case. Here we considered both the modes $n = 1$ and $n = 0$ for $b = 0.1$ and $b = 0.5$. Thus from this we understand that positively charged Dirac field decay faster than negatively charged Dirac field in a positively charged RN black hole background with a fixed b value. i.e., the more possibility for obtaining quasi-normal mode is in the case of black holes perturbed with negatively charged Dirac field.

Figure 6.4 shows the dependence of $Re(E)$ with black hole charge Q with different values of Dirac field charge e from +0.2 to -0.2 for fixed values of b. For all b values $Re(E)$ is increasing with respect to Q. From Figure 6.4, it is clear that $e = -0.2$ have higher $Re(E)$ compared to $e = +0.2$ which implies that negatively charged Dirac field have larger $Re(E)$ value.

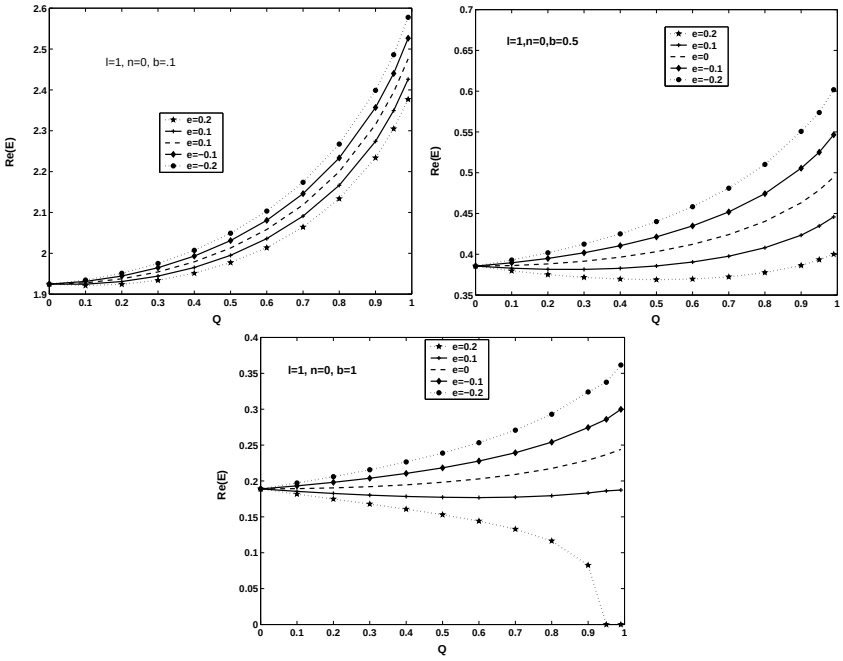

Figure 6.4: Re(E) vs Q for l=1 and n=0 for fixed values of b(0.1, 0.5, 1)

We now check for the imprint of cosmic string on the RN black hole. For this we plot $Im(E)$ versus Q graph for various b values for a fixed field charge e as in Figure 6.5. Thus for the mode $l = 1$, $n = 0$ and when charge of the Dirac field is $e = 0.2$, as Q increases, $|Im(E)|$ at first increases and then decreases. But when $b = 0.1$ the $|Im(E)|$ is smaller compared to others. i.e., decay is small in the case of black hole having cosmic string. This is true only for the positively charged Dirac field and for $e = 0$.

When e becomes negative, it shows another behavior. i.e., for the negatively charged Dirac field, up to some Q value (let it be Q_0) $|Im(E)|$ for $b = 0.1$ is small compared to others. The $|Im(E)|$ for $b = 0.1, 0.5$ and 1 meets near Q_0. After that $|Im(E)|$ values for $b = 0.1$ become larger than all others. i.e., up to Q_0 the decay rate is small for a black hole having cosmic string and then decay rate

increases.

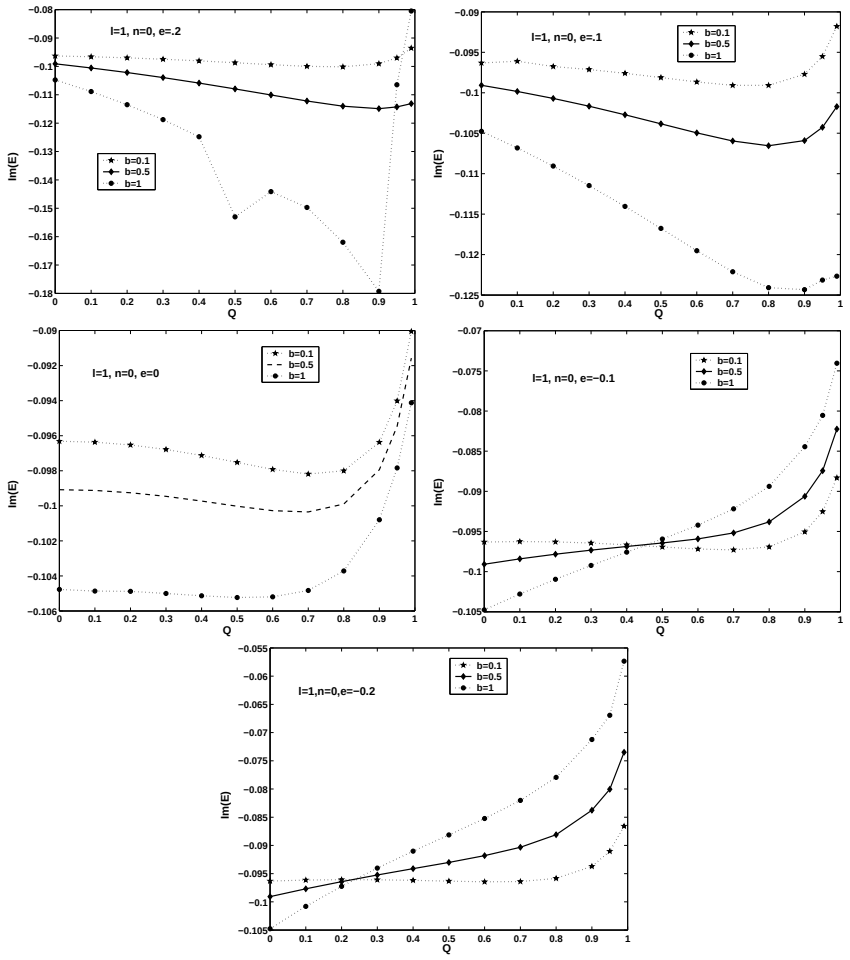

Figure 6.5: Im(E) vs Q for l=1, n=0 for different e(+2 to -2)values

The variation of b with e values for higher modes (for $l = 2$, $n = 0$ and $n = 1$) are shown in Figure 6.6 and Figure 6.7. Here also $|Im(E)|$ behaves same as above. i.e., in the case of negatively charged Dirac field, when the charge of the black hole is high, the effect due to cosmic string is suppressed. This means that if we obtain a response from an RN black hole having small charge perturbed by negatively charged Dirac field, then the more possibility is from black

hole having cosmic string than the one which do not contain it. But if charge is large then more possibility is for black hole which do not contain cosmic string. Figure 6.8 shows the variation of $Re(E)$ with Q for various values of b for a fixed e. Here for all values of e, $Re(E)$ is larger for $b = 0.1$ compared to others. That is the $Re(E)$ has a large value for the black hole having cosmic string.

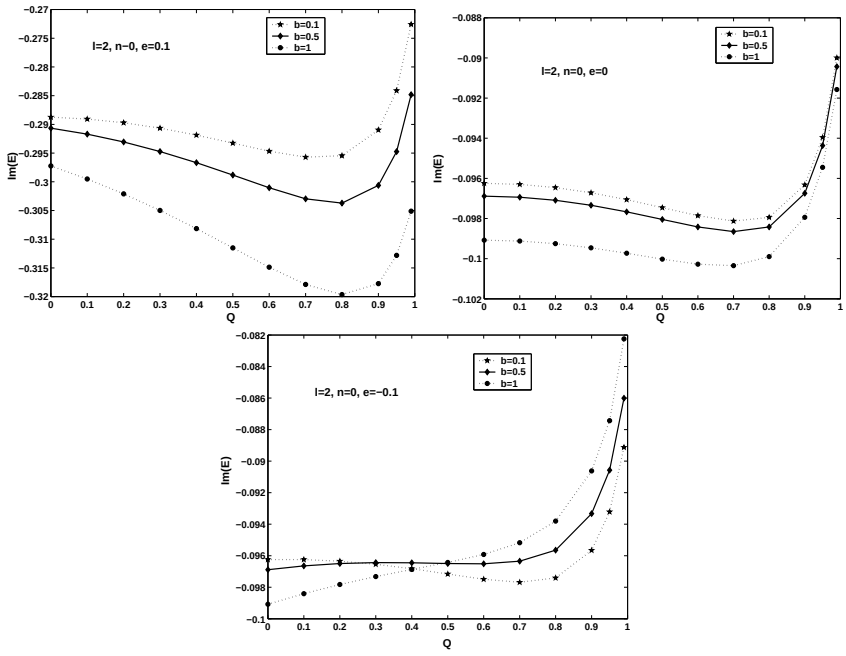

Figure 6.6: Im(E) vs Q for l=2, n=0 for different e(+1 to -1)values

6.4 Conclusion

We have obtained the Dirac equation in RN black hole space-time with a cosmic sting and its deduction into a set of second order differential equations. We have evaluated the quasi-normal mode frequencies for RN black hole space-times having cosmic string perturbed by a massless Dirac field.

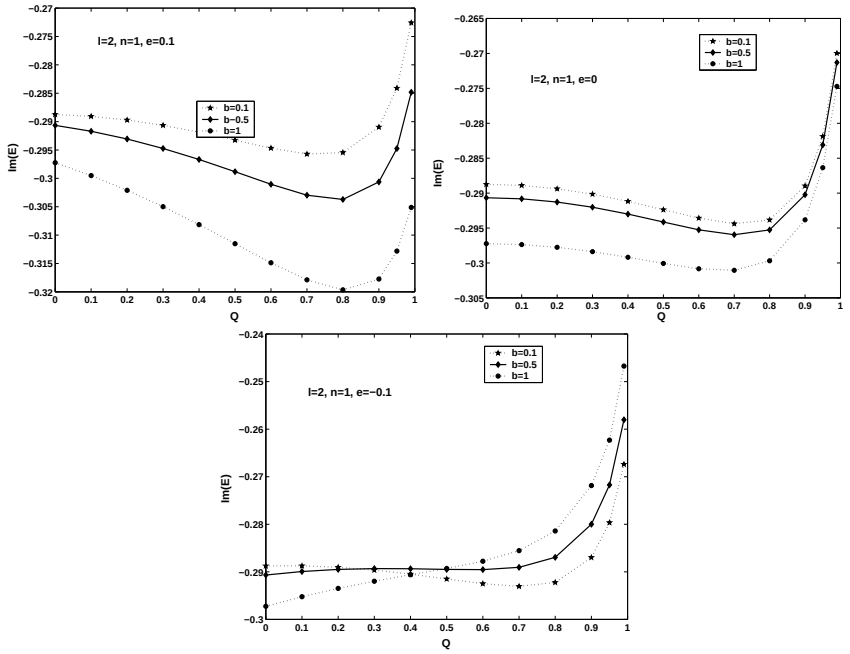

Figure 6.7: Im(E) vs Q for l=2, n=1 for different e(+1 to -1)values

We find that for a fixed value of b, positively charged Dirac field decay faster than negatively charged Dirac field. But when we compare the RN black hole with and without cosmic string, in the case of positively charged Dirac field, decay is less when cosmic string is present. But in the case of negatively charged Dirac field, the RN black hole having cosmic string shows small decay for low values of black hole charge Q but as Q increases its decay rate increases. Whereas, the RN black hole which do not have cosmic string shows rapid decay for low values of Q and as Q increases its decay rate decreases compared to the RN black hole having cosmic string. Thus the effect due to cosmic string will dominate only in the case of RN black hole having small charge perturbed by a negatively charged Dirac field.

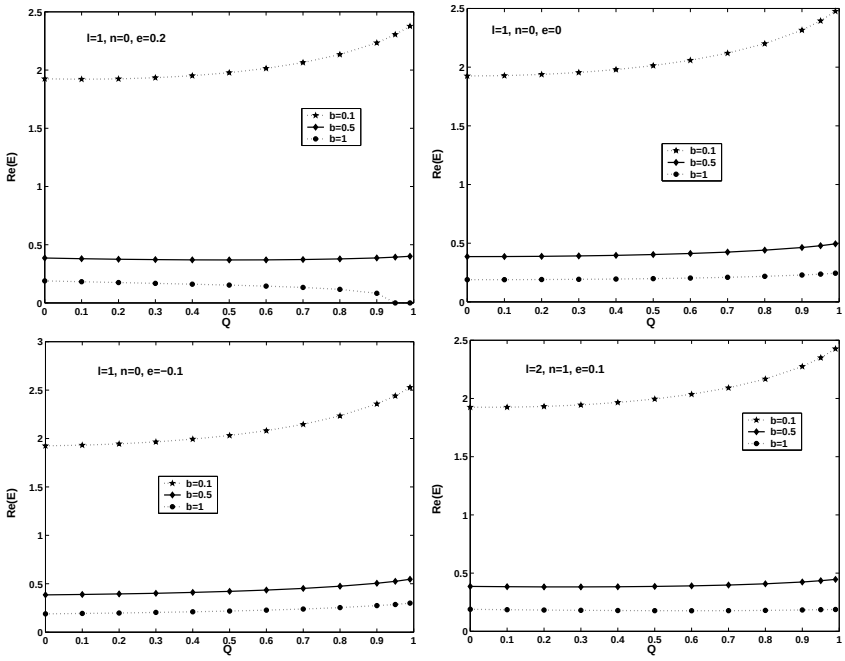

Figure 6.8: Re(E) vs Q for e=+2, 0, -1 for l=1, and the last one is for l=2

7

Results and Conclusion

Black hole space-times are probably the most fascinating objects whose existence is predicted by Einstein's general theory of relativity. The uniqueness and the no hair theorems give strong restrictions on the possible signatures one could look for in astrophysical observations. During the last forty years, numerous mathematical studies have been made in order to understand their properties. In this thesis we have concentrated on the scattering aspect of certain black hole space-time. Following are the main conclusions of this thesis.

1. We have studied the scattering effect of scalar waves in Schwarzschild-de Sitter (SdS), RN extremal and SdS extremal space-times. We have derived expressions for absorption cross sections in the low energy limit for these black hole space-times. Using the property of reflection of waves from horizon, we have obtained expression for the Hawking temperature of SdS black hole and found that for this case the absorption cross section inversely depends on Hawking temperature.

2. We have obtained the expression for absorption cross section of Reissner-Nordstrom black hole, perturbed by charged scalar wave. Here the absorption cross section depends inversely on square of the Hawking temperature. We also find the fact that

the absorption cross section is found to be decreasing if the charge of RN black hole is increasing.

3. The scattering of Dirac waves in a Schwarzschild space-time in the low energy limit is also studied. The absorption cross section of Schwarzschild black hole in Dirac field is found to be 1/8th of absorption cross section of Schwarzschild black hole in scalar field. And the absorption cross section for $k = 2$ in Dirac field is also derived. By plotting the emission spectrum of Schwarzschild black hole in Dirac field with and without reflection we find that the main contribution for the emission spectra comes from the $k = 1$ case, and the higher modes have negligible effect.

4. Using WKB approximation we have evaluated quasi-normal mode frequencies of Schwarzschild, RN extremal, SdS and near extremal SdS black hole space-times having cosmic string perturbed by a massless Dirac field. Here quasi-normal modes with higher mode numbers decay faster than the low-lying ones as in the ordinary case. When the imprint of cosmic string is high, $|Im(E)|$ decreases while $Re(E)$ increases for fixed k, implying the fact that the presence of cosmic string slows down the decay.

5. The influence of cosmic string on the quasi-normal modes of RN black hole background space-time perturbed by positively and negatively charged Dirac fields is studied. The Pöschl-Teller method is used for finding the quasi-normal modes and found that, when perturbing with the positively charged Dirac field, the decay will be less for Reissner Nordstrom black hole having cosmic string. But when we perturb with negatively charged Dirac field it is found that the cosmic string effect will dominate only in the case of RN black hole having small charge.

When the charge of the black hole is increased effect of cosmic string is suppressed.

Future prospects

The gravitational collapse of compact objects to form black holes still remains as not yet a well understood problem in physics. The possibility of detecting gravitational waves from these compact objects in the near future by the LIGO and VIRG laser interferometric detectors has aroused a lot of interest in this topic. It is believed that QNMs carry a unique footprint to directly identify the existence of a black hole. Thus they are expected to play a significant role in the search for gravitational waves and black holes. Furthermore, there are many interesting and deep theoretical questions that one can pose in this situation, some of them are,

1. finding expressions for absorption cross sections of SdS, Reissner-Nordstrom and their extremal cases, perturbed by Dirac field, electromagnetic and Gravitational fields.

2. extending the calculation for finding quasi-normal modes of spherically symmetric black holes having cosmic string perturbed by massive Dirac field and also for rotating black holes.

Bibliography

[1] K. S. Thorne, *Black Holes and Time Warps: Einsteins Outrageous Legacy* (New York: W.W. Norton, New York, 1994).

[2] J. A. Wheeler, Am. Sci. **59**, 1 (1968).

[3] I. D. Novikov and V. P. Frolov, *Physics of Black holes* (Kluwer Academic publishers, 1989).

[4] J. R. Oppenheimer and H. Snyder, Phys. Rev. **56**, 455 (1939).

[5] J. R. Oppenheimer and G. Volkoff, Phys. Rev. **55**, 374 (1939).

[6] B. F. Schutz, *A first course in general relativity* (Cambridge University Press, Cambridge, 1985).

[7] K. Schwarzschild, Sitzber. Deut. Akad. Wiss. Berlin, Kl. Math.-Phys. Tech **s**, 189 (1916).

[8] R. P. Kerr, Phys. Rev. Lett. **11**, 237 (1963).

[9] H. Reissner, Ann. Phys. **50**, 106 (1916).

[10] G. Nordstrom, Proc Kon. Ned. Akad. Wet. **20**, 1238 (1918).

[11] J. M. Bardeen, B. Carter, and S. W. Hawking, Commun. Math. Phys. **31**, 161 (1973).

[12] J. D. Bekenstein, Phys. Rev. Lett **28**, 454 (1972).

[13] J. D. Bekenstein, Phys. Rev. D **27**, 2262 (1983).

[14] S. W. Hawking, Nature **248**, 30 (1974).

[15] S. W. Hawking, Commun. Math. Phys. **43**, 199 (1975).

[16] H. C. Ford, R. J. Harms, Z. I. Tsvetanov, G. F. Hartig, L. L. Dressel, G. A. Kriss, R. Bohlin, A. F. Davidsen, B. Margon, and A. K. Kochhar, Astrophys. J. **435**, L27 (1994).

[17] R. J. Harms, H. C. Ford, Z. I. Tsvetanov, G. F. Hartig, L. L. Dressel, G. A. Kriss, R. Bohlin, A. F. Davidsen, B. Margon, and A. K. Kochhar, Astrophys. J. **435**, L35 (1994).

[18] J. A. H. Futterman, F. A. Handler, and R. A. Matzner, *Scattering from Black holes* (Cambridge University Press, Cambridge, 1988).

[19] J. Hough and S. Rowen, Living Rev.Rel. **3**, 3 (2000).

[20] K. S. Thorne, *Probing black holes and relativistic stars with gravitational waves in Black holes and relativistic stars* (University of Chicago press, New York, 1997).

[21] P. Schneider, J. Ehlers, and E. Falco, *Gravitational lenses* (USpringer Verlag, Berlin,, New York, 1993).

[22] J. A. Wheeler, Phys. Rev. **97**, 511 (1955).

[23] T. Regge and J. A. Wheeler, Phys. Rev **108**, 1063 (1957).

[24] F. A. Handler and R. A. Matzner, Phys. Rev. D **22**, 2331 (1980).

[25] R. A. Matzner, J. Math. Phys. **9**, 163 (1968).

[26] L. D. Landau and E. M. Lifshits, *Quantum Mechanics: Non-Relativistic Theory* (Cambridge University Press, Pergamon, New York, 1977).

[27] C. V. Vishveshwara, Nature **227**, 936 (1970).

[28] R. Ruffini, Phys. Rev. D **7**, 972 (1973).

[29] M. Davis, R. Ruffini, W. H. Press, and R. H. Price, Phys. Rev. Lett. **27**, 1466 (1971).

[30] M. Davis, R. Ruffini, and J. Tiomno, Phys. Rev. D **5**, 2932 (1972).

[31] C. T. Cunningham, R. H. Price, and V. Moncrief, Astrophys. J. **224**, 643 (1978).

[32] C. T. Cunningham, R. H. Price, and V. Moncrief, Astrophys. J. **230**, 870 (1979).

[33] V. D. la Cruz, J. E. Chase, and W. Israel, Phys. Rev. Lett. **24**, 423 (1970).

[34] C. V. Vishveshwara, Phys. Rev. D **1**, 2870 (1970).

[35] S. Chandrasekhar and S. Detweiler, Proc. R. Soc. London A **344**, 441 (1975).

[36] B. F. Schutz and C. M. Will, Astrophys. J. Lett. **291**, L33 (1985).

[37] S. Iyer and C. M. Will, Phys. Rev. D **35**, 3621 (1987).

[38] S. Iyer, Phys. Rev. D **35**, 3632 (1987).

[39] R. A. Konoplya, Phys. Rev. D **68**, 024018 (2003).

[40] V. Ferrari and B. Mashhoon, Phys. Rev. D **30**, 295 (1984).

[41] J. D. Bekenstein, *quantum black holes as atoms proc. VIII Marcel Grossmann Meeting* (World scientific, Singapore, 1999).

[42] R. Penrose, Riv. Nuovo Cimento **1**, 252 (1969).

[43] W. G. Unruh, Phys. Rev. D **14**, 3251 (1976).

[44] N. Sanchez, Phys. Rev. D **16**, 937 (1977).

[45] N. Sanchez, Phys. Rev. D **18**, 1030 (1978).

[46] N. Sanchez, Phys. Rev. D **18**, 1798 (1978).

[47] G. Hooft, gr-qc/0401027 (2004).

[48] M.-L. Yan and H. Bai, gr-qc/0406017 (2004).

[49] S. Perlmutter, C. R. Pennypacker, G. Goldhaber, A. Goobar, and R. A. Muller, Astrophys. J. **483**, 565 (1997).

[50] R. M. Wald, *General Relativity* (University of Chicago Press, Chicago, 1984).

[51] C. W. Misner, K. S. Thorne, and J. A. Wheeler, *Gravitation* (Freeman, San Franciso, 1973).

[52] A. Curir, Gen. Rel. Grav. **13**, 417 (1981).

[53] D. Pavon and J. M. Rubi, Phys. Rev. D **37**, 2052 (1988).

[54] R. K. Su, R. G. Cai, and P. K. N. Yu, Phys. Rev. D **50**, 2932 (1994).

[55] O. Kaburaki, Phys. Lett. A **217**, 315 (1996).

[56] R. A. Matzner, Phys. Rev. D **51**, 1733 (1995).

[57] S. W. Hawking, G. Horowitz, and S. Ross, Phys. Rev. D **51**, 4302 (1995).

[58] C. Teitelboim, Phys. Rev. D **51**, 4315 (1995).

[59] A. Ghosh and P. Mitra, Phys. Rev. Lett. **78**, 1858 (1997).

[60] O. B. Zaslavski, Phys. Rev. Lett. **76**, 2211 (1996).

[61] P. Emparan, Phys. Rev. D **56**, 3591 (1997).

[62] K. Srinivasan and T. Padmanabhan, Phys. Rev. D **60**, 24007.

[63] F.-L. Lin, hep-th p. 9807084 (1998).

[64] M. Y. Kuchiev and V. V. Flambaum, Phys.Rev. D **70**, 044022 (2004).

[65] J. Podolsky, Gen. Rel. Grav. **31**, 1703 (1979).

[66] F. J. Zerilli, Phys. Rev. D **9**, 860 (1974).

[67] V. Moncrief, Phys. Rev.D **9**, 2707 (1974).

[68] V. Moncrief, Phys. Rev.D **10**, 1057 (1974).

[69] V. Moncrief, Phys. Rev.D **12**, 1526 (1975).

[70] S. Chandrasekhar, *The Mathematical Theory of Black holes* (Clarendon, Oxford, 1983).

[71] B. Xanthopoulos, Proc. R. Soc. London **A378**, 73 (1983).

[72] S. Hod and T. Piran, Phys. Rev. D **58**, 024017 (1998).

[73] S. W. Hawking and G. F. R. Ellis, *The large scale structure of space-time* (Cambridge University Press, Cambridge, 1973).

[74] D. Brill and J. A. Wheeler, Rev. Mod. Phys. **29**, 465 (1957).

[75] S. A. Teukolsky, Astrophysical J. **185**, 635 (1973).

[76] W. Unruh, Phys. Rev. Lett. **31**, 1265 (1973).

[77] S. Chandrasekhar, Proc. R. Soc. **A 349**, 571 (1976).

[78] S. Chandrasekhar, Proc. R. Soc. A **A 350**, 564 (1976).

[79] F. Finster, J. Smoller, and S. T. Yau, Phys. Rev. D. **59**, 104020 (1999).

[80] F. Finster, J. Smoller, and S. T. Yau, Commun. Math. Phys. **205**, 249 (1999).

[81] F. Finster, J. Smoller, and S. T. Yau, Phys. Lett. **A259**, 431 (1999).

[82] F. Finster, J. Smoller, and S. T. Yau, J. Math. Phys. **41**, 2173 (2000).

[83] F. Finster, J. Smoller, and S. T. Yau, Commun. Pure Appl. Math. **53**, 902 (2000).

[84] F. Finster, J. Smoller, and S. T. Yau, J. Math. Phys. **41**, 3943 (2000).

[85] F. Finster, J. Smoller, and S. T. Yau, Adv. Theor. Math. Phys. **4**, 1231 (2002).

[86] F. Finster, J. Smoller, and S. T. Yau, gr-qc/0211043 (2002).

[87] F. Finster, N. Kamran, J. Smoller, and S. T. Yau, Commun. Math. Phys. **230**, 201 (2002).

[88] F. Finster, N. Kamran, J. Smoller, and S. T. Yau, gr-qc/0005088 (2000).

[89] R. Fabbri, Phys. Rev. D **12**, 933 (1975).

[90] D. N. Page, Phys. Rev. D **13**, 198 (1976).

[91] D. N. Page, Phys. Rev. D **14**, 3260 (1976).

[92] D. N. Page, Phys. Rev. D **16**, 2402 (1977).

[93] C. Doran, A. Lasenby, S. Dolan, and I. Hinder, Phys. Rev.D **71**, 124020 (2005).

[94] D. G. Boulware, Phys. Rev. D **12**, 350 (1975).

[95] M. Soffel, B. Muller, and W. Greiner, Phys. Rev. D . **22**, 1935 (1980).

[96] R. Jarregui, M. Torres, and S. Hacyan, Phys. Rev. D. **43**, 3979 (1991).

[97] P. M. Alsing, I. Fuentes-Schuller, R. B. Mann, and T. E. Tessier, Phys. Rev. A **74**, 032326 (2006).

[98] R. Kerner and R. B. Mann, arXiv:0710.0612 (2007).

[99] S. B. Giddings and T. Thomas, Phys. Rev. D **65**, 056010 (2002).

[100] S. Dimopoulos and G. Landsberg, Phys. Rev. Lett. **87**, 161602 (2001).

[101] D. M. Eardley and S. B. Giddings, Phys. Rev. D **66**, 044011 (2002).

[102] S. W. Hawking, Phys. Rev. D **14**, 2460 (1975).

[103] G. T. Horowitz and J. MAldacena, Joun. High. Eng. Phys. **0402**, 008 (2004).

[104] M. Y. Kuchiev, Phys. Rev. D **69**, 124031 (2004).

[105] D. R. Brill and J. A. Wheeler, Phys. Rev. D **29**, 465 (1957).

[106] P. B. Groves, P. R. Anderson, and E. D. Carlson, Phys. Rev. D **66**, 124017 (2002).

[107] T. Regge and J. A. Wheeler, Phys. Rev **108**, 1063 (1957).

[108] H. P. Nollert, Class. Quantum. Grav. **16**, R159 (1999).

[109] K. D. Kokkotas and B. G. Schmidt, Living Rev. Rel. **2**, 2 (1999).

[110] R. A. Konoplya, Phys. Lett. B **550**, 117 (2002).

[111] B. Wang, Braz. J. Phys. **35**, 1029 (2005).

[112] H. T. Cho, Phys. Rev. D **68**, 024003 (2003).

[113] Y. J. Wu. and Z. Zhao, Phys. Rev. D **69**, 084015 (2004).

[114] J. Jing, gr-qc/0312079 **v1** (2003).

[115] S. Chen, B. Wang, and R. Su, gr-qc/0701088 **v1** (2007).

[116] A. Vilenkin, Phys. Rep. **121**, 263 (1985).

[117] A. Vilenkin, Phys. Rev. D **23**, 852 (1981).

[118] M. Aryal, L. H. Ford, and A. Vilenkin, Phys. Rev. D **34**, 2263 (1986).

[119] T. W. B. Kibble, J. Phys. A: Math. Gen **9**, 1387 (1966).

[120] A. Vilenkin, Phys. Rev. Lett **46**, 1169 (1981).

[121] T. W. B. Kibble and N. Turok, Phys. Rev. Lett **116B**, 141 (1982).

[122] M. G. Germano, V. B. Bezerra, and E. R. B. de Mello, Class. Quantum Grav. **13**, 2663 (1996).

[123] F. Cooper, A. Khare, and U. Sukhatme, Phys. Rept. **251**, 267 (1995).

[124] R. A. Konoplya and A. Zhidenko, Nucl. Phys. **B777**, 182 (2007).

[125] A. O. Starinets, Phys. Rev. D **66**, 124013 (2002).

[126] V. Cardoso and J. P. S. Lemos, Phys.Rev. D **63**, 124015 (2001).

[127] R. A. Konoplya, Phys. Rev. D **68**, 124017 (2003).

[128] H. R. Beyera, Commun. Math. Phys. **221**, 659 (2001).

[129] L. E. Simone and C. M. Will, Class. Quant. Grav. **9**, 963 (1992).

[130] R. A. Konoplya and A. Zhidenko, Phys. Lett. B **609**, 377 (2005).

[131] A. V. Zhidenko, Phys. Rev. D **74**, 064017 (2006).

[132] R. A. Konoplya, Phys. Rev. D **66**, 084007 (2002).

[133] W. Zhou and J. Zhu, Int. J. Mod. Phys. D **13**, 1105 (2004).

[134] X. He and J. Jing, Nucl. Phys **B755**, 313 (2006).

[135] J. Jing, Phys. Rev. D **72**, 027501 (2005).